Electrospinning of Polymers

The University of Sheffield

By David Norton

Submitted to the University of Sheffield
In fulfilment of the requirements for the award of
Doctor of Philosophy

Declaration

The work described in this thesis was undertaken at the University Of Sheffield between February 2003 and January 2006, under the supervision of Professor A. J. Ryan. Unless otherwise stated, it is the work of the author and has not been submitted in whole or in any part for any other degree at this or any other institute.

February 2006

Signed.....

David Norton

Department of Chemistry
Dainton Building
University of Sheffield
Brook Hill,
Sheffield
S3 7HF

Acknowledgements

I would firstly like to thank Professor A. J. Ryan for giving me the opportunity to work on such a great project. Working for Tony has been a truly fulfilling experience. His balance of close guidance coupled with the freedom he gave me with this project was the ideal mix for me to get the most out of my research. The continued enthusiasm he has shown for the project has proved invaluable for my levels of motivation.

Thanks must go to Dr "James" Linge Wang. His alternative slant on electrospinning and boundless enthusiasm for the subject enabled many great ideas to flourish between us. Thanks also to Rob McKean for the excellent work he has done on the electrospinning machines since starting last year, and thanks to masters student Liang Liang Wang whose work ethic and application was second to none. Many thanks must also go to John Howse for his help in cobbling together bits of kit to make a functional machine. As far as building the machines go none of it would have been possible without the help of technicians Richard Wilkinson and Mike Carr. On the biological side of things my thanks must go to Sun Tao for the novel uses he has found for my fibres and Irene Canton for her help with my biology learning. Cheers to Paul Pickavance for all those coffee breaks (how much money!!) where we could discuss our projects in depth (honest) and to the entire NCD group who have ensured that the past three years have been the most enjoyable of my life. Thanks to Susanna who has kept me more or less stress free for the past two and a half years, I couldn't ask for any more from you.

Finally thanks to my Mum and Dad for giving me so much support throughout my university career and for introducing me to the outdoors at an early age, without which my life would feel so unfulfilling.

Abstract

The electrospinning process is of great utility in the manufacture of non-woven fabrics for a variety of applications including tissue engineering.

A machine has been constructed capable of electrostatically spinning (electrospinning) a wide range of polymer solutions for the production of nano and micrometer diameter polymer fibres and fibrous non-wovens. The key role of these scaffolds in the research is in the making of tissue engineered scaffolds.

Methods have been developed to allow control over the fibre topography enabling the production of fibrous polystyrene (PS) and poly(l-lactide) (PLLA) scaffolds within which skin cells can proliferate and self-organise. A polystyrene scaffold, without cell signalling chemistry, was made by electrospinning and used for co-culture of fibroblasts, keratinocytes and endothelial cells. In the absence of growth serum the single cell cultures did not thrive, but together they did not need growth serum to populate the 3-D structure. When cultured at an air-water interface native spatial organisation was observed, demonstrating that not only does co-culture allow cells to proliferate without serum but also spontaneously self organise into the epidermal/dermal structure.

Control over the fibre surface has also been achieved whereby electrospinning in a variable humidity environment alters the porosity of the fibre surface. The benefits of this surface control have been investigated in terms of the fibre's efficacy at drug delivery. Rates of delivery of a water soluble drug encapsulated within PLLA fibres with modified surface morphologies were monitored. It was shown that the surface pores were insufficiently large to cause a noticeable increase in drug delivery rates compared with totally smooth fibres.

A novel electrospinning technique has been introduced and trialled whereby aligned micro and nanofibres of a range of polymers have been produced. This method represents a breakthrough technology in electrospinning where non-woven products are usually obtained.

List of Figures

Chapter 1 - Introduction

Chapter 2 – The Sheffield Electrospinning Machine

Chapter 3 – Self Organisation of Skin Cells in 3D Electrospun Scaffolds

Chapter 4 – Controlled Porosity of PLLA Fibres

Chapter 5 – Drug Delivery From PLLA Fibres

Chapter 6 – Fibre Alignment

List of Tables

Contents

Chapter 1
Introduction

Chapter 2 – The Sheffield Electrospinning Machine

Chapter 3 - Self Organisation of Skin Cells in 3D-Electrospun Scaffolds

Chapter 4 - Controlled porosity of PLLA fibres

Chapter 5 - Drug Delivery From PLLA Fibres

Chapter 6 - Fibre Alignment

Chapter 7 – Summary and Future Work

Chapter 1 - Introduction

1.1 Electrospinning-The Basics

Electrically powered polymer processing has been known to produce ultrafine polymer fibres since as early as the 1930s, when the electrospinning process was patented by Formhals.[1]

The process is a non-mechanical, electrostatically driven phenomenon, which is used to produce a non-woven matrix of nanoscale to microscale diameter fibres, with an inherently large surface area to volume ratio.

The electrospinning technique for producing ultrafine, sub-micron to micron diameter fibres, is related to the process of electrostatic spraying, which was first analysed by Rayleigh more than 100 years ago.[2]In electrostatic spraying, charge of typically 5-30 kV is injected into a liquid droplet from an electrode. The charged liquid is separated some distance from a second electrode (target) of opposite polarity to establish a static electric field. A so-called Taylor Cone forms through distortion of the liquid droplet due to the competing forces of the static electric field and the liquid's surface tension. For liquids with a finite conductivity, charged droplets are dispersed from the tip of the Taylor Cone[3,4] and are delivered to the target. If the liquid consists of a polymer melt or a polymer in solution and the concentration of that polymer is sufficiently high to cause molecular chain entanglement, a fibre, rather than a droplet, is drawn from the tip of the Taylor cone.[5-12]

The fibres are produced using a rather simple experimental set-up, the basic components being a high-voltage source, a grounded rotating collector mandrel with a speed controller, a source electrode, and a polymer solution of suitable concentration to cause entanglements. (figure 1.1). In addition to this a focussing ring was added to stabilise the extruded jet. Below this critical concentration chain entanglements are insufficient to stabilise any jet leading to spraying of droplets.

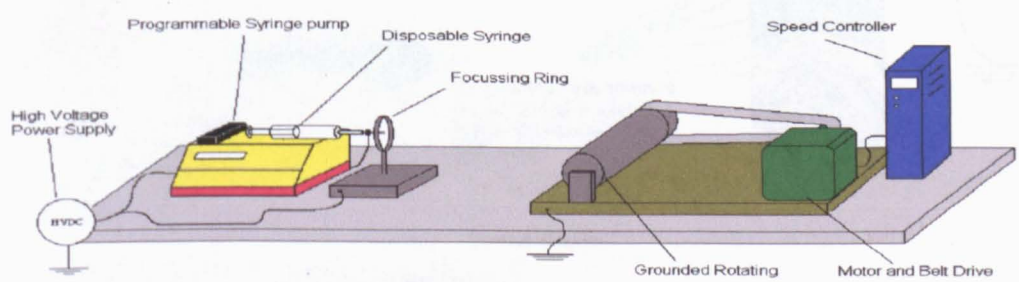

Figure 1.1 The electrospinning rig.

In this process the electrically charged polymer solution is held in a syringe fitted with a blunt tip needle, which is directed towards the grounded collector. An electric field is set up between the needle tip and the collector, and the polymer solution is slowly pumped through the syringe. On passing through the needle the solution becomes charged, as does the droplet on the end of the needle. An equilibrium is set up between the surface tension of the droplet and the attraction of the charged solution for the grounded collector. The droplet distorts in the electric field, charges within the droplet migrating to the surface, which is facing the collector. The accumulation of charge causes a protrusion to appear on the end of the droplet, distorting the droplet into a conical Taylor cone.[13] The charge per unit area at the tip of the cone increases as its radius decreases until the attraction is so strong that surface tension is overcome, and a jet of polymer solution is extruded toward the collector.[6] (figure 1.2)

During acceleration toward the collector solvents evaporate and the jet becomes unstable in the electrostatic field. This bending instability rearranges the jet into a series of connected loops, which in turn become unstable leading to secondary and tertiary loops. The jet therefore becomes a very complicated whipping system attached to a straight initial jet.[8,14] This rapid whipping of the jet on its approach to the collector leads to enormous increases in jet length at a relatively short distance from its origin. This result is a reduction of the jet diameter to the sub-micron range.[15]

Over the working distance between origin and collector, solvent evaporates, leaving extremely fine, charged fibres, which are electrostatically attracted to the

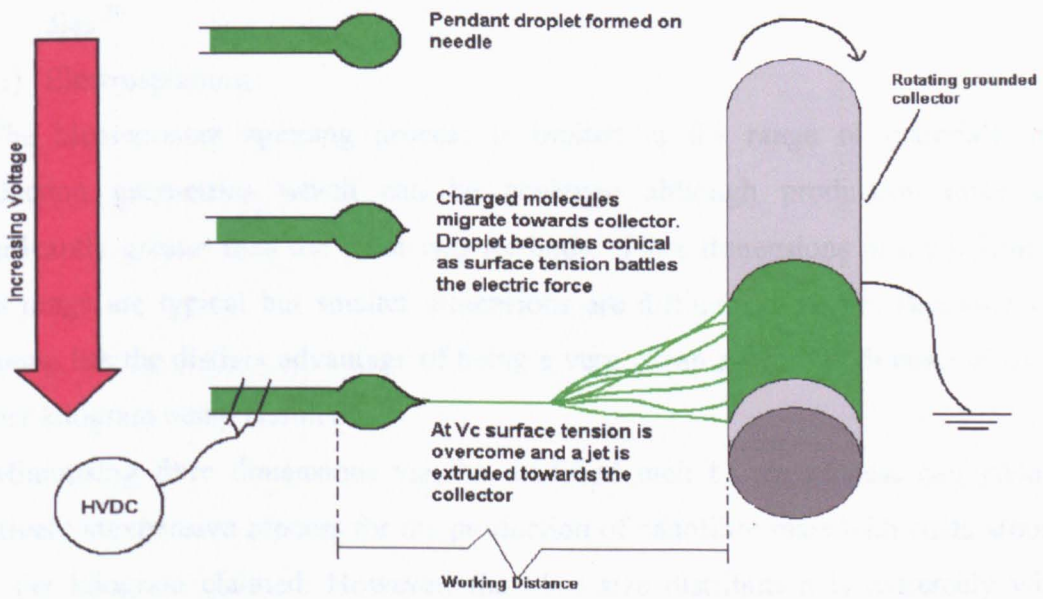

Figure 1.2 Schematic showing jet formation at V_c.

collector. The random nature of deposition gives rise to a porous, non-woven microstructure, which can be used in many applications, from filters through to tissue scaffolds (section 1.3). The morphology of electrospun fibres depends on the processing parameters of the system. Parameters such as solution concentration (viscosity), electrical conductivity of the solution, solvent parameters such as volatility, surface tension, polymer parameters such as molecular weight, solubility, and other parameters such as electric field strength, deposition distance, feeding rate and collector type (rotating drum or flat plate)[16] all affect the nature of the final product.

By altering these parameters the morphology of the electrospun fibres and the non-woven mat can be fine-tuned to the intended application.

1.2 Nanofibres as Functional Products-the Feasibility of Electrospinning

Interest in nanofibres and microfibres has recently escalated greatly principally in the fields of biomedicine for tissue scaffolds and drug delivery media, filtration devices and barrier fabrics as well as ultra-high surface area materials for sensor and catalysis applications(section 1.3).

There are three principal techniques for the production of nanofibres.

1) Bicomponent fibre spinning (melt or solution) where one of the components is soluble and can be removed to leave remnant nano-fibres.[17-19]
2) Conventional melt blown fibres produced at low flow rates using multi orifice dies.[20]
3) Electrospinning.

The bicomponent spinning process is limited in the range of materials and production geometries which can be achieved although production rates are significantly greater than the other two methods. Fibre dimensions in the 0.5μm to 1μm range are typical but smaller dimensions are difficult to obtain. Bicomponent spinning has the distinct advantage of being a very cheap process with costs of $1 to $5 per kilogram being claimed.[21]

Minimising fibre dimensions via the modified melt blown process can yield a relatively inexpensive process for the production of nanofibre mats with costs around $10 per kilogram claimed. However, the fibre size distribution is extremely wide ranging from <1μm up to 10μm and thus material performance is anticipated to be

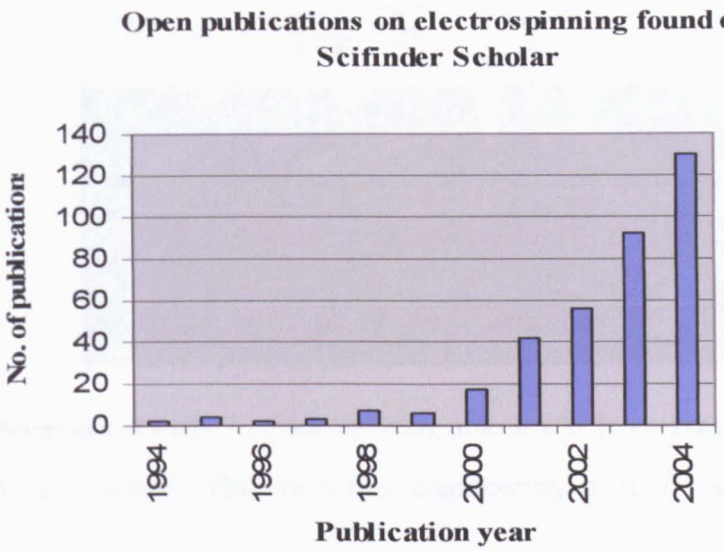

Figure 1.3 Bar chart showing number of open publications on electrospinning up to 2004.

significantly poorer. In order to get highly specialised materials a tight reign needs to be held over fibre diameter uniformity. When the distribution of diameters is large the properties of the material are harder to predict and optimise, which makes the modified melt blown process rather limited in its application.

Electrospinning has the advantage that an extremely wide range of polymers can be spun as long as they can be solubilised. Since the 1980s and especially in recent years the electrospinning process has regained more attention, probably due to a surging interest in nanotechnology as ultrafine fibres of a wide range of polymers can be easily fabricated with this process. The geometries of electrospun products are also relatively simple to alter by changing one of many process parameters. Figure 1.3 shows how the number of non-patent publications on electrospinning has increased over the last 10 years.

However, despite all this research into the process since its conception over 70 years ago there has been little commercial exploitation of electrospinnning. The limiting factor in commercialisation stems from the low production rates of the process which are typically grams per hour. Therefore, unless the production rate of the technique can be increased by several orders of magnitude, the cost of nanofibre production may continue to relegate electrospinning to the laboratory bench.

Scale-up from the laboratory level has been an ongoing problem with the process. The use of multiple spinnerets leads to complications in electrostatic repulsion between adjacent nozzles and subsequent unpredictability of the jet path. Non-continuity of the process is also a serious limiting factor in scale-up. At present most electrospinning experiments are non-continuous as a result of droplet drying. Once the droplet dries a Taylor cone is no longer able to form and electrospinning ceases until

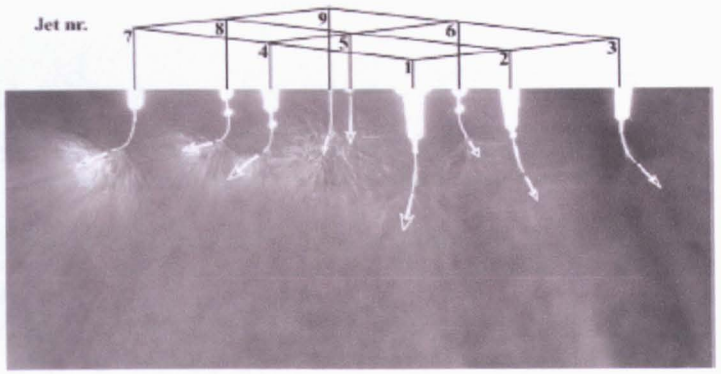

Figure 1.4 A photograph of a nine jet electrospinning process with jets arranged in a 3x3 matrix.[18]

the droplet is renewed. This provides engineering difficulties when scale-up is considered.

Much work has been done on multiple needle electrospinning investigating the interactions of many charged jets. A recent paper by Theron et al presented work done experimentally and by modelling on multiple jet arrays.[22] They found that when spinning with a small number of jets (2 or 3), the Coulombic interactions between adjacent jets caused repulsion and divulgence of jets. Maybe surprisingly they found that the introduction of more jets negated this effect and resulted in collection of fibres over a small and ultimately predictable area. They reported that an array of 9 needles separated by a distance of 1cm created a stable spinning condition for the polymer studied hence increasing rate of nanofibre production ninefold. (Figure 1.4) These experiments were performed vertically where dry droplets would just drop off the needle tip onto the collector leading to non-uniformity of the product but with the advantage of maintaining continuity of the spinning process.

Another method to overcome the scale-up problem this has been proposed and patented by Jirsak Oldrich et al who have developed a needleless spinning technique whereby the fibres originate from a turning "screw" half submerged in the polymer solution.[23] This method ensures constant renewal of the solution surface without the problem of needle clogging and enables spinning over a large area. Needleless electrospinning is an attractive target for engineers as it has the potential for easing scale up problems. (Figure 1.5)

The submerged rotating screw is charged and the screw blades cause accumulation of charge in a small volume of solution. The screw blades effectively act as charge concentrators fulfilling the function of the needle in the conventional process. By constantly refreshing the polymer solution in the bath a continuous electrospinning

a) b)

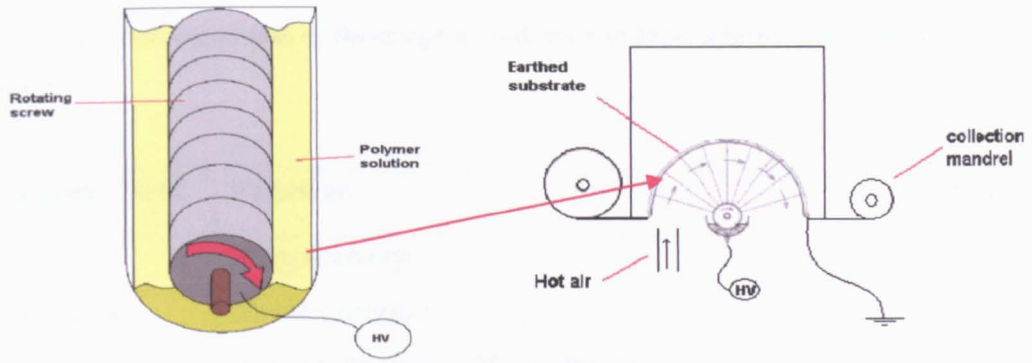

Figure 1.5 Oldrich's Needleless electrospinning a) the screw delivery system b)the conveyor. [19]

process is achieved. The earthed substrate upon which the fibres are collected is a tightly woven metal mesh from which the product can be easily removed.

1.3 Applications of Electrospun products

There are a broad range of applications envisaged for the application of nano-fibre technology all based on the exponential increase in fibre properties as the diameter reduces to ever smaller dimensions.

Smaller fibre diameters open up exciting possibilities in the area of cell growth proliferation. Non-woven matrices of nano/micro fibres typically have a porous topography into which cells can grow and proliferate giving rise to possible applications as tissue scaffolds.[24-26]

The increased modulus of smaller diameter fibres opens up possibilities of nano-composite manufacture. Combined spinning of multiple polymers would enable these composites to have a wide range of properties.

Spinning of conductive substrates could allow production of nano-wires, and the permeability and high surface area of such materials opens up many opportunities in the areas of catalysis (using activated fibres), filtration, and drug delivery. A summary of proposed uses and their approximate market value is given in table 1.1.[21]

Table 1.1 Commercial uses of electrospun products and their approximate market value (where known).[21]

Application Field	Function	Value
Life Sciences	Drug delivery Blood filtration Wound dressings (2D scaffolds)	US$40bn
Tissue Engineering	Tubular shapes for blood vessels, nerve regeneration etc 3D scaffolds for bone, cartilage, muscle regeneration Porous skin membrane	US$3.5bn US$200m US$1.5bn
Filtration	Liquid Gas Molecular Particulates	eSpin & Donaldson US$50m
Protective Clothing	Low air impedance Biological, chemical, gas and aerosol barrier	JSLIST ~US$1bn
Sensors	Thermal Piezo (Bio)Chemical (Fluorescent) Optical	??
Cosmetics	Skin cleansing Skin healing Skin therapies	??
Others	Micro/nano electronics Electrostatic dissipation EMI shielding Photovoltaics Lightweight composites Functional composites (eg shape change) High efficiency/functional catalysts	??

1.3.1 Medical Applications

Of the envisaged applications those in the medical field are perhaps most advanced in their definition and development.

Medical applications can be divided broadly in to two major fields these are tissue engineering/scaffolds and drug delivery. Through the selection of appropriate materials, electrospun nanofibre webs are ideally suited to meet the requirements for two and three dimensional scaffold geometries namely promotion of cell adhesion and enhancement of cell growth, retention of differentiated cell function, biodegradability / biocompatibility, high porosity, high surface area/volume ratio, mechanical strength, uniformly distributed and interconnected pore structure and processability into desired shape.

Scaffolds in sheet form can be used for wound dressings or porous skin membranes and can be post processed into the form of tubes for artificial arteries or nerve guides or alternatively provide scaffolds for the generation of tendon, cartilage[24], muscle[27-30] (figure 1.6), skin[24-26,31],bone[24,31] or heart tissue.[32] (figure 1.7) Tissue engineering of skin will be addressed in length in Chapter Three.

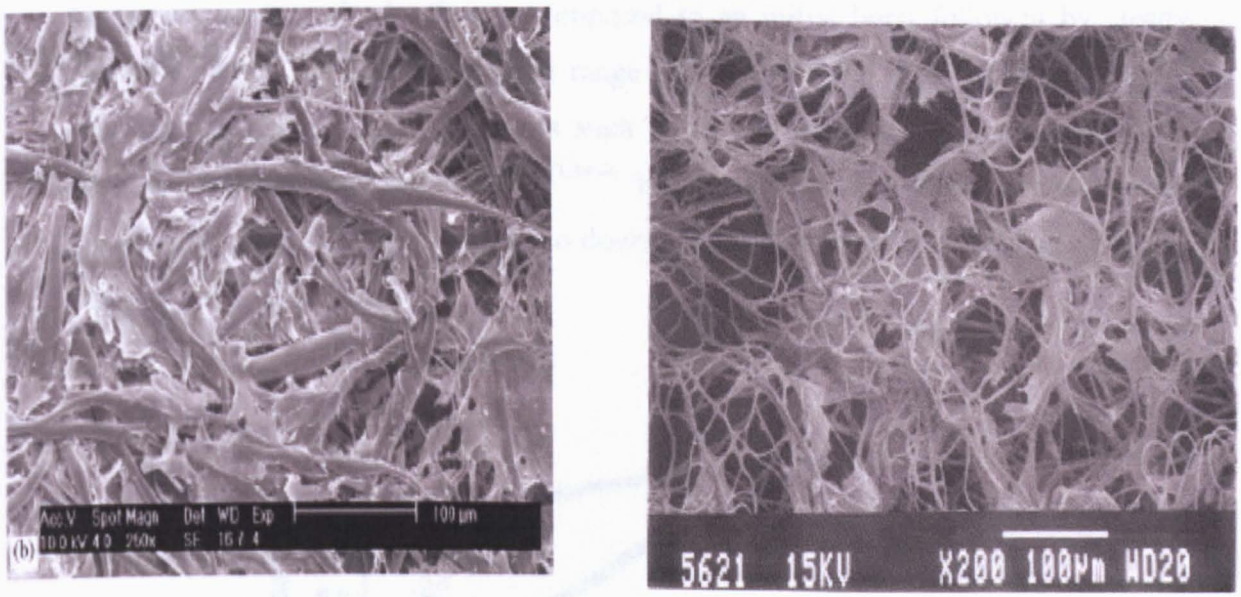

Figure 1.6 SEM micrographs of a) bone construct and b) smooth muscle on PVLA. [31]

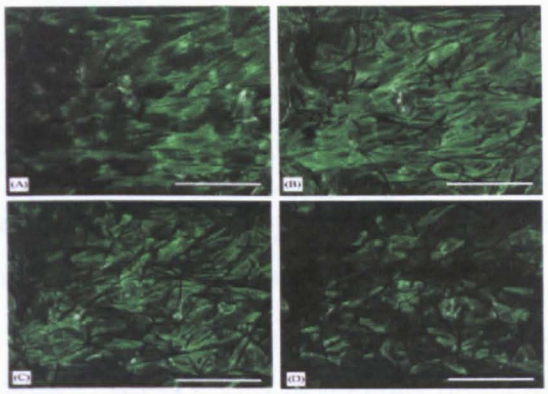

Figure 1.7 Confocal laser scanning microscopy images of cardiac myocytes (green) on as-spun PLLA membranes (black) at different depths from the upper surface A)2μm from surface B) 4μm C) 6μm D) 8μm showing penetration of cells. Scale bar is 50μm.[28]

1.3.2 Drug release

The controlled delivery of drugs can be achieved via a range of means requiring the high surface area to volume ratio of nano/microfibres. Through encapsulation of a drug within electrospun fibres a great amount of control can be enforced upon the release characteristics of that drug.[33-36] Release is dependent on many easily tunable properties such as fibre diameter, porosity and degradation rate of the polymer.

Figure 1.8 shows how release of tetracycline (a water soluble antibiotic) from cellulose fibres is highly dependent upon fibre diameter with large diameter fibres giving a more sustained release as opposed to an initial burst followed by steady release[37]. Work has been done on a range of polymers and drugs with much of it focusing on biodegradable polymers such as PLLA and collagen[38] and antibiotics such as Mefoxin[34] and tetracycline.[33,39,40] The modes of drug release are still under question but their efficacy is under no doubt. Work on drug release from electrospun fibres is covered in Chapter 5.

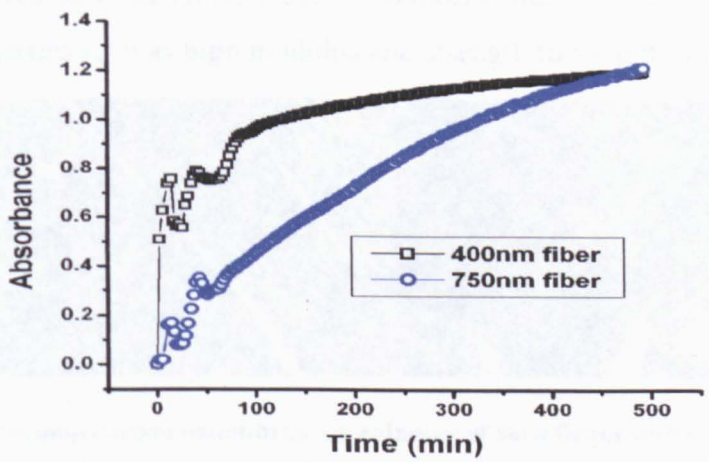

Figure 1.8 Release curves EC/tetracycline composite fibers in aqueous solution, with the same concentration of tetracycline in the fibers (tetracycline : EC=1:10). [33]

1.3.3 Barriers and Filtration

In addition to the biomedical device area a number of applications for barrier materials and filtration have been evaluated.[41-47]

For example the military have been developing the joint services lightweight integrated suit technology (JSLIST). This technology offers resistance to liquid (rain) intrusion, air permeability to maintain wearer comfort, tear strength and fabric weight requirements for harsh environments, chemical protection from a variety of liquid- and vapour-phase chemical contaminants and durability for hours of wear and heavy laundering. JSLIST is a material with comparable properties to commercially available Gore-Tex^{tm} fabrics but with additional chemical protection and durability. Preliminary investigations have indicated that compared to conventional textiles, electrospun nanofibres present both minimal impedance to moisture vapour diffusion and extreme efficacy in trapping aerosol particles.

Currently, companies such as Donaldson and eSpin[48] claim to be producing 10000m^2 per day of electrospun material for filtration purposes.[21] The uses of their product include water and air purification, fuel cell membranes, heating and air conditioning, industrial pollution control and military vehicles.

1.3.4 Composite Technology

Further areas of significant potential arise in the field of nano-composites especially based on carbon and ceramic nanofibres. Co-spinning of 2 or more polymers may yield useful mechanical properties.[49-60] With reinforcement by carbon or ceramic fibres such as Kevlar, these composite materials can provides superior structural properties such as high modulus and strength to weight ratios.

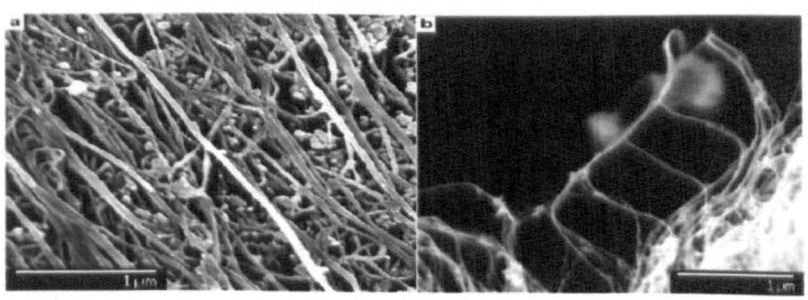

Figure 1.9 Electrospun carbon nanofibres. Co-spinning of such fibres with conventional polymer fibres could lead to interesting properties.[61]

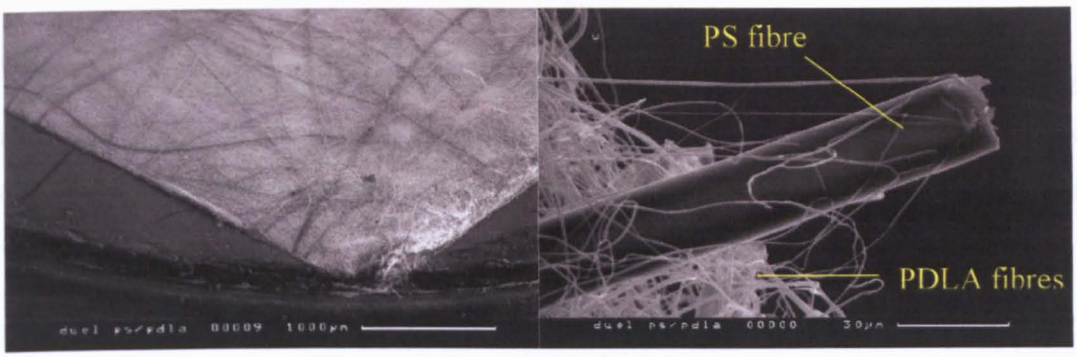

Figure 1.10 SEM micrograph of PDLA fibres co-spun with PS. The PS fibres are the large dark fibres (see chapter 2.4.1 for experimental details)

Polymer nanofibre composites from electrospinning are still in the early stages of developments due to the inherent difficulty in solubilising and spinning these materials but carbon nanotubes have been spun(figure 1.9)[53] as have composites of polystyrene and poly (D,L- lactide) (figure 1.10) whereby the larger PS fibres provide mechanical strength to the otherwise flimsy PDLA scaffold.

1.3.5 Catalysis

The field of electrospinning is also attractive for catalysis. The high surface area coupled with a surface functionalised polymer could act as supported catalyst for many applications from fuel cells to large scale chemical production. Coupled with composite technology for increased durability and the potential products become very attractive to industrialists. So far research has concentrated on the functionalising of fibre surfaces with enzymes.[62,63]

1.3.6 Absorbency

Spinning of surface modified polymers yield high surface area, porous products which can have ultra absorbent properties.[64-66] For example a cellulose based agricultural polymer can be functionalised to absorb fertiliser and pesticide for ground reclamation / decontamination. Once spun into nano/microfibres it becomes a functional product with an extremely high surface area to volume ratio. This concept can be extended to gas absorption in landfill covers and even hydrogen storage for fuel cells which turn the gas into electricity through controlled combination with oxygen in an electrochemical cell.[67]

Today the storage of hydrogen is the biggest challenge for the broadrange introduction of fuel cell technology. Carbon nanofibre technology is still in its infancy but the hydrogen storage capability is claimed to be very high even up to 3 times its own weight in hydrogen.[68]

1.3.7 Sensors and reactive polymers

Electrospinning of specialised polymers could yield materials able to act as sensors such as junction thermocouples, optical sensors [69](e.g. fluorescent polymer sensitivity related to surface area), pH sensors made from poly(aniline),[70] and shape change composites via piezo electric nanofibre webs (electro active polymers (EAP)).[69,71-74]

EAPs show a mechanical response to an electrical stimulus so when spun into nanofibres and stretched over a lightweight frame they can cause pronounced movements.[75] Alignment of such fibres will cause larger, more predictable movements (figure 1.11).

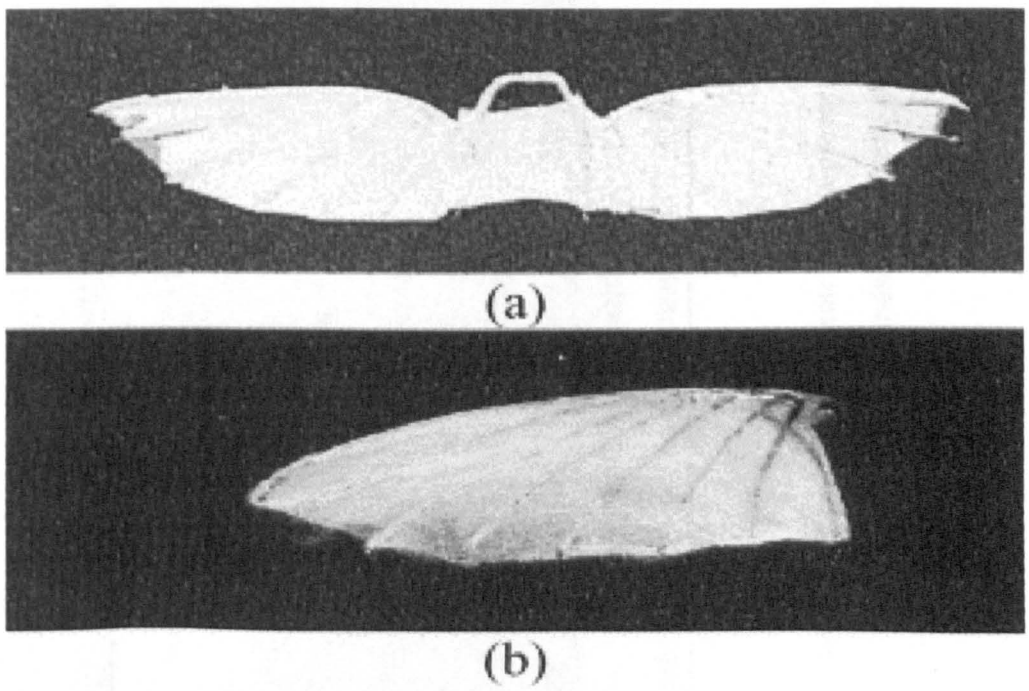

Figure.1.11 TrF1 fibres electrospun onto MAV wing frames. (a) Double wing configuration, approximate dimensions are 15.2 cm×5.1 cm;. (b) Single wing configuration, approximate dimensions are 10.2 cm×6.4 cm. Polymer is copolymer of Polyvinyl di-fluoride PVDF and Trifluoroethylene (TrFE).[75]

1.4 Which polymers have been spun?

The table below gives an idea of the range of materials which have been electrospun, and the possible/intended applications of the processed polymers. The most important experimental parameters have been included where known. This table is by no means definitive and intended only as a guide.

Table 1.2 Electrospun polymers and their uses.

Polymer	Mn($gmol^{-1}$)	Solvent	V(kV)	wt%	Characteristics of electrospun nanofibres	Applications	Ref
Piezoelectric Copolymers*	Various	DMF	20-25	20	Tough/durable fibres-electrically responsive	Micro-air vehicle wing skin.	75
PLLA (poly(L-lactic acid))	150000	DCM	35-45	5	Pitted fibres, Biodegradable	Filters, drug release, tissue engineering	41,76-78
PC (polycarbonate)	2800	DCM	35-45	15	Pitted fibres	Filters	41
Polyvinylcarbazole	1100000	DCM	35-45	7.5	Pitted fibres	Filters	41
Poly(ethylene-co-vinyl alcohol)	Various	70% 2 propanol/water	15	56-70	biocompatible, hydrophilic yet H2O insoluble	Tissue engineering scaffold	27

PCL (Poly(ε-caprolactone))	80000	MC/DMF, or Chloroform	20-25	15	biodegradable, rubbery-improves elasticity	Tissue engineering scaffold, Drug loading.	79
PEO (poly(ethylene oxide)	400000	H20	18-24	10	thin fibres-small pore size-can be blended with silk for biocompatibility	Filters/ tissue engineering scaffold	42 80
PGA (Poly(glycolic acid))	Unknown	MC/DMF	20-25	15	biodegradable	Tissue engineering scaffold	16
PDLA (Poly(D,L-lactic acid))	Unknown	MC/DMF	20-26	15	biodegradable	Tissue engineering scaffold, drug loading and release	16
PVA (poly(vinyl-alcohol)	86000	H2O	19	10	Fibres can be calciniated with alumina-borate oxide	Fire protection, material reinforcement	51

Fibrinogen	Unknown	1,1,1,3,3,3-hexafluoro-2-propanol (HFIP)	15-30		Biocompatible and biodegradable	Wound healing	[81]
Poly(acrylic acid)-poly(pyrene methanol) copolymer + polyurethane latex	50000(PAA-PM)	DMF	15-20	18.6	Fluorescent polymer	Fluorescence quenching optical sensors for metal ions	[69]
Polyethylene terephthalate	10000-20000	DCM/TFA	15	4	Structurally stable	Nanoscale wires/ropes etc	[6]
Recombinant Proteins	Various	H2O	18	5-20	Biocompatible and biodegradable	Tissue engineering	[82]
Polystyrene	190000	THF,CS2, toluene, DMF, THF/DMF	10-20	~30	Cheap- easy to spin	Cell culturing, filters	[83]
Polyaniline/PEO	900000(PEO)	Chloroform(doped with 10-camphorsulphonic acid)	25	2-4	Conducting nanofibres	Specialist materials	[84]

SLPF (silk like polymer with fibronectin functionality)		Formic acid	20	1.6-12.4	Biocompatible, structural stability, biofunctionality	Tissue engineering, Neural prosthetic devices	[85]
Nylon 6		HFIP	30	10		Advanced fabrics, textiles	[52]
Polyacrylonitrile	22000	DMF	-	-	Textile fibre polymer	Advanced fabrics, textiles	[6]
Bombyx Mori Silk and PEO	PEO 900000	H20	4.8-8.8	25	Natural Protein, biocompatible	Biomaterial Scaffolds	[80]
Collagen		HFIP	15-30	various	Biocompatible, resorbable	Tissue engineering,	[38]

*Poly(vinylidene fluoride)-trifluoroethylene copolymer

1.5 Experimental Set Up

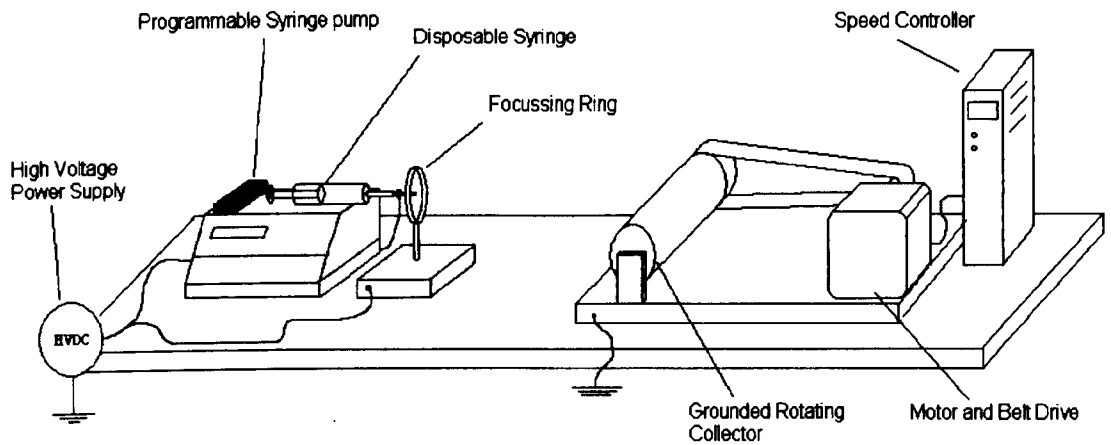

Figure 1.12 The Electrospinning Apparatus.

Figure 1.12 shows a basic electrospinning rig. The syringe pump is programmable in order to maintain a droplet on the needle tip, which is connected to the high voltage power supply with a crocodile clip. Also attached to the power supply is a metal focussing ring, which has the effect of confining the polymer jet to a smaller target area by altering the electric field between the needle and the collector.[7]

Similar focussing devices have been made using multiple ring systems[42] which can focus the jet to a very small area, effectively funnelling the jet down a repulsive electronic gradient.(figure 1.13)

The arrows in Figure 1.13 denote the direction of the electrostatic field lines and arrow length denotes qualitative field strength.

Most electrospinning set-ups don't use any form of focussing device. The fibre mat topography may well be altered by using such devices. By having such a defined electrostatic field, jet instabilities are reduced so fibre deposition may not be as chaotic. Extensive studies of such effects have yet to be undertaken. The power supply usually has a range of 0 to 35kV, which will cater for most electrospinning situations, and current should be 0A.

The collector can vary dramatically, although for many applications a rotating drum is used. Rotating and translating devices have also been used extensively as have simple flat metal plates. The main advantage of rotating collectors is to enable collection over a longer time scale and coat a larger area than is possible using a flat plate.

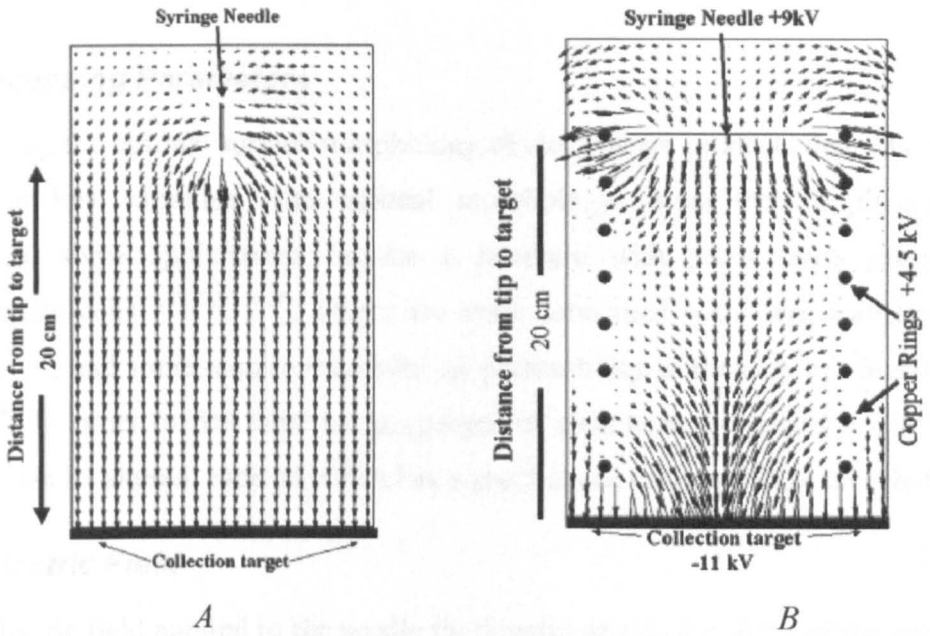

Figure 1.13 Field lines in A) non focussed and B) focussed electrospinning devices. [38]

Coating of objects other than metal collectors is very easy. By placing the object in the electric field, between needle and collector it will itself become coated. This is particularly useful for collecting fibres on scaffolds in order to make seamless membranes.[75]

1.6 Processing Parameters

Obtaining the optimal surface morphology of electrospun products depends upon a number of key variables. The optimal morphology varies from application to application, some applications require a structure with pores large enough to accommodate cells[24,25,27,31,38,86], others are more concerned with fibre diameter than pore size[51,84], and some require increased air permeability(in the case of "breathable" textiles).[87] In order to fine tune the properties of electrospun products a number of variables can be altered, each of which has a pronounced effect on fibre morphology.

1.6.1 Electric Field

The electric field applied to the needle tip directly affects the shape of the initiating droplet. With all other variables (such as feeding rate, viscosity etc) kept constant, an increase in voltage directly affects the shape of the initial droplet and the resulting morphology of the fibres.[13]

Each polymer/solvent solution has a critical voltage (V_c) associated with it, this being the voltage at which spinning commences. When the voltage is slowly increased from 0 to V_c the surface of the liquid becomes charged to the same potential via the motion of ions/polarised polymer molecules through the liquid. As the electric field is increased the droplet becomes more and more prolate (Taylor Cone).When V_c is reached, the electric field is high enough that the attraction toward the grounded collector overcomes the forces associated with the surface tension. From the tip of the Taylor cone a quasi-stable, electrically charged jet is ejected. [88]

This critical voltage is not necessarily the voltage that produces the ideal fibre morphology. Investigations into the effects of increasing voltage beyond the critical voltage carried out on a solution of PDLA in DMF showed that increasing voltage lead to more beaded fibres.[16] As the electrospinning process is self-accelerating, there is a fine balance to be struck between feeding rate of solution and applied voltage.

Even when the feeding rate is faster than the jet could carry the fluid away, a Taylor cone is maintained at the bottom of the droplet and fibres are extruded in the way described. As voltage is increased, there comes a point where the fluid is jetting away from the tip faster than the solution is getting fed into the system. When this happens, the droplet retreats into the needle tip and jetting is initiated from within the

spinneret. The resulting fibres are of greater diameter and are more beaded as a result of wetness as thicker fibres have more solvent to evaporate.

The situation described above however is not particularly useful to the chemist. When electrospinning, the aim is to always strike a balance between all the parameters in the system to get a self-sustaining jetting situation. In the situation where feeding rate is increased with increased electric field, a far more useful observation about fibre morphology is made, that fibres are more defined, drier and of smaller diameter.[75] This is almost the opposite of what happens when feeding rate is kept constant. If the Taylor cone is maintained at higher voltage by altering the feeding rate, distortion of the cone will be greater at high V due to the increased attraction to the grounded collector. The tip of the cone through which the jet is extruded will be smaller, therefore the jet will be finer. The jet will also be accelerated faster toward the collector plate as a result of the increased potential gradient. The fine jet coupled with the added acceleration leads to very fast solvent evaporation and the collection of fine, dry, well-defined fibres.[83,89,90]

1.6.2 Concentration

Of all the variables that can be altered, concentration of polymer solution has the most drastic effect upon the morphology of the electrospun fibres. Increasing concentration of a polymer solution has the effect of increasing the viscosity of the solution as the number of entanglements between polymer chains increase.[20] Varying concentration just a little can yield a great increase in viscosity.[16]

Consistently it has been shown that increasing the viscosity up to the process limiting concentration of the polymer solution leads to the formation of more uniform, well-defined fibres (figure 1.14). At low viscosity beaded structures are often observed. The beads are interlinked by extremely fine nanofibres(figure 1.15). As concentration increases, the number of bead structures goes down and the morphology becomes more fibrous and uniform. The fibre diameter also increases steadily with increasing viscosity.[27,75,81,91]

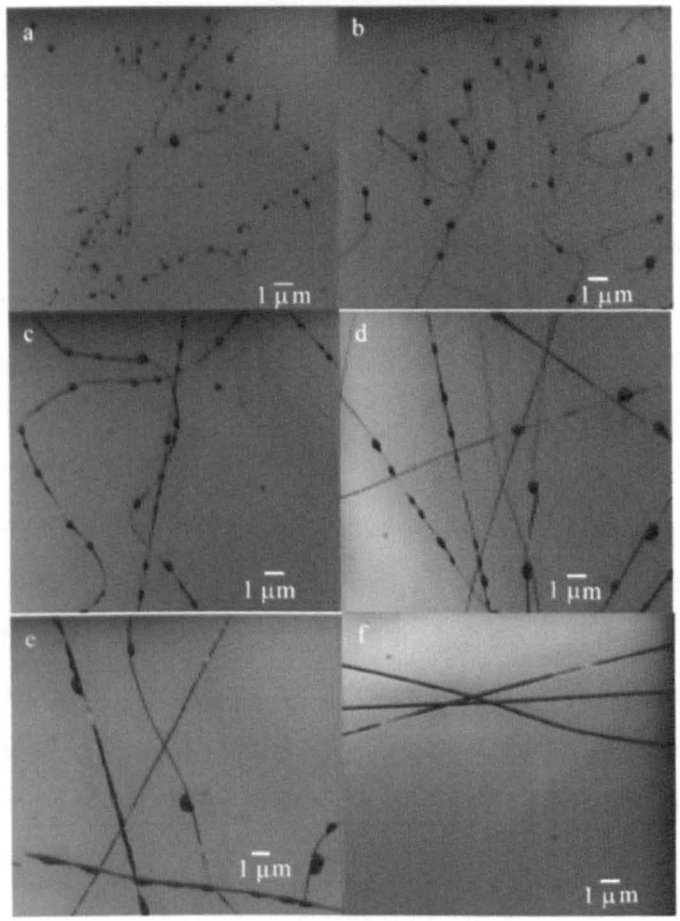

Figure 1.14 Optical microscope images (5× enlargement) of PS fibres electrospun from THF as a function of PS concentration: (a) 18 wt %; (b) 20 wt %; (c) 25 wt %; (d) 28 wt %; (e) 30 wt %; (f) 35 wt %. [21]

As viscosity of the solution increases it becomes more difficult to distort the droplet in to a Taylor cone in order to initiate jet formation. The Taylor cone is less prolate at the time of jet formation so the jet is initially wider. At higher concentration the jet is also more difficult to elongate under the acceleration of the electric field so the collected fibres are fatter than those produced from more dilute solutions.

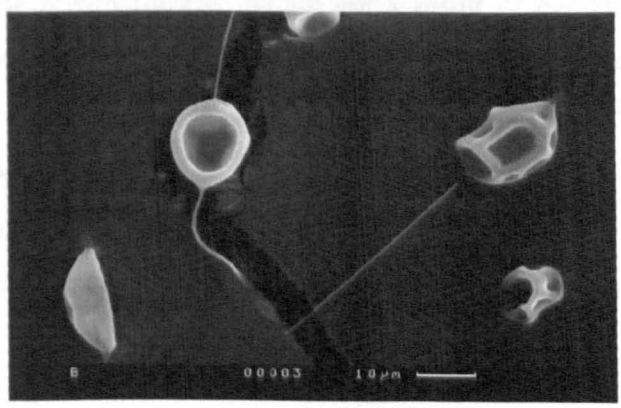

Figure 1.15 SEM micrograph of PS beaded fibres spun at 15wt%, too low in concentration for complete fibre formation.

1.6.2.1 Role of polymer chain entanglements in electrospinning

Entanglements between polymer chains in an electrospinning solution determine whether or not fibres will be obtained.[92] Increasing the concentration of a solution increases the number of overlapping chains and consequently increases the number of entanglements.[20] Too few entanglements in a solution means no fibres will be obtained, too many and the solution may be too viscous to process.

This balancing act is played out every time a new polymer solution is spun, and the perfect spinning concentration is usually determined through repeated iteration. Recently Shenoy et al reported a theoretical method of predicting the ideal spinning concentration using M_e (the entanglement molecular weight – the average molecular weight between entanglements in a polymer melt) and M_w (the weight average molecular weight).[92] The theory predicted the production of fibres in a good solvent at a concentration whereby there was an average of 2.5 entanglements per polymer chain, corresponding to a concentrated polymer solution with much overlap of molecules. The theory has been tested for PS solutions and found to work for polydisperse PS in a good solvent, but be less accurate for monodisperse PS solutions.[93]

1.6.3 Modification of the fibre surface

Recent studies on PS systems reveal nanopores on the surface of the extruded fibres as well as ribbon-like fibre morphology. As concentration was increased the nanopores on the surface became more uniform in shape and size. The reasons for these morphological changes are not fully understood, although theories have been put forward explaining the possible role of Thermally Induced Phase Separation (TIPS), and Vapour Induced Phase Separation in nanopore formation.[83] Further possibilities include breath figures, which are a result of evaporative cooling of the polymer surface as solvent is evaporated from the jet. Moisture from the air condenses on the jet in the form of droplets, which remain upon the surface and act as hard spheres. Upon drying of the jet, the water leaves indentations upon the fibre in the form of pores (figure 1.16).[94] Concentration of water in the air (humidity) has recently been shown to aid the proliferation of nanopores upon the surface of electrospun fibres.[72,95]

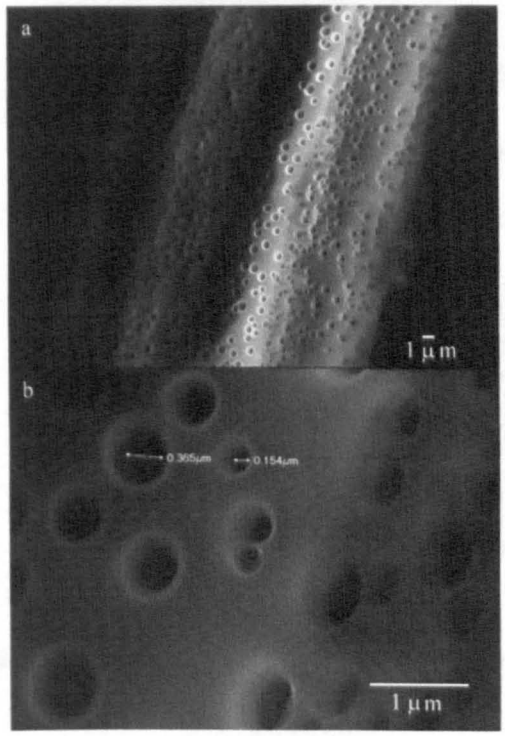

Figure 1.16 (a) SEM micrograph of PS fibre electrospun from CS_2 at 30 wt %; (b) higher magnification showing porous morphology.[83]

This could be as a result of increased numbers of breath figures due to condensed water, or by affecting vapour induced phase separation. This phenomenon has been studied further in chapter 4 on the surface of PLLA fibres whereby it was found that the surface morphology could be controlled using modified electrospinning conditions.

1.6.4 Deposition distance

Deposition distance (also known as working distance) has very little effect on the diameter or surface morphology of the nanofibres. The most noticeable effect of increasing working distance is that collected fibres are drier and more defined. When working distance is low, solvent cannot evaporate fully before the collector is reached. This often leads to beaded structures and inhomogeneous regions as a result of trapped solvent.(figure 1.17)[75,83]

The literature suggests that thinner fibres result when longer spinning distances are used[71,79] but results found during this research suggests that this is not the case. Fibres collected over shorter distances may well bear the appearance of being thicker but this can be attributed to the fibres being solvated. Once the fibres have been spun beyond a critical distance to become fully unsolvated any further increase in distance has no effect on fibre diameter.

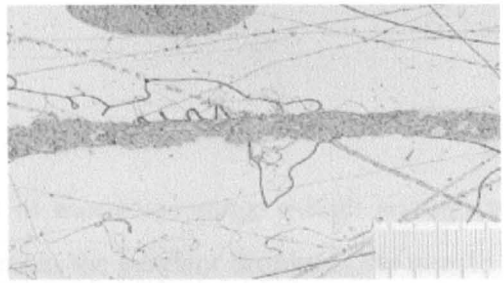

(a)

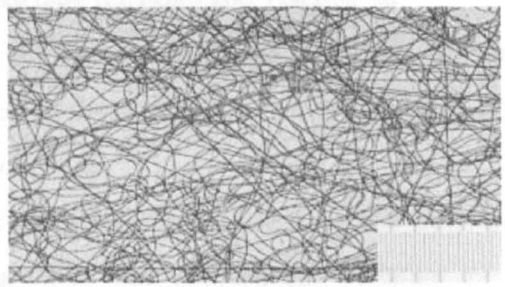

(b)

Figure 1.17 Electrospinning of TrF1 from THF deposition distance a) 7.6cm b) 25.4cm.[71]

Optimising deposition distance depends upon all other processing parameters. For less volatile solvents often a greater deposition distance is required in order to produce dry fibres. In order to collect over greater distances it would require an increase in potential, to increase acceleration and improve chances of fibre collection. Deposition distance is so inherently linked to all other variables that it is mainly a matter of iteration to find the correct length.

1.6.5 Feeding Rate

The effect of feeding rate has been discussed in 1.2.1 with respect to electric field strength. Increasing feeding rate when all other parameters are kept constant has very little effect on fibre morphology. The droplet on the end of the spinneret builds up, the Taylor cone becomes more distorted (with the possibility of multiple cones on the one droplet), but fibres are still extruded at the same rate. Controlling the feeding rate is a fine art and should be the last parameter to be altered in order to optimise it with the rest of the system. The ideal situation, whatever the viscosity/electric field etc is to maintain a single, uniform droplet on the tip of the spinneret. If this can be achieved, equilibrium will be set up between flow rate and extrusion rate and the device will run smoothly to produce regular fibre topography.[16,83]

1.6.6 Solvent system

In order to form fibres in electrospinning, a high enough viscosity and surface tension are required to maintain the pendant droplet at the needle tip. The solvent used must therefore affect high surface tensions and viscosities.[27]

Another requirement of the solvent is a high dielectric constant and conductivity. Solvents, which are deficient in these respects, will yield large, amorphous fibre mats, if indeed spinning takes place at all.[83]

Increasing the conductivity/dielectric constant of the solvent system i.e. adding Dimethylformamide(DMF)(which has a dielectric constant of 38.3) to Methylene Chloride(MC) (dielectric constant of 9.1), will yield thinner fibres. The molecules in the pendant drop will become more highly polarised; the Taylor cone more prolate; the extruded jet finer and the acceleration toward the collector much faster. The fibres are stretched more over the working distance and will be finer.[79]

Solvent volatility, which is closely related to surface tension, has a great effect on electrospinning. Extremely volatile solvents such as CS_2 do not constitute good electrospinning solvents. The vapour pressure is so high that the polymer droplet on the needle will almost instantly form a skin, thus hindering jet formation.[83]

The other extreme is a high boiling solvent such as toluene. Collected fibres are often still solvated, and in the specific case of toluene, which has a low dielectric constant, jet initiation is difficult in the first place.

An example of a good electrospinning solvent, which *does* have a high boiling point, is water. Water is the solvent of choice for electrospinning of PEO as it has good surface tension, it is highly polarisable, and clean. With sufficient attention paid to the other processing parameters, it is easy to obtain well defined, dry fibres from PEO in water.[15,42,80,96]

1.6.7 Temperature

The effect of temperature on the electrospinning of polymer solutions has not been studied on any great depth and is rather an intuitive matter. Increasing the air temperature around the electrospinning apparatus will have an effect on the rate of solvent evaporation from the fibres, giving rise to drier fibres over shorter distances. Polymer solutions have different behavioural qualities when heated or cooled depending upon the polymer/solvent system and may become thicker or thinner depending upon the dominant molecular interactions within the solution[97]. Large

fluctuations in temperature should therefore be avoided during electrospinning experiments or when repeating electrospinning experiments.

1.6.8 Ionic Salt Addition

As a general rule, the addition of ionic salts to an electrospinning solution leads to the formation of fibres with a smaller average diameter.[16] As discussed earlier, fibres spun from low concentrations are often beaded. Addition of ionic salts reduces the number of beads also.

This behaviour can be explained as follows. Adding salts to the solution results in a higher net charge on the surface of the jet as well as the jet actually carrying more electric charge. The force imparted upon the ions by the electric field is far greater than the force felt by the polymer molecules themselves, due to the ions having the greater charge density and mobility throughout the solution. The result is an increase in the elongation forces imposed upon the jet under the electrical field, which leads to finer fibres being produced.

The extent of elongation depends upon the salt used. Ionic salts whose ions are small (thus have a higher charge density), are more mobile within a jet under the influence of an external electric field. As a result, the elongation forces associated with the addition of ionic salts with small ions (such as Sodium Chloride NaCl), are greater than those associated with large ions (such as Potassium Phosphate KH_2PO_4) as predicted by the Debye-Huckel theory.[98]

For organic solvent systems, salts such as PF (Pyridinium formiate) must be used which are soluble in less polar organic solvents such as dichloromethane. PF is a volatile salt, which is completely vaporised off with the solvent during electrospinning thus not contaminating the final product. As with the polar salts described above it has the effect of removing beads and elongating fibres, leading to fine, uniform nanofibres.[91]

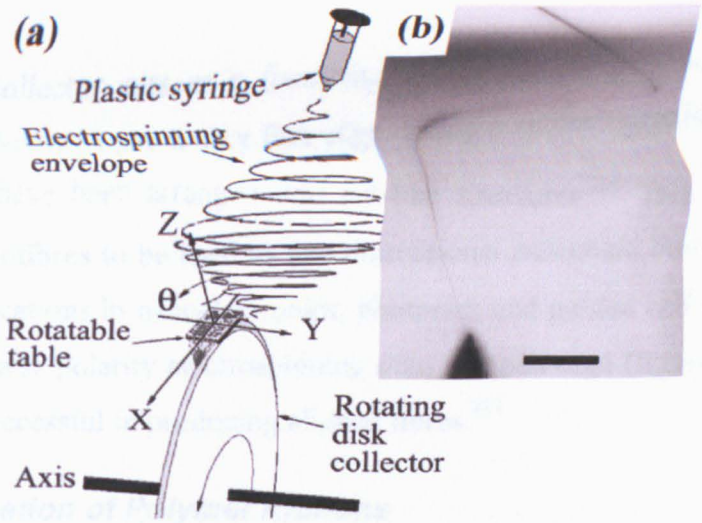

Figure 1.18 a) a schematic of electrospinning onto a gounded disc edge and the associated focussing of the jet and b) fast shutter speed image of fibre focussed onto disc edge.[11]

1.6.9 Collector Type

The collector type used can have a bearing on the topography of the non-woven mat. Collection of fibres on a flat collector plate leads to the random array of fibres typical of electrospun products. Collecting upon a rotating drum however can induce some degree of parallel alignment of fibres, whilst still maintaining an extremely porous product.[16,27,81]

Possible applications of electrospun nanofibres of conductive polymers are in the field of micro- and optoelectronics.[99] These applications do not require the non-woven mat structure commonly associated with electrospinning, but more often individual nanofibres. Work has been done on electrospinning of conducting polymers onto the sharpened edge of a spinning disc (figure 1.18). So far it has been shown that this is a good method for producing single, parallel-aligned nanofibres.[14] This is a good example of the collector affecting the electrostatic field in order to control deposition.

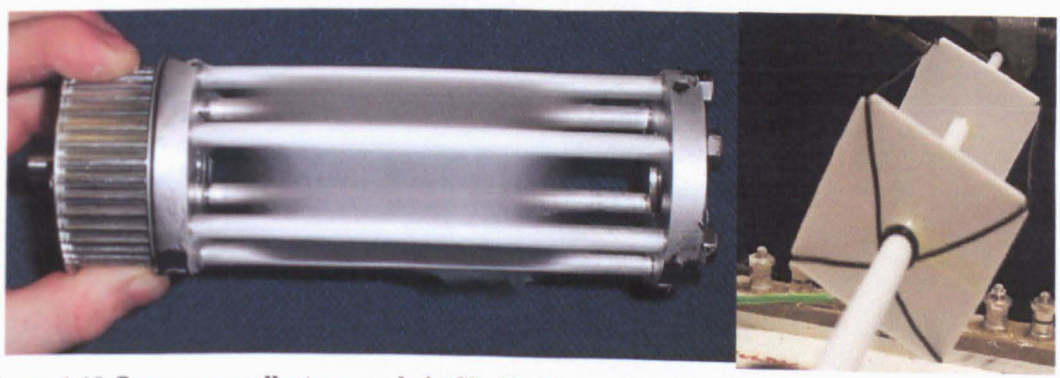

Figure 1.19 Open cage collectors made in Sheffield.

Here, the collector acts as a focussing device for the polymer jet with single nanofibres collecting upon a very fine edge. Using a similar spinning disc approach, single fibres have been arranged into net-like structures.[100] This approach enables individual nanofibres to be used as one-dimensional nanoscale building blocks, with potential applications in nanoelectronics, photonics and guided cell culture Chapter 6 deals with reverse polarity electrospinning onto an open cage (figure 1.19) which has proved very successful in producing aligned fibres.[101]

1.6.10 Formation of Polymer Ribbons

It has been observed that although many electrospun polymer fibres are spherical in cross-section a great number have a more ribbon-like structure.[102] Recent investigations have shown that the spinning of PS from THF results in ribbon structures being formed.(figure 1.20).The mechanics of such ribbon formation is discussed in chapter 2.3.1. The ability to predict and control ribbon formation has not yet been achieved, nor the comparative advantages of each structure been elucidated.

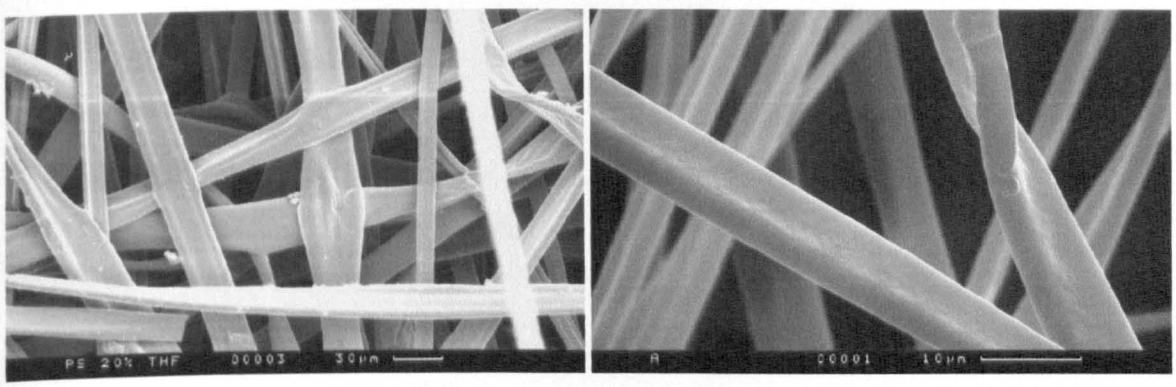

Figure 1.20 Polystyrene ribbons formed from electrospinning 20 wt% solution of PS in THF at 15kV.

1.7 Summary

Primarily it is important to produce the optimum fibre mat topography for the required purpose. The large number of parameters which have an effect on the product make electrospinning a powerful tool for obtaining target fibrous structures.

In the case of biological scaffolds the main aims could be to maximise cell adhesion or penetration throughout the scaffold. This requires a systematic approach, altering the many processing parameters in order to produce the ideal matrix. Pore size and mat density are the prime structural features that need to be monitored for cell penetration, with fibre surface being more important for adhesion, with rough, tape-like fibres probably being preferred to smooth cylinders.

As long as an apparatus is built which is capable of accommodating these parameter changes then most requirements of the potential electrospinning market can be met.

1.8 Aims and Objectives

The aim of this project was to construct a piece of apparatus capable of producing electrospun fibres of a wide range of polymers with controllable properties such as morphology, topography, and fibre alignment.

Once this had been achieved this apparatus was used to produce electrospun fibres for a variety of purposes. Specifically, fibres were produced for the manufacture of tissue engineering scaffolds upon which skin cells were grown. The target structure of the 3-Dimensional scaffold had a topography of suitable dimensions to allow proliferation of skin cells throughout it.

By altering the surface morphology it was anticipated that the drug delivery properties of electrospun fibres could be controlled. The drug Tetracycline was encapsulated within poly(l-lactide) fibres with different surface porosities and the release of the drug into an aqueous system monitored. The porosity of fibres was changed in order to change the rate of delivery from the fibres. Tetracycline was chosen as it is a model drug which is cheap to purchase and easily detectable using U.V spectroscopy.

Controlling the alignment of electrospun polymers would represent a breakthrough in electrospinning technology and is one of the main aims of the project. Electrospun materials are generally non-wovens as a result of the whipping phenomenon commonly encountered with this process. Utilising a novel reverse polarity apparatus to eliminate whipping, it was anticipated that alignment of fibres will be achieved.

1.9 References

1. Formhals, A. *US patent 1 975 504* **72** (1934).
2. Rayleigh. On the instability of jets. *London Math Soc* **10**, 4-13 (1878).
3. Taylor, G. I. Disintegration of Water Drops in an Electric Field. *Proceedings of the Royal Society of London*, 383-397 (1964).
4. Taylor, G. I. Electrically Driven Jets. *Proceedings of the Royal Society of London* **Series A**, 453-475 (1969).
5. Doshi, J. & Reneker, D. H. Electrospinning Process and Applications of Electrospun Fibers. *Journal of Electrostatics* **35**, 151-160 (1995).
6. Reneker, D. H. & Chun, I. Nanometre diameter fibres of polymer, produced by electrospinning. *Nanotechnology* 7, 216-223 (1996).
7. Jaeger, R., Bergshoef, M. M., Batlle, C. M. I., Schonherr, H. & Vancso, G. J. Electrospinning of ultra-thin polymer fibers. *Macromolecular Symposia* **127**, 141-150 (1998).
8. Reneker, D. H., Yarin, A. L., Fong, H. & Koombhongse, S. Bending instability of electrically charged liquid jets of polymer solutions in electrospinning. *Journal of Applied Physics* **87**, 4531-4547 (2000).
9. Hohman, M. M., Shin, M., Rutledge, G. & Brenner, M. P. Electrospinning and electrically forced jets. I. Stability theory. *Physics of Fluids* **13**, 2201-2220 (2001).
10. Hohman, M. M., Shin, M., Rutledge, G. & Brenner, M. P. Electrospinning and electrically forced jets. II. Applications. *Physics of Fluids* **13**, 2221-2236 (2001).
11. Lorrando, L. & Manley, R. Electrostatic Fibre Spinning from Polymer Melts. *Journal of polymer Scince - Polymer Physics Edition* **19**, 909-920 (1981).
12. Zeleny, J. The Electrical Discharge From Liquid Points, And a Hydrostatic Method of Measuring the Electric Intensity at their Surfaces. *Physical Review* **3**, 69-91 (1914).
13. Yarin, A. L., Koombhongse, S. & Reneker, D. H. Taylor cone and jetting from liquid droplets in electrospinning of nanofibers. *Journal of Applied Physics* **90**, 4836-4846 (2001).
14. Theron, A., Zussman, E. & Yarin, A. L. Electrostatic field-assisted alignment of electrospun nanofibres. *Nanotechnology* **12**, 384-390 (2001).

15. Shin, Y. M., Hohman, M. M., Brenner, M. P. & Rutledge, G. C. Electrospinning: A whipping fluid jet generates submicron polymer fibers. *Applied Physics Letters* **78**, 1149-1151 (2001).

16. Zong, X. H. et al. Structure and process relationship of electrospun bioabsorbable nanofiber membranes. *Polymer* **43**, 4403-4412 (2002).

17. Kanno, K. et al. in *Jpn. Kokai Tokkyo Koho* 6 pp. ((Toray Industries, Inc., Japan). Jp, 1975).

18. Saito, K., Saji, Y. & Ikegami, S. in *Jpn. Kokai Tokkyo Koho* 3 pp. ((Toho Beslon Co., Ltd., Japan). Jp, 1975).

19. Okazaki, T., Sumi, T. & Kusunose, T. in *Jpn. Kokai Tokkyo Koho* 11 pp. ((Japan Exlan Co., Ltd., Japan). Jp, 1974).

20. Wilkinson, A. N., Ryan, A.J. Polymer Processing and Structure Development. Kluwer, Amsterdam, 1998. (1999).

21. Dutton, R. N. Preliminary evaluation of the technology status and market potential for electrospinning. *Patent Viability Report* (2005).

22. Theron, S. A., Zussman, E. & Yarin, A. L. Experimental investigation of the governing parameters in the electrospinning of polymer solutions. *Polymer* **45**, 2017-2030 (2004).

23. Oldrich, J Process for producing nanofibers of polymer solution by electrostatic spinning and apparatus for making the same. *patent number CZ20032421*(2004).

24. Li, W. J., Laurencin, C. T., Caterson, E. J., Tuan, R. S. & Ko, F. K. Electrospun nanofibrous structure: A novel scaffold for tissue engineering. *Journal of Biomedical Materials Research* **60**, 613-621 (2002).

25. Shortkroff, S., Li, Y., Thornhill, T. S. & Rutledge, G. C. Cell growth on electrospun PCL scaffolds. *Abstracts of Papers of the American Chemical Society* **224**, 102-PMSE (2002).

26. Sun, T. et al. Self-Organization of Skin Cells in Three-Dimensional Electrospun Polystyrene Scaffolds. *Tissue Engineering* **11**, 1023-1033 (2005).

27. Kenawy, E. R. et al. Electrospinning of poly(ethylene-co-vinyl alcohol) fibers. *Biomaterials* **24**, 907-913 (2003).

28. Mo, X. M., Xu, C. Y., Kotaki, M. & Ramakrishna, S. Electrospun P(LLA-CL) nanofiber: a biomimetic extracellular matrix for smooth muscle cell and endothelial cell proliferation. *Biomaterials* **25**, 1883-1890 (2004).

29. Xu, C. Y., Inai, R., Kotaki, M. & Ramakrishna, S. Aligned biodegradable nanofibrous structure: a potential scaffold for blood vessel engineering. *Biomaterials* **25**, 877-886 (2004).

30. Xu, C., Inai, R., Kotaki, M. & Ramakrishna, S. Electrospun Nanofiber Fabrication as Synthetic Extracellular Matrix and Its Potential for Vascular Tissue Engineering. *Tissue Engineering* **10**, 1160-1168 (2004).

31. Yoshimoto, H., Shin, Y. M., Terai, H. & Vacanti, J. P. A biodegradable nanofiber scaffold by electrospinning and its potential for bone tissue engineering. *Biomaterials* **24**, 2077-2082 (2003).

32. Zong, X. et al. Electrospun fine-textured scaffolds for heart tissue constructs. *Biomaterials* **26**, 5330-5338 (2005).

33. Kenawy, E. R. et al. Release of tetracycline hydrochloride from electrospun poly(ethylene-co-vinylacetate), poly(lactic acid), and a blend. *Journal of Controlled Release* **81**, 57-64 (2002).

34. Kim, K. et al. Incorporation and controlled release of a hydrophilic antibiotic using poly(lactide-co-glycolide)-based electrospun nanofibrous scaffolds. *Journal of Controlled Release* **98**, 47-56 (2004).

35. Sanders, E. H., Kloefkorn, R., Bowlin, G. L., Simpson, D. G. & Wnek, G. E. Two-Phase Electrospinning from a Single Electrified Jet: Microencapsulation of Aqueous Reservoirs in Poly(ethylene-co-vinyl acetate) Fibers. *Macromolecules* **36**, 3803-3805 (2003).

36. Tan, S. T., Wendorff, J. H., Pietzonka, C., Jia, Z. H. & Wang, G. Q. Biocompatible and biodegradable polymer nanofibers displaying superparamagnetic properties. *ChemPhysChem* **6**, 1461-1465 (2005).

37. Wang, L. Electrospinning Cellulose derivative fibres.*PhD Thesis*(2004).

38. Matthews, J. A., Wnek, G. E., Simpson, D. G. & Bowlin, G. L. Electrospinning of collagen nanofibers. *Biomacromolecules* **3**, 232-238 (2002).

39. Bajpai, A. K., Bajpai, J. & Shukla, S. Release dynamics of tetracycline from a loaded semi-interpenetrating polymeric material of polyvinyl alcohol and poly(acrylamide-co-styrene). *Journal of Materials Science: Materials in Medicine* **14**, 347-357 (2003).

40. Markman, C., Fracalanzza, S. E. L., Novaes, A. B., Jr. & Novaes, A. B. Slow release of tetracycline hydrochloride from a cellulose membrane used in guided tissue regeneration. *Journal of Periodontology* **66**, 978-83 (1995).

41. Bognitzki, M. et al. Nanostructured fibers via electrospinning. *Advanced Materials* **13**, 70-+ (2001).

42. Deitzel, J. M., Kleinmeyer, J. D., Hirvonen, J. K. & Tan, N. C. B. Controlled deposition of electrospun poly(ethylene oxide) fibers. *Polymer* **42**, 8163-8170 (2001).

43. Deitzel, J. M. et al. Electrospinning of polymer nanofibers with specific surface chemistry. *Polymer* **43**, 1025-1029 (2002).

44. Ding, B., Kimura, E., Sato, T., Fujita, S. & Shiratori, S. Fabrication of blend biodegradable nanofibrous nonwoven mats via multi-jet electrospinning. *Polymer* **45**, 1895-1902 (2004).

45. Hajra, M. G., Mehta, K. & Chase, G. G. Effects of humidity, temperature, and nanofibers on drop coalescence in glass fiber media. *Separation and Purification Technology* **30**, 79-88 (2003).

46. Jin, H. J., Fridrikh, S. V., Rutledge, G. C. & Kaplan, D. L. Electrospinning Bombyx mori silk with poly(ethylene oxide). *Biomacromolecules* **3**, 1233-1239 (2002).

47. Tsai, P. P., Schreuder-Gibson, H. & Gibson, P. Different electrostatic methods for making electret filters. *Journal of Electrostatics* **54**, 333-341 (2002).

48. eSpin. www.eSpintechnologies.com.

49. Balkus, K. J., Madhugiri, S. & Ferraris, J. Electrospun nanofiber composites. *Abstracts of Papers of the American Chemical Society* **224**, 332-COLL (2002).

50. Bergshoef, M. M. & Vancso, G. J. Transparent nanocomposites with ultrathin, electrospun nylon- 4,6 fiber reinforcement. *Advanced Materials* **11**, 1362-1365 (1999).

51. Dai, H. Q., Gong, J., Kim, H. & Lee, D. A novel method for preparing ultra-fine alumina-borate oxide fibres via an electrospinning technique. *Nanotechnology* **13**, 674-677 (2002).

52. Fong, H., Liu, W. D., Wang, C. S. & Vaia, R. A. Generation of electrospun fibers of nylon 6 and nylon 6- montmorillonite nanocomposite. *Polymer* **43**, 775-780 (2002).

53. Gao, J. et al. Large-Scale Fabrication of Aligned Single-Walled Carbon Nanotube Array and Hierarchical Single-Walled Carbon Nanotube Assembly. *Journal of the American Chemical Society* **126**, 16698-16699 (2004).

54. Huang, Z.-M., Zhang, Y. Z., Kotaki, M. & Ramakrishna, S. A review on polymer nanofibers by electrospinning and their applications in nanocomposites. *Composites Science and Technology* **63**, 2223-2253 (2003).

55. Kameoka, J. et al. A scanning tip electrospinning source for deposition of oriented nanofibres. *Nanotechnology* **14**, 1124-1129 (2003).

56. Lee, Y. H. et al. Electrospun dual-porosity structure and biodegradation morphology of Montmorillonite reinforced PLLA nanocomposite scaffolds. *Biomaterials* **26**, 3165-3172 (2005).

57. Li, D., Wang, Y. & Xia, Y. Electrospinning nanofibers as uniaxially aligned arrays and layer-by-layer stacked films. *Advanced Materials (Weinheim, Germany)* **16**, 361-366 (2004).

58. Li, D. & Xia, Y. Electrospinning of nanofibers: Reinventing the wheel? *Advanced Materials (Weinheim, Germany)* **16**, 1151-1170 (2004).

59. Min, B.-M., You, Y., Kim, J.-M., Lee, S. J. & Park, W. H. Formation of nanostructured poly(lactic-co-glycolic acid)/chitin matrix and its cellular response to normal human keratinocytes and fibroblasts. *Carbohydrate Polymers* **57**, 285-292 (2004).

60. Ziegler, D., Sung, C., Dolukhanyan, T. & Schreuder-Gibson, H. L. Microcharacterization of composite membranes of electrospun nanofibers and microparticles. *Microbeam Analysis 2000, Proceedings*, 171-172 (2000).

61. Wang, Y., Serrano, S. & Santiago-Aviles, J. J. Conductivity measurement of electrospun PAN-based carbon nanofiber. *Journal of Materials Science Letters* **21**, 1055-1057 (2002).

62. Jia, H. F. et al. Enzyme-carrying polymeric nanofibers prepared via electrospinning for use as unique biocatalysts. *Biotechnology Progress* **18**, 1027-1032 (2002).

63. Kim, K. et al. Control of degradation rate and hydrophilicity in electrospun non-woven poly(d,l-lactide) nanofiber scaffolds for biomedical applications. *Biomaterials* **24**, 4977-4985 (2003).

64. Hansen, L. M., Kataphinan, W., Reneker, D. H. & Smith, D. J. Production of superabsorbent electrospun nanofibers. *Abstracts of Papers, 227th ACS*

National Meeting, Anaheim, CA, United States, March 28-April 1, 2004, PMSE-303 (2004).

65. Layman, J. M. et al. Development of the biohemostat - a treatment modality for high pressure bleeding based on super-absorbent polymers and electrospun membranes. *Polymer Preprints (American Chemical Society, Division of Polymer Chemistry)* **44**, 94-95 (2003).

66. Bhide, M. Controlled release of nitric oxide from electrospun nanofiber transdermal matrices. *Abstracts, 35th Great Lakes Regional Meeting of the American Chemical Society, Chicago, IL, United States, May 31-June 2*, 251 (2003).

67. Chu, B., Hsiao, B. S. & Fang, D. in *PCT Int. Appl.* 55 pp. ((The Research Foundation of State University of New York, USA). Wo, 2002).

68. Lakeman J.B, B. D. J. The Role of Fuel Cells in the Supply of Silent Power for Operations in Littoral Waters. *NATO/OTAN* (2004).

69. Wang, X. Y. et al. Electrospun nanofibrous membranes for highly sensitive optical sensors. *Nano Letters* **2**, 1273-1275 (2002).

70. Chen, H. & Hsieh, Y.-L. Ultrafine hydrogel fibers with dual temperature- and pH-responsive swelling behaviors. *Journal of Polymer Science, Part A: Polymer Chemistry* **42**, 6331-6339 (2004).

71. Athreya, S. A. & Martin, D. C. Impedance spectroscopy of protein polymer modified silicon micromachined probes. *Sensors and Actuators a-Physical* **72**, 203-216 (1999).

72. Bognitzki, M. et al. Preparation of fibers with nanoscaled morphologies: Electrospinning of polymer blends. *Polymer Engineering and Science* **41**, 982-989 (2001).

73. Wang, X. Y., Lee, S. H., Ku, B. C., Samuelson, L. A. & Kumar, J. Synthesis and electrospinning of a novel fluorescent polymer PMMA-PM for quenching-based optical sensing. *Journal of Macromolecular Science-Pure and Applied Chemistry* **A39**, 1241-1249 (2002).

74. Zussman, E., Yarin, A. L. & Weihs, D. A micro-aerodynamic decelerator based on permeable surfaces of nanofiber mats. *Experiments in Fluids* **33**, 315-320 (2002).

75. Pawlowski, K. J. et al. Electrospinning of a micro-air vehicle wing skin. *Polymer* **44**, 1309-1314 (2003).

76. Yang, F. et al. Fabrication of nano-structured porous PLLA scaffold intended for nerve tissue engineering. *Biomaterials* **25**, 1891-1900 (2004).

77. Guidoin, M.-F., Guidoin, R., Frayssinet, P., Legrand, A. & How, T. Poly-L-Lactide Surfaces Subjected to Long-Term Cell Cultures. Cell Proliferation and Polymer Degradation. *Artificial Cells, Blood Substitutes, and Biotechnology* **33**, 411-422 (2005).

78. Yang, F., Murugan, R., Wang, S. & Ramakrishna, S. Electrospinning of nano/micro scale poly(L-lactic acid) aligned fibers and their potential in neural tissue engineering. *Biomaterials* **26**, 2603-2610 (2005).

79. Lee, K. H., Kim, H. Y., Khil, M. S., Ra, Y. M. & Lee, D. R. Characterization of nano-structured poly(epsilon-caprolactone) nonwoven mats via electrospinning. *Polymer* **44**, 1287-1294 (2003).

80. Jin, H. J., Fridrikh, S., Rutledge, G. C. & Kaplan, D. Electrospinning bombyx mori silk with poly(ethylene oxide). *Abstracts of Papers of the American Chemical Society* **224**, 408-POLY (2002).

81. Wnek, G. E., Carr, M. E., Simpson, D. G. & Bowlin, G. L. Electrospinning of nanofiber fibrinogen structures. *Nano Letters* **3**, 213-216 (2003).

82. Huang, L. et al. Generation of synthetic elastin-mimetic small diameter fibers and fiber networks. *Macromolecules* **33**, 2989-2997 (2000).

83. Megelski, S., Stephens, J. S., Chase, D. B. & Rabolt, J. F. Micro- and nanostructured surface morphology on electrospun polymer fibers. *Macromolecules* **35**, 8456-8466 (2002).

84. Norris, I. D., Shaker, M. M., Ko, F. K. & MacDiarmid, A. G. Electrostatic fabrication of ultrafine conducting fibers: polyaniline/polyethylene oxide blends. *Synthetic Metals* **114**, 109-114 (2000).

85. Buchko, C. J., Kozloff, K. M. & Martin, D. C. Surface characterization of porous, biocompatible protein polymer thin films. *Biomaterials* **22**, 1289-1300 (2001).

86. Boland, E. D., Wnek, G. E., Simpson, D. G., Pawlowski, K. J. & Bowlin, G. L. Tailoring tissue engineering scaffolds using electrostatic processing techniques: A study of poly(glycolic acid) electrospinning. *Journal of Macromolecular Science-Pure and Applied Chemistry* **38**, 1231-1243 (2001).

87. Gibson, P., Rivin, D., Kendrick, C. & Schreuder-Gibson, H. Humidity-dependent air permeability of textile materials. *Textile Research Journal* **69**, 311-317 (1999).

88. Shin, Y. M., Hohman, M. M., Brenner, M. P. & Rutledge, G. C. Experimental characterization of electrospinning: the electrically forced jet and instabilities. *Polymer* **42**, 9955-9967 (2001).

89. Deitzel, J. M., Kleinmeyer, J., Harris, D. & Tan, N. C. B. The effect of processing variables on the morphology of electrospun nanofibers and textiles. *Polymer* **42**, 261-272 (2001).

90. Buchko, C. J., Chen, L. C., Shen, Y. & Martin, D. C. Processing and microstructural characterization of porous biocompatible protein polymer thin films. *Polymer* **40**, 7397-7407 (1999).

91. Jun, Z., Hou, H. Q., Schaper, A., Wendorff, J. H. & Greiner, A. Poly-L-lactide nanofibers by electrospinning - Influence of solution viscosity and electrical conductivity on fiber diameter and fiber morphology. *E-Polymers*, art. no.-009 (2003).

92. Shenoy, S. L., Bates, W. D., Frisch, H. L. & Wnek, G. E. Role of chain entanglements on fiber formation during electrospinning of polymer solutions: good solvent, non-specific polymer-polymer interaction limit. *Polymer* **46**, 3372-3384 (2005).

93. Wang, L. L. Fourth Year Thesis- Electrospinning of PS. *Masters Thesis*(2005).

94. Srinivasarao, M. Three-Dimensionally Ordered Array of Air Bubbles in a Polymer Film. *Science* **292**, 79 (2001).

95. Casper, C. L., Stephens, J. S., Tassi, N. G., Chase, D. B. & Rabolt, J. F. Controlling Surface Morphology of Electrospun Polystyrene Fibers: Effect of Humidity and Molecular Weight in the Electrospinning Process. *Macromolecules* **37**, 573-578 (2004).

96. Huang, L., Nagapudi, K., Apkarian, R. P. & Chaikof, E. L. Engineered collagen-PEO nanofibers and fabrics. *Journal of Biomaterials Science-Polymer Edition* **12**, 979-993 (2001).

97. Ryan A, J. W. A. N. Polymer processing and structure development. **Kluwer Academic Publishers** (1998).

98. Atkins, P. W. The Elements of Physical Chemistry. *Oxford University Press*, 414 (1996).

99. Lennhoff, J. D. in *U.S. Pat. Appl. Publ.* 18 pp., Cont.-in-part of U.S. Ser. No. 884,796. ((Physical Sciences, Inc., USA). Us, 2005).

100. Zussman, E., Theron, A. & Yarin, A. L. Formation of nanofiber crossbars in electrospinning. *Applied Physics Letters* **82**, 973-975 (2003).

101. Sun, T. et al. Tissue Engineering: Nano, Micro or Macro-fibres? *Submitted for assessment* (2005).

102. Koombhongse, S., Liu, W. X. & Reneker, D. H. Flat polymer ribbons and other shapes by electrospinning. *Journal of Polymer Science Part B-Polymer Physics* **39**, 2598-2606 (2001).

Chapter 2

The Sheffield Electrospinning Machine (SESM)

The process of building a machine suitable for the electrospinning of polymers was one of constant development. A basic rig was built first comprising no mechanical parts, which was then developed into the more sophisticated rigs now used for advanced electrospinning. Each stage of development was a natural response to the limitations of the previous rig. This chapter documents the development of the Sheffield Electrospinning machine over the course of this project.

2.1 SESM Mkl Pipette Apparatus

The most simple electrospinning apparatus has no mechanical parts and is driven wholly by gravity and electrostatics. This was the first rig built and gave an insight into the fluid mechanics of electrospinning.

Firstly a highly viscous solution of the chosen polymerwas prepared and loaded into a standard glass pipette. The viscosity of the solution is such that a droplet is maintained at the pipette tip when the pipette is mounted vertically. In this situation equilibrium is set up between the droplet surface tension, gravity, and the pressure of the column of solution. In the event of this equilibrium being unattainable, the angle of the pipette can be changed from the vertical so that the downward pressure on the droplet is reduced. Once a stable situation was attained a narrow wire could be passed into the end of the pipette so that it became submerged in the polymer solution. This wire was connected to a high voltage power supply (Brandenburg Alpha 11 30kV)

Directly below the suspended droplet is a metal plate covered in aluminium foil (for easy sample removal), which was earthed. This plate acted as the collector. The distance from droplet to collector was dependent upon the polymer/solvent system in use (less volatile solvents requiring greater distance in order to evaporate fully and vice versa) but usually varies between 10 and 30cm.

Once the wire was in place and droplet suspended, a voltage was applied (5kV-30kV) to the wire. At the critical voltage (V_c) the polymer jet was extruded toward the collector. The chosen voltage was such that the rate of jet extrusion matches the rate of droplet renewal. It was exceptionally difficult to achieve this situation with such a

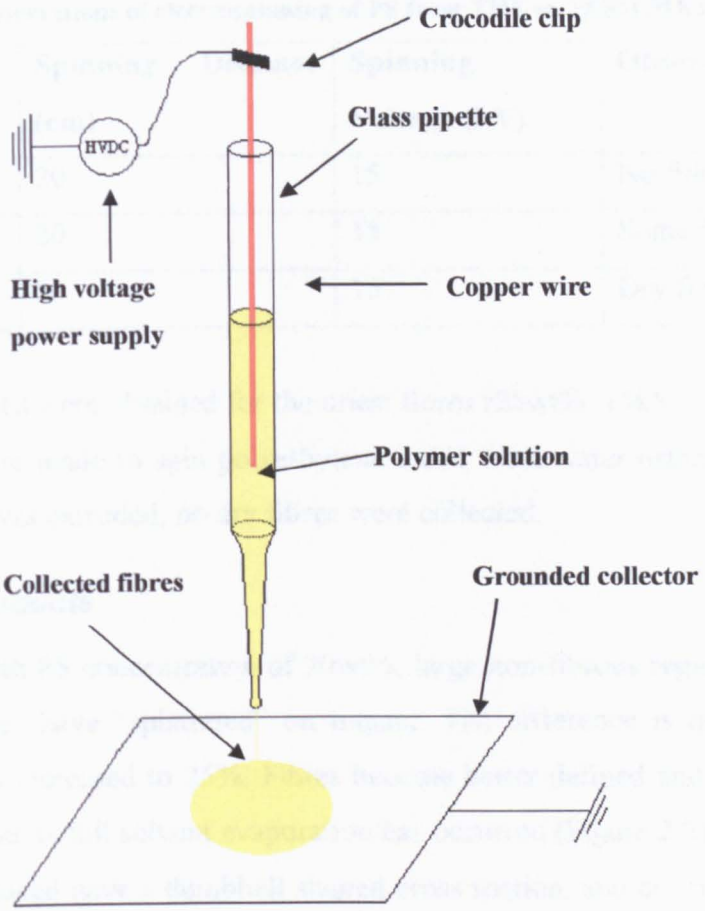

Figure 2.1 Diagram of Pipette Electrospinning apparatus SESM Mk1.

set up as the rate of droplet renewal slows as the column of solution, and the corresponding pressure it exerts decreases.

The fibre jet whipped extensively before arrival at the collector plate, as there was no electric field refinement (focussing) with this set up. This aids with the drying process but means that the fibres are collected over a large area creating much unnecessary mess and wastage.

Fibres were collected on the Aluminium foil, which could then be removed from the metal plate, placed in a sealed bag and stored.(figure 2.1)

2.1.1 Electrospinning on Mkl

2.1.1.1 PS in THF

Polystyrene (PS) with a molecular weight of 1.7×10^5g mol^{-1} was dissolved in different volumes of THF to give three solutions of varying concentration. A potential of 15 kV was applied to the submerged needle and fibres collected on the foil.

Table 2.1 Early observations of electrospinning of PS from THF on SESM MK1

Concentration (wt%)	Spinning Distance (cm)	Spinning Voltage (kV)	Observations
15	20	15	No fibres, good jet
20	20	15	Some fibres, wet
25	20	15	Dry fibres poor jet

SEM micrographs were obtained for the driest fibres (25wt%, 15kV)

Attempts were made to spin polyethylene oxide from water using the pipette rig. Although a jet was extruded, no dry fibres were collected.

2.1.2 Mkl Products

In figure 2.2 with PS concentration of 20wt%, large non-fibrous regions can be seen, where wet fibres have "splattered" on impact. The difference is quite clear when concentration is increased to 25%. Fibres become better defined and the non-fibrous regions disappear as full solvent evaporation has occurred (Figure 2.2).

The fibres produced have a dumbbell shaped cross section, and are ribbon-like rather than cylindrical. The formation of such polymer ribbons is discussed later in this chapter and previously in chapter 1.6.10.

With concentrations of less than 25% polymer jet formation was observed however, incomplete solvent evaporation lead to the collection of non-fibrous polymer rather than fibres. At 25% however, the PS solution was extremely viscous and the droplet ceased to reform at the pipette tip as the column of solution and the corresponding liquid pressure decreased. The result of this was that the jet only remained stable for a short period of time and only limited collection could take place.

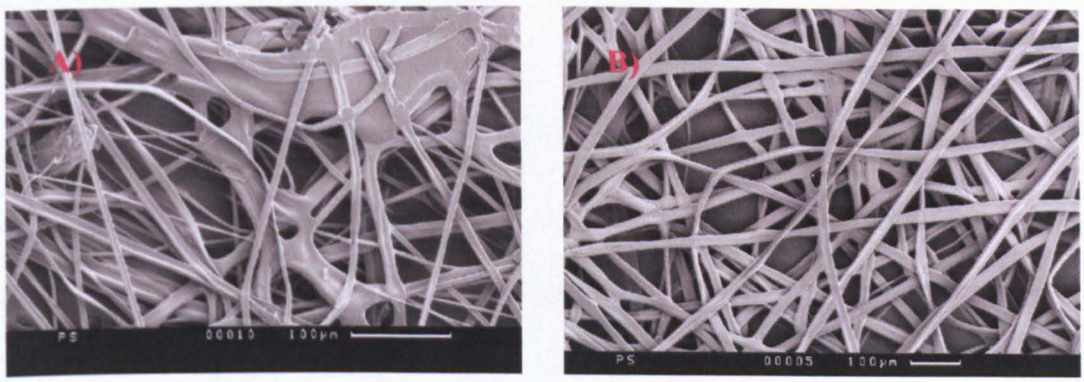

Figure 2.2 SEM micrograph of A) PS 20wt% in THF from pipette rig and B) PS 25wt% in THF from pipette apparatus.

It can be seen clearly in the SEM pictures that these are not very thick samples, as the plate behind the sample can be observed.

2.2 *SESM MkII Continuous droplet renewal and rotating collector*

This iteration of electrospinning apparatus was designed to overcome the problem of droplet cessation by constantly renewing the droplet mechanically. As opposed to the vertical pipette rig, this set up shoots fibres horizontally toward a rotating collector and is mounted upon an insulated Perspex table (figure 2.3).

The polymer solution is prepared and loaded into a plastic syringe and all air bubbles removed by tapping the syringe wall when it is held vertically. A disposable blunt ended needle is then attached to the syringe (the gauge of this needle is altered depending upon the particular experiment, with thicker needles being used for more viscous solutions) which is connected to a high voltage power supply via a length of insulated wire and a crocodile clip. The syringe is then mounted on a programmable syringe pump and pumped until a droplet appears at the needle tip.

At a set distance from the needle tip is a rotating grounded drum collector, covered in aluminium foil, which is set in motion. The rotating drum was built by the University Central Workshop and was subject to constant modification.

At this point the power supply is turned on and the voltage applied to the needle increased until the jet initialises at V_c. After a short time the droplet will disappear so the syringe pump is started in order to renew the droplet. Many iterations must be performed until the pump speed comes into equilibrium with the rate of droplet disappearance.

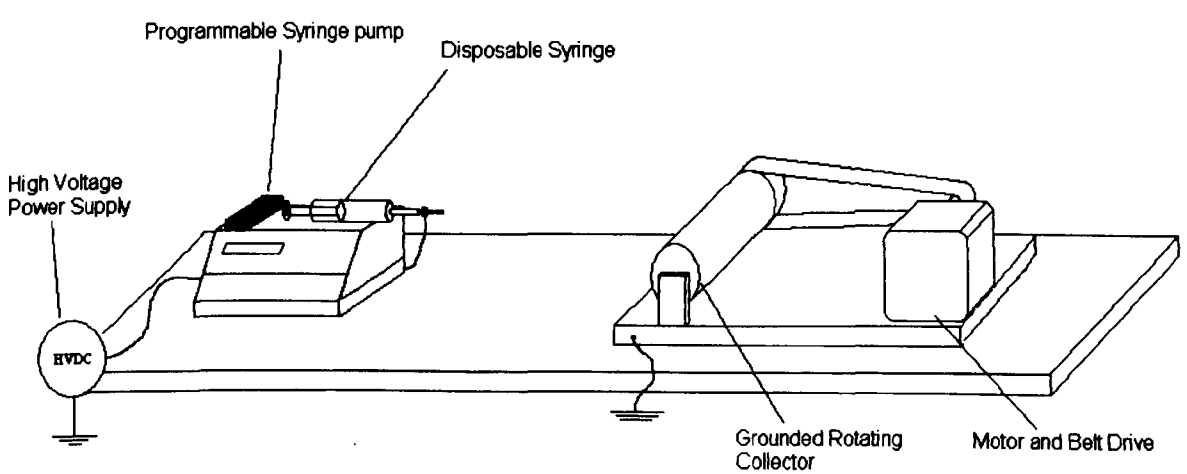

Figure 2.3 SESM MkII.

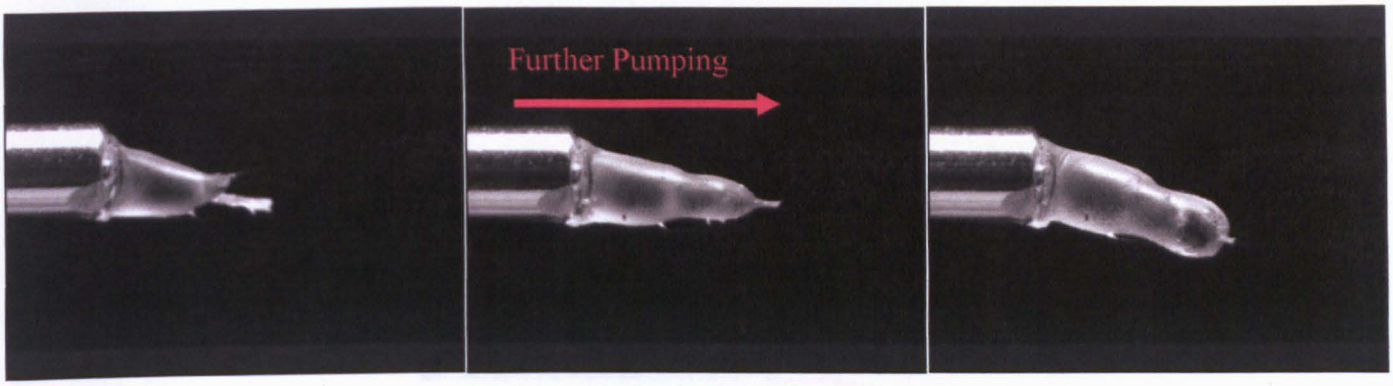

Figure 2.4 Spinning cessation due to excess solvent evaporation. A thick "skin" around the droplet prevents further jet formation regardless of pump rate.

In order to successfully collect dry product, the parameters associated with this rig must be fine-tuned. Once pump speed, voltage and collector distance are all optimised, dry product can be collected almost indefinitely until the solution runs out or the drum becomes insulated by the product. When this happens, the jet is seen to redirect itself to the next nearest grounded object. At this point pumping is stopped, as any further spinning is futile as the small increase in collected product will be outweighed by the time taken to collect it. This is a major drawback with SESM MkII as the ability to produce thick mats was seen as a priority for potential cell culture work.

When using this set up with extremely volatile solvents the droplet often dries up, halting the spinning. In this situation knocking the dried polymer off the needle tip with a long insulated rod reinitialises the droplet but failure to due so results in cessation of spinning. (Figure 2.4 (taken with a high magnification video camera))

Sometimes the droplet will only partly dry, forming a thin "skin" around the solution. When this occurs, the jet will often initiate from a place on the droplet where this "skin" is thinnest and the electrospinning process will continue. A problem with this is that often from one droplet multiple jets can arise. These jets will duly repel each other and cease to travel toward the collector. (Figure 2.5)

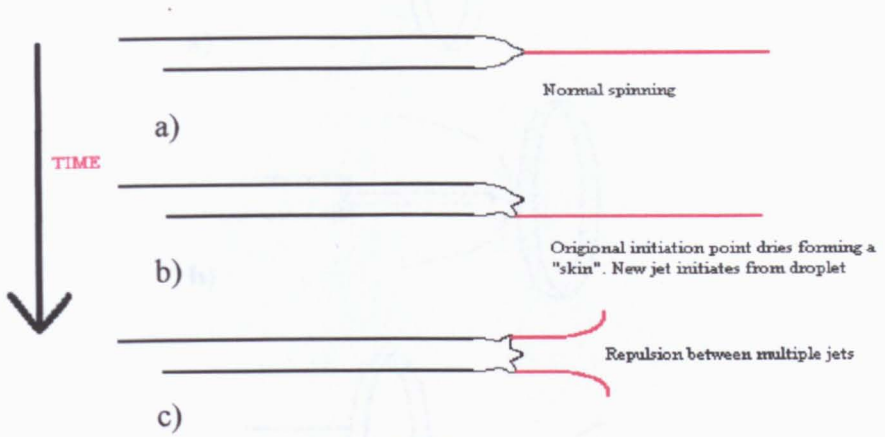

Figure 2.5 Cartoon showing the development of multiple jets through droplet drying and their subsequent repulsion. a) shows a normal electrospinning situation. b) the droplet dries partially and forms a solid skin, spinning re-initiates from the weakest point in this skin. c) a situation arises where more than one re-initiated jet will form from the sides of the original, dry droplet. These jets can repel each other.

To minimise the formation of multiple jets and maintain a single coherent source, a form of focussing device was deemed the next essential development step.

2.3 SESM MkIII Focussing

The problems of multiple jet formation due to droplet drying, and that of the jet being attracted to other grounded objects, are reduced by the inclusion of a focussing ring around the needle tip. When one jet dries up the next is forced by the charged ring to travel in the direction of the collector due to funnelling of charge, and secondary jets no longer form. The aluminium/copper ring is positioned near the very tip of the needle and is charged to the same voltage as the needle itself. If the ring is placed too far back along the needle, only small focussing effects will be noticed; too far forwards and the jet will become unstable and even shoot backwards. Once the ring is correctly positioned the jet is stable for longer and can be focussed on its target of the rotating drum more easily. (Figure 2.6)

The focussing ring reduces the area of the collector over which the polymer is collected and forces further deposition once the drum begins to become insulated. Insulation is still a limiting factor for deposition but only after a thick (up to 1mm) sample is built up.

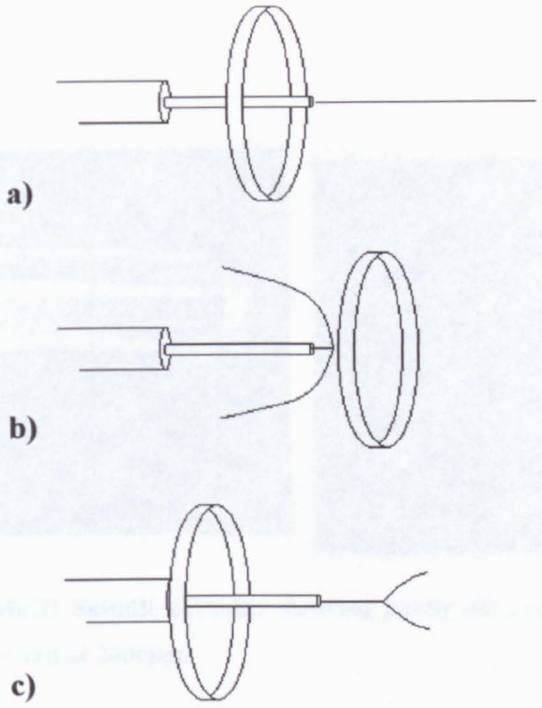

Figure 2.6 In a) the ring is positioned perfectly and a single focussed jet is accelerated from the needle tip b) ring is too far forward causing repulsion of jet c) ring is too far back so jet is not stabilised-multiple jets will still occur.

Another development for MkIII was that of variable rotation speed for the collector drum. This was achieved by connecting the belt drive to a variable speed controller purchased from Scientific Laboratory Supplies. This enabled a range of rotation speeds from 60 r.p.m to 300 r.p.m to be realised. Figure 2.7 shows the complete set-up.

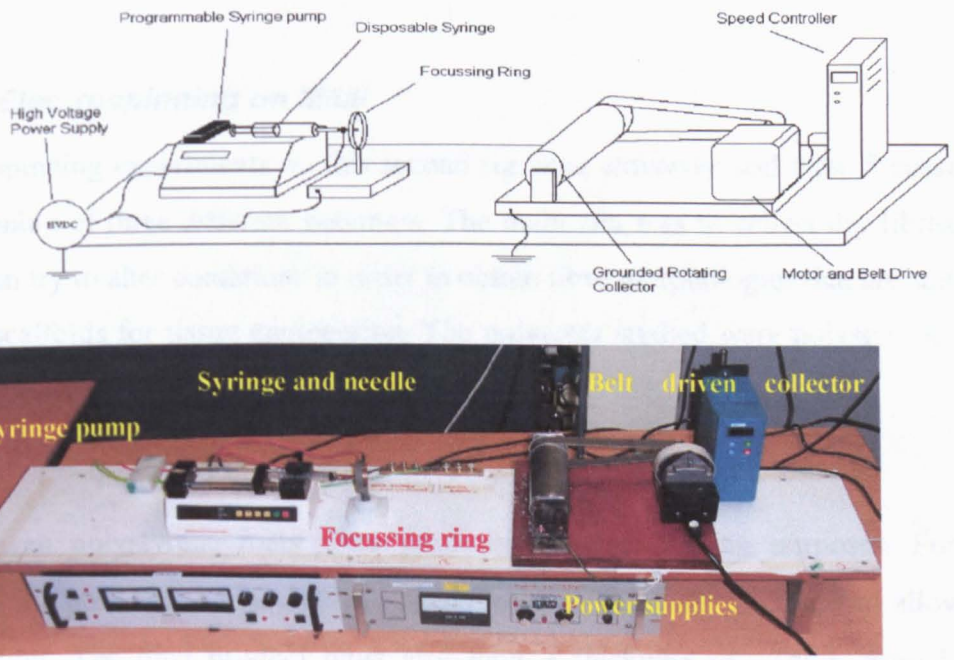

Figure 2.7 Diagram and photograph of SESM MkIII.

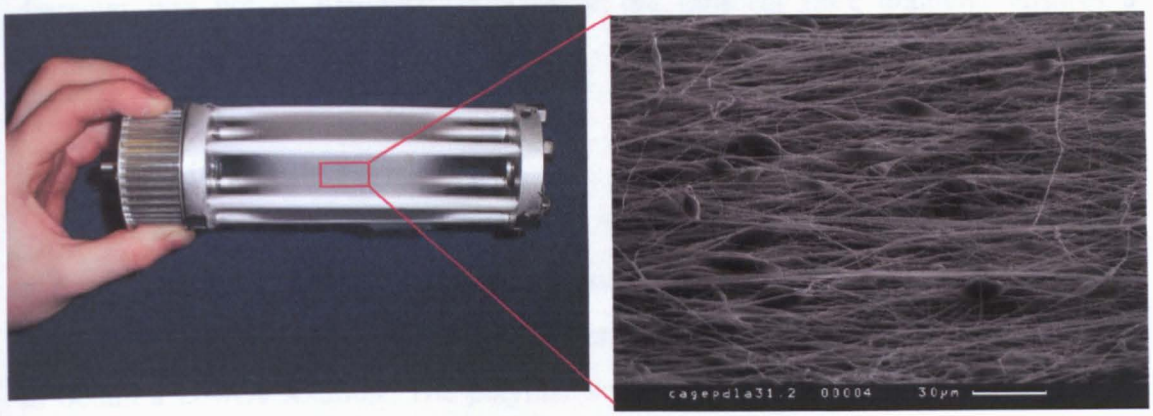

Figure 2.8 Detachable MkIII Spindle collector showing partly aligned PDLA fibres spun from 40wt% PDLA/DMF collected at 200rpm.

The drum could also be replaced with a spindle collector such as that shown in figure 2.8. Collecting on a spindle creates a less tightly packed product due to looser winding over the spindle bars than the winding which occurs around a drum. With fast enough rotation of the spindle some alignment can be induced in the way the fibres lay down rather like cotton over a spindle. (discussed at length in chapter 5)

The combined developments of MkIII enabled full control of droplet delivery to the needle tip, jet focussing on the target, product collection speed, voltage and working distance. MkIII proved a very effective rig for production of moderately thick (insulation is still a problem for collection of mats thicker than 1mm), single polymer electrospun products.

2.3.1 Electrospinning on MkIII

Electrospinning experiments on this second rig were extensive and were focussed on the spinning of three different polymers. The main aim was to collect dry fibres, and only then try to alter conditions in order to obtain fibre morphologies that are suited to use as scaffolds for tissue engineering. The polymers studied were polystyrene (PS), poly(D,L-lactide) and poly(L-lactide)

2.3.1.1 Polystyrene (PS)

Non-woven polystyrene mats were produced for cell-seeding purposes. For this purpose the pore size between fibres needs to be in the order of 30µm to allow cell penetration. The final product must also have a thickness of ~1mm. Actual fibre

diameter was not of particular importance but uniform fibre diameter ensures a uniform average pore size.

Polystyrene in Tetrahydrofuran

Sterile non-treated polystyrene(PS) microwells were ground up into a fine powder, and subsequent GPC analysis showed the average molecular weight of the PS to be 190000 kg mol^{-1} .The PS was dissolved in tetrahydrofuran (THF) under gentle stirring to obtain a 20wt% solution. The polymer solution was delivered at a constant flow rate (10-15ml/hr) via a syringe pump to a disposable 22GA blunt end needle. Upon applying a high voltage (17.5kV), a fluid jet was ejected toward the rotating (~800rpm) grounded collector at a distance of 20cm, upon which dried PS fibres were collected in the form of a non-woven fabric. This was continued until the fabric insulated the collector which occurred at ~0.8mm thickness

SEM micrographs were taken of the products to observe their structure (figure 2.9)

The fibres are in the form of collapsed tubes that have a dumbbell shaped cross section. (Figure 2.10) The mechanics of such ribbon formation occurs through the formation of thin skins upon the surface of the fluid jet. Solvent evaporates from the surface of the jet first, leaving a polymer-rich skin around a solvent-rich interior.

Over the jet path the solvent inside the tube escapes and atmospheric pressure collapses the tube into a flat ribbon structure. If the skin on the tube surface is particularly stiff, perfectly flat ribbons are not obtained, but ribbons with a 'dumbbell-shaped' cross-section. This structure is also formed as a result of electrical repulsion between the opposite sides of the tube since the jet is carrying charge. This self-repulsion hinders the formation of perfectly flat ribbons (figure 2.10). The tubes either side of the flattened section may be empty or filled.

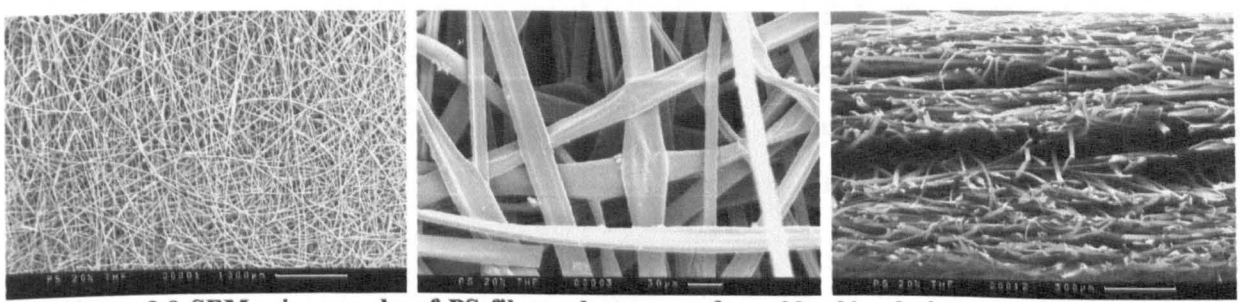

Figure 2.9 SEM micrographs of PS fibres electrospun from 20wt% solution, showing uniform fibre diameter and pore size (~30μm) and a fabric thickness of ~1mm.

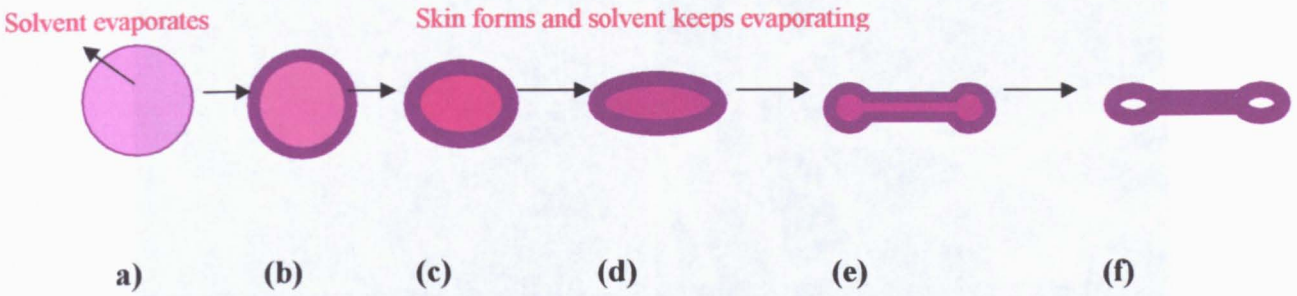

Figure 2.10 Schematic showing collapse of skin on jet. Dumbbell shaped cross-section in (e) occurs due to inflexibility of tube walls and self-repulsion of the tube sides[1].

Polystyrene in methylethylketone/dimethylformamide (1:1)

PS solutions were also prepared from a mixed solvent system of 1:1 MEK/DMF. This solvent mixture has a higher dielectric constant that THF alone, so jet formation occurred at lower voltage. The polymer solution was delivered at a constant flow rate (10-15ml/hr) via a syringe pump to a disposable 19GA blunt end needle

The boiling point of this solvent system is higher than THF so many problems were experienced with wet fibres. In order to alleviate this problem, the collector was placed further from the needle (30cm).

Table 2.2 Early observations of electrospinning of PS from DMF/MEK on SESM MKIII.

PS Concentration Wt%	Voltage (kV)	Distance(cm)	Observations
5	15	30	Jet formation, but non-fibrous product collected
10	15	30	Spluttery discharge, leaving disk of solidified polymer on collector, no mechanical stability. Few fibres.
15	15	30	Soft fabric, rather like cotton wool in texture. Some tensional strength. Fibres produced(see figure 2.11)

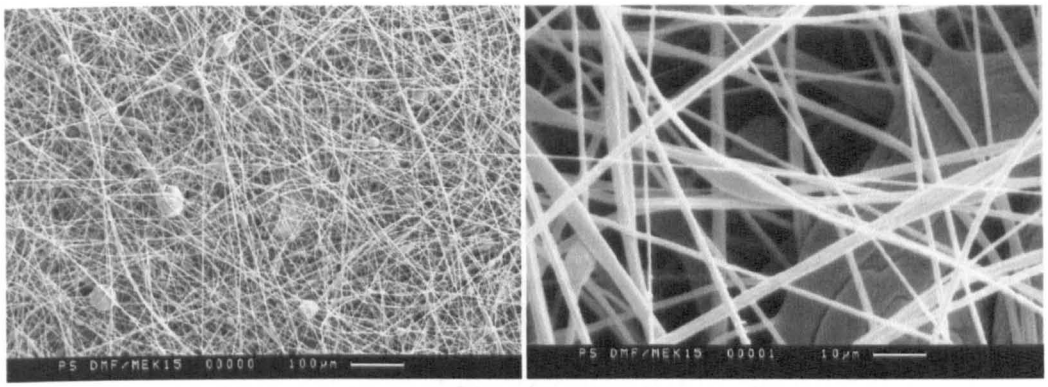

Figure 2.11 SEM micrograph of PS 15wt% in DMF/MEK (1:1) at low and high magnification.

The fibres produced with this solvent system are finer than those produced from THF solutions as the lower viscosity of the solutions enables easier deformation of the fluid jet (figure 2.11). DMF and MEK are also very polar solvents with greater ability to transfer charge to earth with the dielectric constant of DMF being 36.7 and MEK being 18.5, compared to THF which is 7.6. The application of high voltage to more polarisable solutions leads to finer jets being produced as well as greater acceleration of the jet within the electric field. The increased acceleration means finer fibres are yielded as the extension forces acting upon the elastic jet are greater. This leads to a finer jet being expelled. The boiling point of this solvent system is 147°C which is higher than THF (64.8°C) so many problems were had with wet fibres due to incomplete solvent evaporation. These fibres can also be seen to have a dumbbell ribbon structure.

Poly(D,L-lactide)/(PDLA)

PDLA (average mol.wt.75000-120000 $gmol^{-1}$) was dissolved in dimethyl formamide (DMF), under gentle heating to give solutions of 35wt% and 40wt% concentration. The polymer solution was delivered at a constant flow rate (15ml/hr) via a syringe pump to a disposable 20GA blunt end needle. Upon applying a high voltage (20-22.5kV), a fluid jet was ejected toward the rotating (~800rpm) grounded collector at a distance of 20cm, upon which PDLA fibres were collected in the form of a non-woven fabric. Insulation of the drum occurred at a fabric thickness of 0.2mm. Fibre morphology was checked by SEM (figures 2.12 and 2.13).

To check for complete dryness, a small sample of each fabric was dissolved in deuterated chloroform and analysed by NMR.

Table 2.3 Early observations of electrospinning of PDLA from DMF on SESM MKIII

Concentration (wt%)	Voltage(kV)	Observations
35	20	No droplet drying. Fibres elastic at first but become brittle after 30mins
40	22.5	No droplet drying. Fibres remain elastic after collection

NMR analysis of the fabrics showed DMF to still be present in the mat spun from 35wt% solution, and no trace of DMF in that spun from 40wt% solution (NMR data not shown.). The presence of DMF in the 35wt% mat led to the brittle nature of the fabric, highlighting the need for complete solvent evaporation especially when the product has a load or stress bearing purpose. Complete solvent evaporation is also essential if the scaffold is to be used for tissue engineering purposes as residual solvent could lead to cell death.

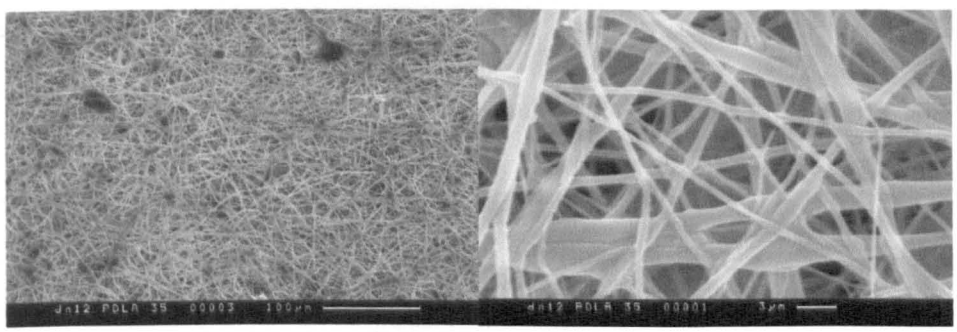

Figure 2.12 SEM micrographs of PDLA fibre from 35wt% DMF solutions, showing non-fibrous regions and non-uniform fibre diameter/pore size, characteristic of incomplete drying.

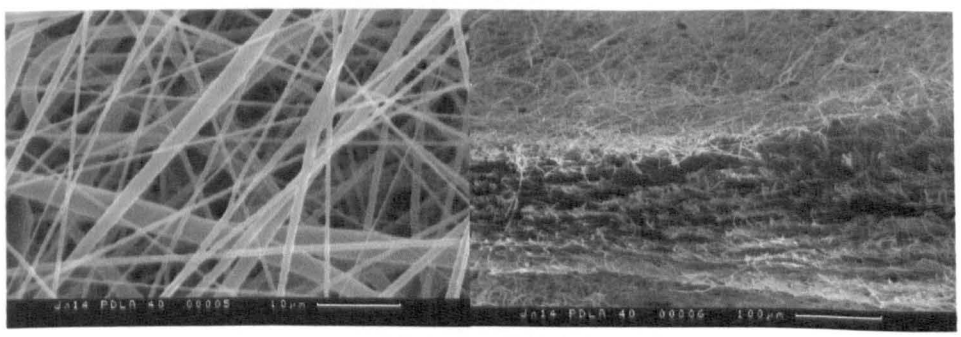

Figure 2.13 SEM micrographs of PDLA fibre spun from 40wt% DMF solutions. Uniform fibre diameter. Cross section shows 0.2mm thickness.

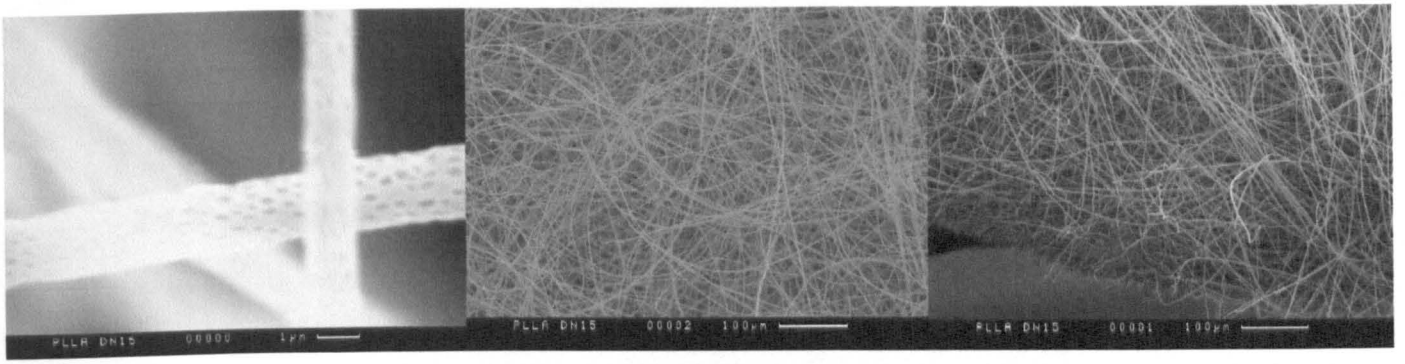

Figure 2.14 SEM micrographs of PLLA fibres electrospun from 5wt% solution in DCM, showing uniform fibre size and porous fibre morphology.

Poly(L-lactide)/ PLLA

PLLA (M_w152000 $gmol^{-1}$) was dissolved in dichloromethane (DCM), to give a solution of 5wt% concentration. The Polymer solution was delivered at a constant flow rate (15ml/hr) via a syringe pump to a disposable 20GA blunt end needle. Upon applying a high voltage (25kV), a fluid jet was ejected toward the rotating (~200rpm) grounded collector at a distance of 15cm, upon which PLLA fibres were collected in the form of a non-woven fabric. Insulation of the drum occurred at a fabric thickness of 0.2mm.

The collected fabric was subject to SEM in order to determine fibre morphology (figure 2.14).

PLLA is more crystalline than PDLA and the fibres produced were more brittle and gave a "fluffier" product as the more rigid fibres will not pack as closely together as less crystalline ones. The porous surface morphology is difficult to explain but is explored in more detail in chapter 4.

2.4 MkIII modifications

2.4.1 Dual Spinning

A modified version of SESM MKIII couples two electrospinning rigs together in order to enable co-spinning of 2 different polymers.

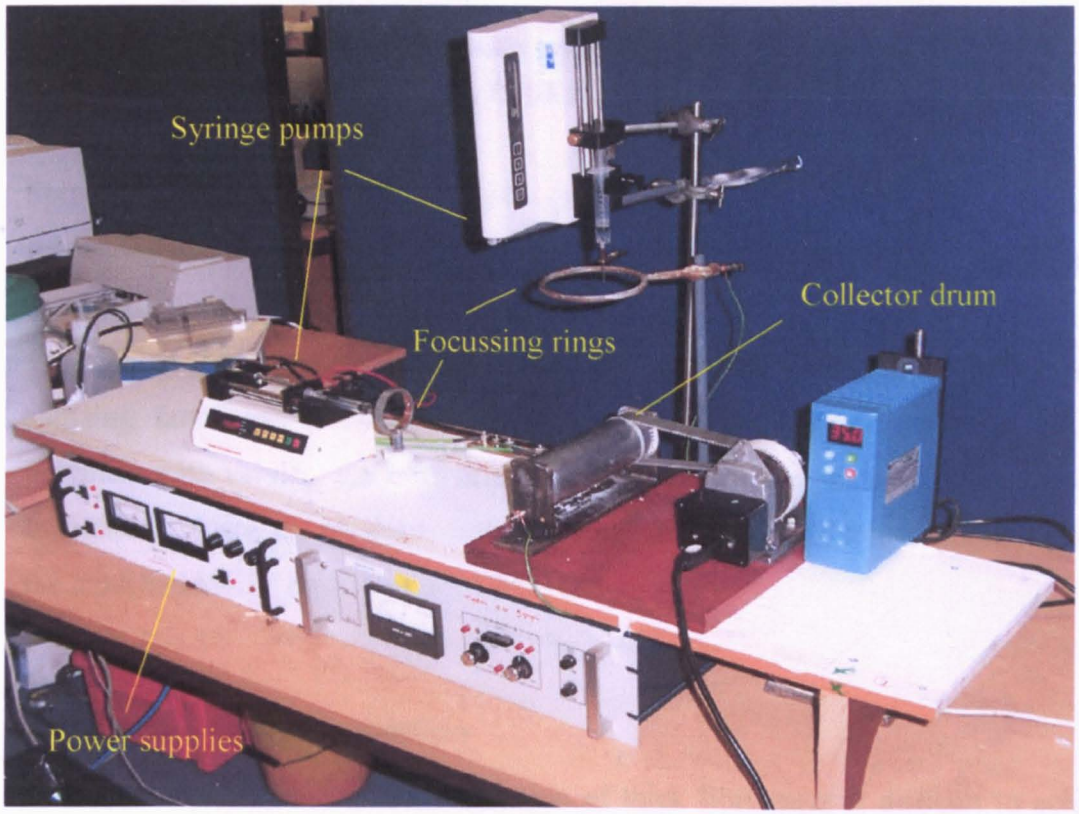

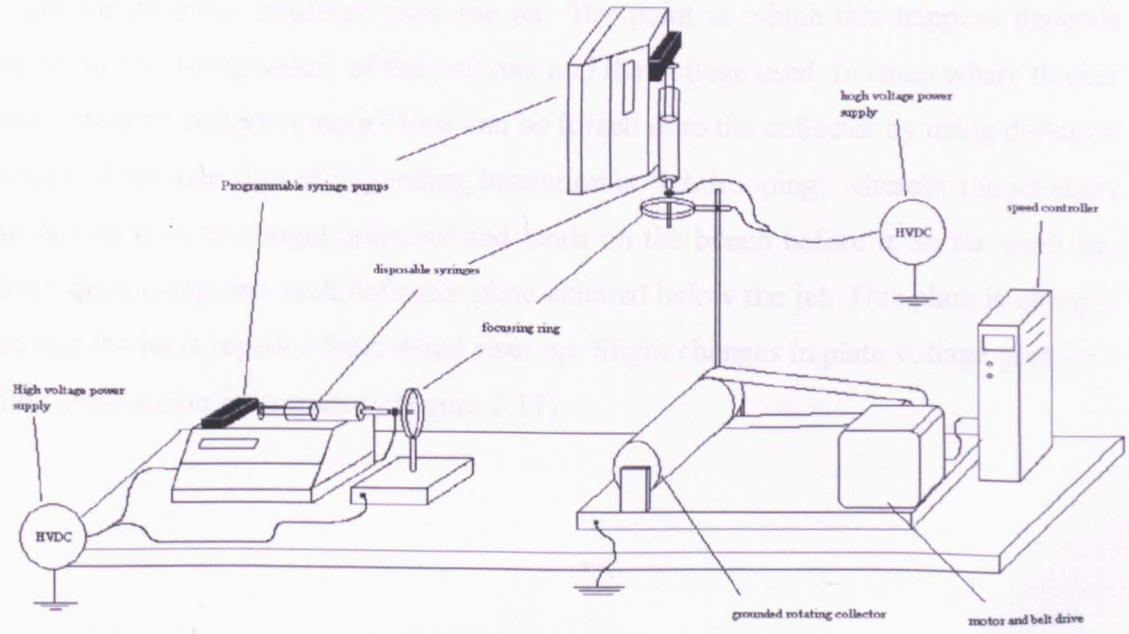

Figure 2.15 the modified MKIII rig for co-spinning.

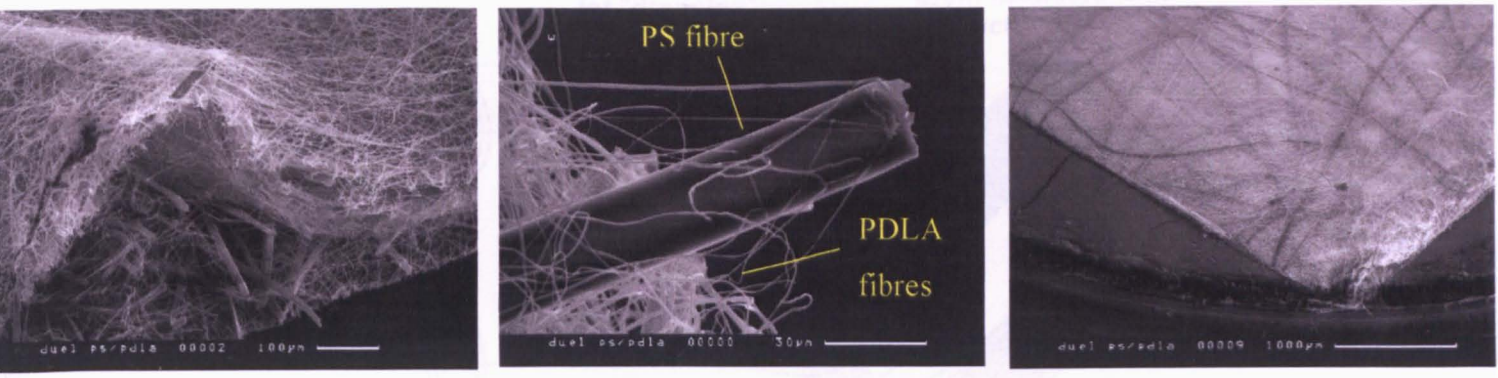

Figure 2.16 Composites of PS/PDLA spun on modified MkIII rig PS spun from 20wt% PS in THF at 20cm, PDLA spun from 40wt% PDLA in DMF at 25cm.

Spinning one polymer conventionally (horizontally) and one vertically ensures no repulsion between the two jets, and when targeted on the same collector a composite material of the two polymers is obtained. (figure 2.15)

Spinning of polymers with different characteristics opens up possibilities of spinning functional composites with increased tensile strength or blending bulk polymers with varying amounts of activated polymer for more specialised purposes. In figure 2.16 are shown some SEM micrographs of PS/PDLA composites spun on the modified MKIII rig.

2.4.2 Overcoming Insulation

As previously discussed the collection of thick fibre mats is difficult to achieve. Once a certain thickness of polymer is deposited upon the collector the earthed collector becomes insulated from the jet. The point at which this happens depends upon the insulating ability of the polymer and the voltage used. In cases where thicker mats must be collected more fibres can be forced onto the collector by using deflector plates. A tell-tale sign of impending insulation is "jet drooping" whereby the jet starts to fall short of the target collector and lands on the bench before it So far work has been done using one such deflector plate situated below the jet. This plate is charged so that the jet is repelled from it and rises up. Slight changes in plate voltage give very fine control over jet trajectory (figure 2.17).

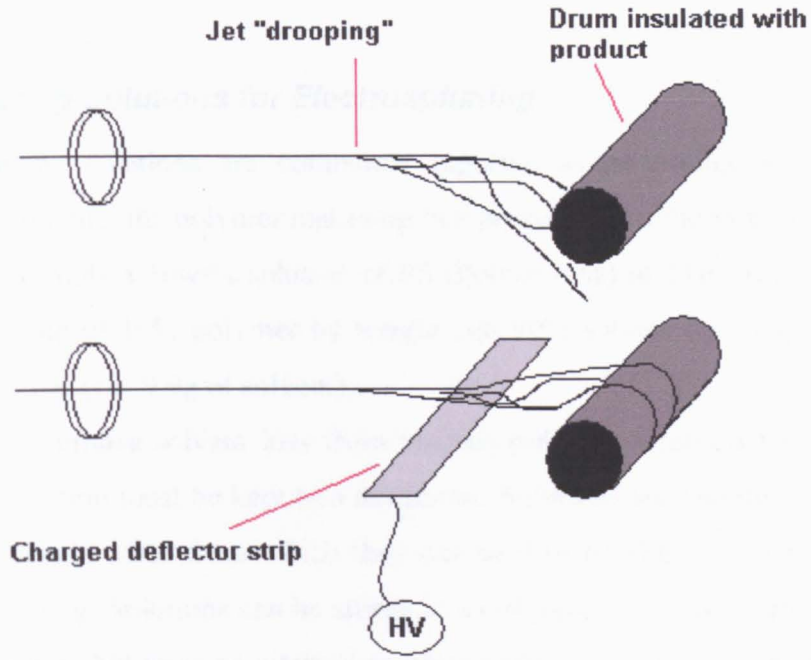

Figure 2.17 showing the effect of a deflector plate below the jet.

Using even one strip proves very useful in the collection of thicker materials. Once the drum becomes insulated the jet begins to "droop" and fibres no longer collect on the drum. The inclusion of the charged plate redirects the fibres back onto the drum enabling more product to be collected. There comes a point however, when the added complications of deflector plates outweigh the improvements in material thickness. With more and more product collecting on the drum it becomes increasingly difficult to force/deflect more fibres to be collected. When dealing with non-wovens it seems illogical to expend too much energy in making thick materials as layering thinner ones will yield a topographically identical product.

2.5 *Further developments*

The SESM is in a constant state of flux, with both major and minor modifications being undertaken as the particular circumstances dictate. Most of the electrospinning performed in Sheffield takes place on a MkIII rig. However, this rig is limited to the production of randomly oriented, non-woven products. In essence such products can be viewed as traditional electrospun products, but more advanced products need more advanced machines. In Chapters 4 and 5 two different SESMs are introduced which are capable of producing both aligned and porous fibres.

It is felt that coverage of these two machines warrants a chapter each as the technology is more complex and the results more extensive.

2.6 Preparing Solutions for Electrospinning

Electrospinning solutions are commonly reported as percentage weight (wt%) solutions meaning that the polymer makes up that percentage of the total weight of the solution. For example a 10wt% solution of PS (Polystyrene) in THF (tetrahydofuran) would be made up of 10% polymer by weight and 90% solvent by weight (i.e. 0.1g PS in a total of 10g (i.e. 9.9g of solvent)).

In order to minimise solvent loss from viscous polymer solutions the amount of transferral of solution must be kept to a minimum. Solutions are therefore formulated in screw-top sample tubes from which they can be directly drawn into a disposable syringe for spinning. Solutions can be stored in a refrigerator to reduce any chance of solvent evaporation but must be warmed to room temperature prior to spinning as the viscosities of polymer solutions are very responsive to changes in temperature (see 1.6.7).

2.7 Preparing Electrospun Samples for Scanning Electron Microscopy (SEM)

The major analysis tool for electrospun fibres is microscopy and in particular Scanning Electron Microscopy(SEM). This particular form of microscopy allows resolution of samples down <20nm.

The Scanning Electron Microscope (SEM) is a microscope that uses electrons rather than light to form an image. There are many advantages to using the SEM instead of a light microscope.

The SEM has a large depth of field, which allows a large amount of the sample to be in focus at one time. The SEM also produces images of high resolution, which means that closely spaced features can be examined at a high magnification. Preparation of the samples is relatively easy since most SEMs only require the sample to be conductive. The combination of higher magnification, larger depth of focus, greater resolution, and ease of sample observation makes the SEM one of the most heavily used instruments in research areas today.

In order to make the sample conductive it is attached to an aluminium stub and placed in a sputter coater (figure 2.18). The sputter coater works under an argon atmosphere to deposit a thin layer of gold on the surface of the sample thus rendering it conductive[2].

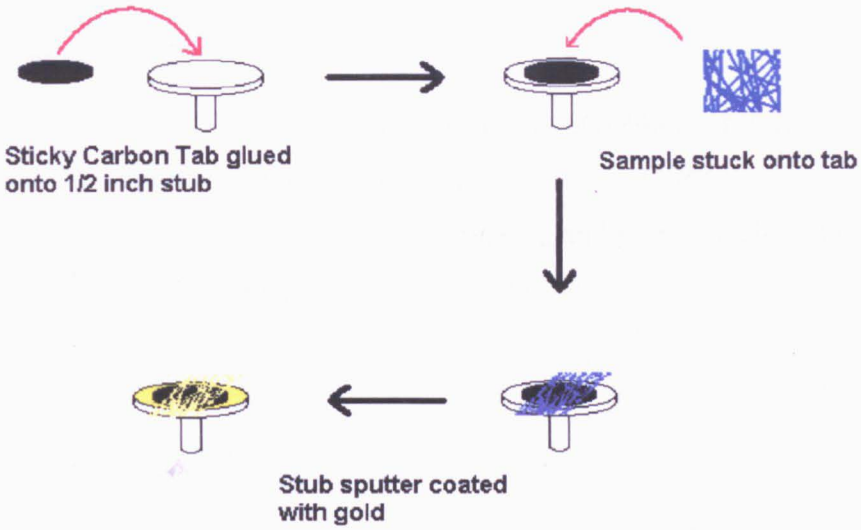

Figure 2.18 Sample mounting for SEM of electrospun fibres.

The conductive stub is then placed into the sample chamber of the SEM and held under vacuum. A schematic of the SEM is shown in figure 2.19. A beam of electrons is produced at the top of the microscope by heating of a metallic filament. The electron beam follows a vertical path through the column of the microscope. It makes its way through electromagnetic lenses which focus and direct the beam down towards the sample. Once it hits the sample, other electrons (backscattered and secondary) are ejected from the sample. Detectors collect these electrons, and convert them to a signal that is sent to a viewing screen producing an image.

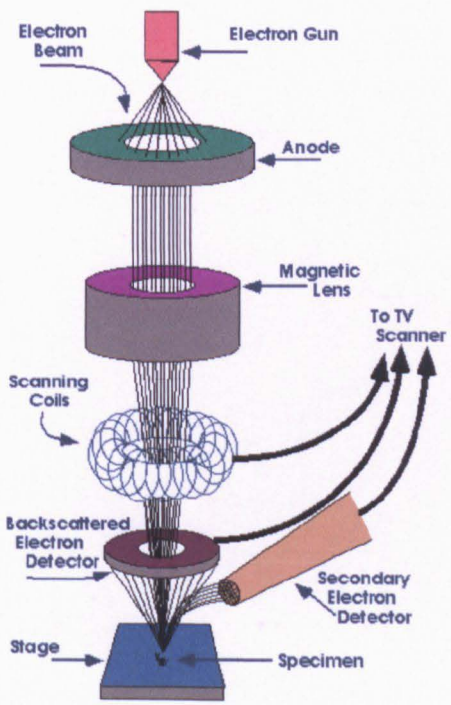

Figure 2.19 Schematic of the Scanning Electron Microscope(SEM).

2.8 References

1. Reneker, D. H. & Chun, I. Nanometre diameter fibres of polymer, produced by electrospinning. *Nanotechnology* 7, 216-223 (1996).
2. Chescoe, D. The operation of transmission and scanning electron microscopes. *Oxford : Oxford University Press, 1990* (1990).

3.1 Introduction

The skin is often referred to as the largest organ in the human body. This applies to exterior surface, as it covers the body, appearing to have the largest surface area of all the organs. Moreover, it applies to weight, as it weighs more than any single internal organ, accounting for about 15 percent of body weight. For the average adult human, the skin has a surface area of between 1.5-2.0 square meters most of it being 2-3 mm thick. The average square inch of skin holds 650 sweat glands, 20 blood vessels, and more than a thousand nerve endings[1,2]. As the interface with the surroundings, it plays the most important role in protecting against pathogens, and when it is damaged the body becomes extremely vulnerable. Minor damage to the skin is quickly repaired by the body but more extensive damage such as that inflicted by a severe burn is often beyond natural repair. Partial thickness and full thickness burns refer to the extent of damage to the skin the latter resulting in damage to all the skin layers down to the subcutaneous tissue(figure 3.1) In such cases there is often a need for a synthetic substitute for the damaged skin. The structure of skin and the effect of a full thickness burn are shown in figure 3.1.

Modern tissue engineering has long been focused on the need to construct a synthetic product to speed recovery of extensively damaged skin. There are currently a number of commercially available skin tissue engineered products with each one taking a slightly different approach to wound healing. The basic approach of the available products is to create a scaffold upon which skin cells are seeded and can proliferate. The cells should be able to proliferate within this matrix and the "live" matrix surgically attached over the wound acting as a temporary barrier to infection

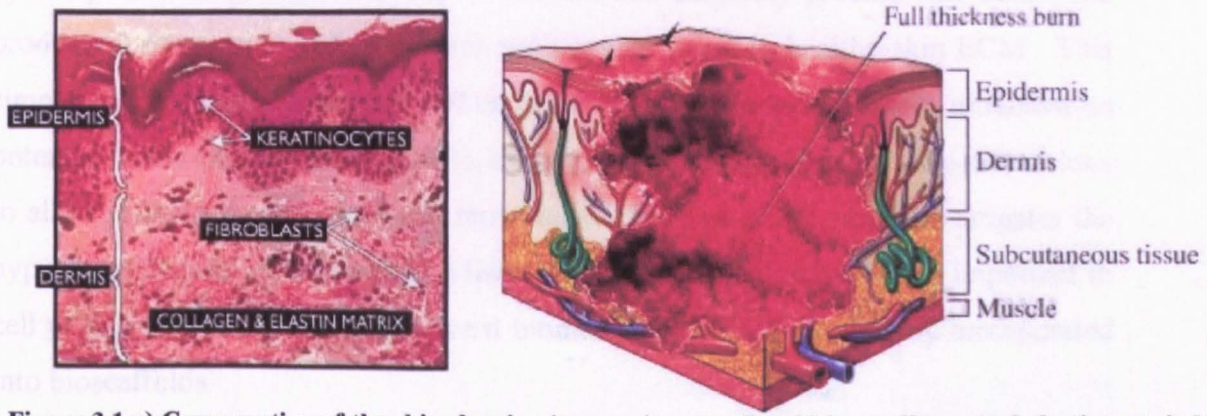

Figure 3.1 a) Cross-section of the skin showing its constituent cells within a collagen and elastin matrix b) cartoon showing extent of damage of a full thickness burn [1]

As the cells proliferate and take hold in the matrix they should start to combine with and become accepted by the wound bed actively re-populating it with skin tissue. Most available products use synthetic scaffolds which often contain animal sourced collagen (Biobrane, Transcyte, Apligraft and Integra) upon which non-donor (neonatal) skin cells are usually seeded. Some are wholly sythetic scaffolds (Dermagraft) which again must be seeded with neonatal fibroblasts. Often these scaffold are biodegradeable and will start to be resorbed by the body once the scaffold takes hold . Another approach is to use acellular cadaver dermis upon which host cells can be seeded. However, as with many of these products, the success of cell repopulation requires the use of bovine calf serum to provide the scaffolds with enough nutrients and growth factors.

Much research in tissue engineering focuses on synthesis of complex 3-Dimensional polymer scaffolds containing functional biomolecules to which cells are introduced. Typical scaffolds are macroscopically porous in order to permit cellular entry into the matrix and essentially mimic the extra cellular matrix (ECM) of collagen and elastin found in skin tissue.

The loose fashion in which electrospun fibres are laid upon one another produces a naturally porous non-woven structure with an inter-fibre pore size unique to the spinning conditions. Such scaffolds are not an ECM mimic as their structure bears little topological resemblance to ECM and they are devoid of any molecular cues. The collagen fibres in skin ECM are commonly oriented to some degree as opposed to the random orientation found in non-woven electrospun products. These scaffolds should however, provide an environment through which cells are free to propagate and self assemble. By spinning a biodegradable scaffold it is expected that as the cells proliferate, the scaffold will be resorbed by the body and replaced by ECM produced by the proliferating cells. It is hoped that this self-assembly process will enable the production of oriented collagen fibres such as that found in healthy skin ECM. This simple self assembly approach makes electrospun products extremely attractive as potential tissue engineering scaffolds, as long as the scaffold is of suitable dimensions to allow relatively unhindered cell movement. This part of the study investigates the hypothesis that the dimensions of a tissue engineering scaffold are more important to cell proliferation than the conventional biomolecular cues so commonly incorporated into bioscaffolds.

In order for cells to migrate through a scaffold the inter-fibre pore size must be in the region of 50μm[3-6]which necessitated the production of thick fibres as increasing the fibre diameter decreases the packing density in the matrix[7,8]Growth of cells on unmodified electrospun scaffolds has been widely reported[3,4,9-11]but their 3-Dimensional proliferation and organisation has never been studied.

It was of primary importance to see whether or not cells could proliferate in unmodified fibrous matrices. Polystyrene (PS) was chosen as it is a non-biological material with no cell signalling or spatial information, for which cells generally show no preference. In effect PS acted as a negative control.

This control material was seeded three types of human skin cell; fibroblasts, keratinocytes and endothelial cells. A fibroblast is a cell that makes the structural fibres and ground substance of connective tissue helping to bind the skin cells together. Keratinocytes are the major cell type of the epidermis, making up about 90% of epidermal cells and endothelial cells are responsible for the lining of blood vessels within the skin. These three cell types make up the cellular portion of human skin which are held in a porous collagen and elastin matrix (figure 3.1). These cells were cultured in a number of ways. Firstly they were cultured separately from one another and then co-cultured, whereby the different cell types were grown together on the scaffold. In addition to this, half of the experiments were performed in the presence of a serum(containing growth factors and proteins derived from foetal calves and used in most cell culturing experiments), and half were grown in a serum-free environment. It was anticipated that the co-culturing of different cell types would lead to a symbiosis between them and dispense with the need for serum which carries with it a risk of disease transmission (such as Bovine Spongiform Encephalopathy (BSE) which can give rise to Creutzfeldt-Jakob Disease (CJD)) if the tissue engineered construct is subsequently implanted in humans. Co-culturing would hopefully give rise to the cells producing their own spatial cues. Coupled with the unhindered movement of cells throughout a sufficiently porous scaffold this would preferably lead to the different cell types self-organising and thus mimicking their natural order in human skin (figure 3.1).

There are two main mechanisms of cell adhesion on artificial scaffold materials in tissue engineered products: Direct non-receptor mediated cell-material binding and receptor-mediated binding through ECM molecules or their minimal adhesion sequences.

Non-receptor mediated cell adhesion is based on non-specific cell-material interactions via weak chemical bonding; such as hydrogen bonding, electrostatic, polar or ionic interactions between molecules present in the cell surface, and functional chemical groups of the polymers that conform the scaffold[12,13]. Although these types of interactions constitute the first step in the adhesion event of the cells to the tissue engineered scaffold, they do not provide an adequate transmission of signals from the extracellular environment into the cell. If the cells are not able to find or produce ECM molecules in a relatively short period of time (from 24 to 48 hours after seeding) they unavoidably will undergo apoptosis[14-16].

To enable a more functional receptor-mediated cell adhesion onto a tissue engineered scaffold the presence of ECM molecules (i.e. fibronectin, collagen, laminin or vitronectin) is needed within the scaffold (synthetic) or produced by the cells. Although there are many types of cell surface adhesion receptors, cell-ECM adhesion is primarily mediated by members of the integrin family. It is hoped in this study that the cells will indeed produce their own ECM molecules to enable cell adhesion to the unmodified polymer scaffold.

Integrins are transmembrane heterodimeric glycoproteins composed of α and β subunits. Thus far, 17 α and 8 β subunits have been identified, and there are at least 22 functional heterodimers in mammalian cells. Multiple combinations of alpha beta subunits result in a vast number of receptors with differential affinity to certain ECM molecules[16,17]. Different integrin type receptors in the cell recognise specific amino acid sequences within multiple ECM molecules. For example, Arg-Gly-Asp (RGD) sequence of fibronectin is recognised by α2β1 integrin, but the same sequence in vitronectin is recognised by αvβ3 receptor[16-19]. Once ligand binding is achieved by cellular integrin receptors, these last ones are recruited into microdomains in the cellular membrane called "focal adhesion sites". In these regions, integrins interact with structural molecules of the cytoskeleton as well as with signalling molecules; thus influencing intracellular responses important for cell behaviour and ultimately the decision between cell proliferation and differentiation or apoptosis[19-21].

The proliferation of the cells throughout the electrospun scaffolds was monitored as was the 3-Dimentional histology of the synthetic tissue. It was found that electrospun PS fabrics with a pore size in the region of 50μm could support the

proliferation and of skin cells in accordance with previously reported work[3-6]. Also co-culturing of the cells at an air-water interface led to a degree of self-organisation within the scaffold.

Polystyrene is not a commonly used tissue engineering material. Such materials are generally biocompatible, and more commonly biodegradable and easily reabsorbed by the body. PS was always therefore, a precursor material which would give a valuable insight into cell behaviour in electrospun scaffolds but never be taken into the clinic. Reconstructed cell/ PS fibre scaffolds could however provide a valuable material for *in vitro* screening of skin tissue.

Poly(l-lactide) (PLLA) is biodegradable polymer which has been widely used in tissue engineering applications[10,22-25]and been accepted into clinical use. Consequently PLLA was chosen as a target material for electrospun scaffolds in skin reconstruction. Information gleaned from the PS experiments indicated that signalling information was not necessary for cell proliferation and organisation within electrospun scaffolds. The overriding factor in a scaffold's ability to support such growth is its morphology. PLLA scaffolds were therefore produced with pore sizes comparable to those found in the PS scaffolds. This necessitated many iterations of the electrospinning procedure (section 3.4.1).

The majority of the work covered in this chapter has been published in *Tissue Engineering.*[1]

This work has been a collaboration between myself and Sun Tao of the Engineering Materials department of the University of Sheffield. All electrospinning was carried out by myself and the scaffolds delivered to Sun Tao ready for cell culture. Many iterations of scaffold were produced in order to find the ideal scaffolds to work with. 2-Dimensional and 3-Dimensional cell culture was carried out by Sun-Tao with significant practical and conceptual input from myself including cutting and preparation of the scaffolds prior to seeding. All cell staining and histology work was carried out by Sun Tao.

3.2 Experimental - Growing Skin on Polystyrene

3.2.1 Electrospinning Processing

Sterile non-treated polystyrene (PS) microwells were ground into a fine powder, and subsequent GPC analysis showed the weight average molecular weight of the PS to be 190 000 $gmol^{-1}$. The PS was dissolved in tetrahydrofuran (THF) under gentle stirring to obtain a 20wt% solution. The polymer solution was delivered at a constant flow rate (10-15ml/hr) via a syringe pump to a disposable 22GA blunt end needle. Upon applying a high voltage (17.5kV), a fluid jet was ejected toward a rotating(~800rpm) grounded collector at a distance of 20cm, upon which dried PS fibres were collected in the form of a non-woven fabric. This was continued until the fabric insulated the collector which occurred at ~0.8mm thickness. The spinning took place on a MKIII electrospinning apparatus (section 2.3)

3.2.2 Cell Culture

Normal human keratinocytes and fibroblasts were isolated and cultured following the method of Goberdhan et al[26] and Ralston et al[27].. The microvascular endothelial cell line (HuDMEC) was grown according to methods described by Sahota et al[28]. Cell culture areas were $1cm^2$ and volume of the cell suspension $0.3cm^3$.This was performed by Sun Tao in the Department of Engineering Materials with help from myself.

3.2.3 Skin composite preparation

Reconstructed skin containing fibroblasts, endothelial cells and keratinocytes was prepared using a slight modification of the method described by Chackrabarty et al[29]. For the 3-D experiments on electrospun scaffolds, stainless steel rings of $1cm^2$ internal diameter were applied to one side of a 1.8 cm^2 section of electrospun polystyrene scaffold. Cells in single or co-culture populations were introduced in 0.5 ml culture medium to the upper surface and kept submerged for 18 hours, after which they were raised to an air-liquid interface and cultured for 14 days in the presence or absence of serum. Medium was replenished three times per week. For 2-Dimensional experiments cells were cultured for 14 days in tissue culture wells, the surface of which was coated by a thin PS film. This film was produced through evaporation of a solution of PS in Tetrahydrofuran in the well[30].

3.2.4 *Preparing Sections from Scaffolds for Microscopy*

Cell containing scaffolds were washed with saline solution and embedded in epoxy resin. 50 μm sections were cut from the resin block and sections ground to 5 μm (see section 4.3 for analogous procedure).

Assessment of cell viability was achieved by using MTT and Hoechst 33342 / propidium iodide stains (see glossary). Full experimental details have been published[30].

3.2.5 *Immunofluorescence microscopy*

Immunofluorescence is the labeling of antibodies or antigens with fluorescent dyes. Immunofluorescently labelled tissue sections are commonly studied using a fluorescence microscope or by confocal microscopy.

Most commonly immunofluorescence employs two sets of antibodies; a primary antibody is used against the antigen of interest. Subsequently a secondary, dye-coupled antibody that recognizes the primary antibody is used.Primary antibodies are usually created to be specific to antigens found one one cell type.

Monolayer cultures were fixed in formaldehyde (which prevents further metabolic activity in the sample), permeabilised (where the membrane is made permeable to allow antibodies into the cell for the purposes of immunostaining) and cut ready for viewing under the microscope[30]. Keratinocyte cells were identified by labeling for pancytokeratin and involucrin antigens. Endothelial cells were identified by labeling for von Willebrand's factor (vWF) and DAPI was used to label total cell nuclei. Appropriate secondary dye-coupled antibodies were used to create a sufficient response for immunofluescence microscopy[30].

3.3 Results and Discussion

3.3.1 2-Dimensional Cell Culture

Prior to introducing cells to the 3-dimensional electrospun scaffold a number of experiments were performed on PS thin films. By culturing combinations of fibroblasts, keratinocytes and endothelial cells on this 2-D substrate (both with and without serum present) the optimum ratio of each cell type could be determined. The same ratio would then be used on the 3-D scaffold. The total metabolic activity of the cells was measured using MTT and the total cell number calculated using Hoechst 33342/propidium iodide (PI). (see glossary)

Normal human fibroblasts (5.0×10^5), keratinocytes (5.0×10^5), and a combination of fibroblast (2.5×10^5) and keratinocytes (2.5×10^5) were cultured initially for 7 and 14 days on a 2D polystyrene film made by evaporation of a PS solution from Tetrahydrofuran (THF). Fibroblast and keratinocyte cells formed separate colonies when co-cultured in Greens medium either with or without serum proteins (Figure 3.2a and b) (but did not survive when cultured separately in the absence of serum). The cells were just as prolific in serum free co-culture (Figure 3.2e) as in serum containing co-culture (Figure 3.2g) indicating a high degree of cooperation and mutual support between these cells. This was confirmed by assessing cell number and viability (Figure 3.2f and h). Fibroblast viability at day 7 in serum culture was higher than at day 14 (Figure 3.2g and h). Keratinocyte viability in serum culture was 60-70% between day 7 to 14, but had a combined viability of 80% when co-cultured with fibroblasts (Figure 3.2g and h).Single culture and co-culture of normal human fibroblasts and endothelial cells ($5x10^5$) was similarly investigated at 7 and 14 days (Figure 3.2c and d). Viability measurements by MTT showed that endothelial cells did not perform well in serum-free conditions, either alone or with fibroblast cells (Figure 3.2i). However, significantly higher endothelial cell viability was demonstrated in co-culture compared to fibroblast single culture (Figure 3.2j). The co-culture of fibroblast and endothelial cells in Greens medium demonstrated higher viability in the presence of serum with viability of over 90% for co-cultures of fibroblasts and endothelial cells (Figure 3.2k and l). In conclusion it was found that on a 2-D substrate even in the absence of serum, keratinocytes and endothelial cells could thrive as long as they were co-cultured with fibroblasts, eliminating the need for bovine serum and its associated risk of disease transferral. Fibroblasts have the ability

to secrete growth factors upon which the other cell types can live. Endothelial cells however performed less well without serum however, even when co-cultured with fibroblasts.

3.3.2 Cell Culture in 3-Dimensions

To investigate cell culture in 3-Dimensions, normal human fibroblasts, keratinocytes and endothelial cells or combinations of cells (in the ratios optimised in the 2-D experiments) were introduced to the upper surfaces of electrospun polystyrene scaffolds (Figure 3.4i). The total cell number for each culture was $5.0x10^5$, except in the case of the three cell-type co-culture where $2.5x10^5$ of each cell type was seeded. The cells were cultured for 7 and 14 days in Greens medium (both with and without serum protein)(Figure 3.3a). The MTT viability of single cultures under serum free conditions were significantly lower than for serum containing cultures (Figure 3.3b-e), in agreement with the 2-D data. However, the viability of fibroblasts and keratinocytes in co-culture (with or without serum) was also high, indicating the advantage of co-culture (Figure 3.3b-c). Viability of fibroblasts did not drop after 14 days in 3D as in 2D. In 2D the fibroblasts become confluent in the culture well by 14 days and have nowhere else to go so cannot proliferate further. In 3-D scaffolds the cells do not become confluent within the matrix and can therefore proliferate over a longer time period.

MTT viability, (which is a quantitative indication of how healthy the culture is) for fibroblasts and endothelial cells in co-culture under serum-free conditions was lower than that in serum, but was significantly higher than the culture of fibroblasts or endothelial cells alone (Figure 3.3d-e).In 2-D culture there was seen to be no symbiosis between endothelial cells and fibroblasts so this increased viability is a function of the scaffold's morphology. The viability of fibroblast, keratinocyte and endothelial cell three-cell co-culture without serum was equivalent to that with serum in accordance with the 2-D data(Figure 3.3b-c). Theses serum-free conditions underpin their success with the presence of fibroblasts and their ability to secrete growth factors into the system.

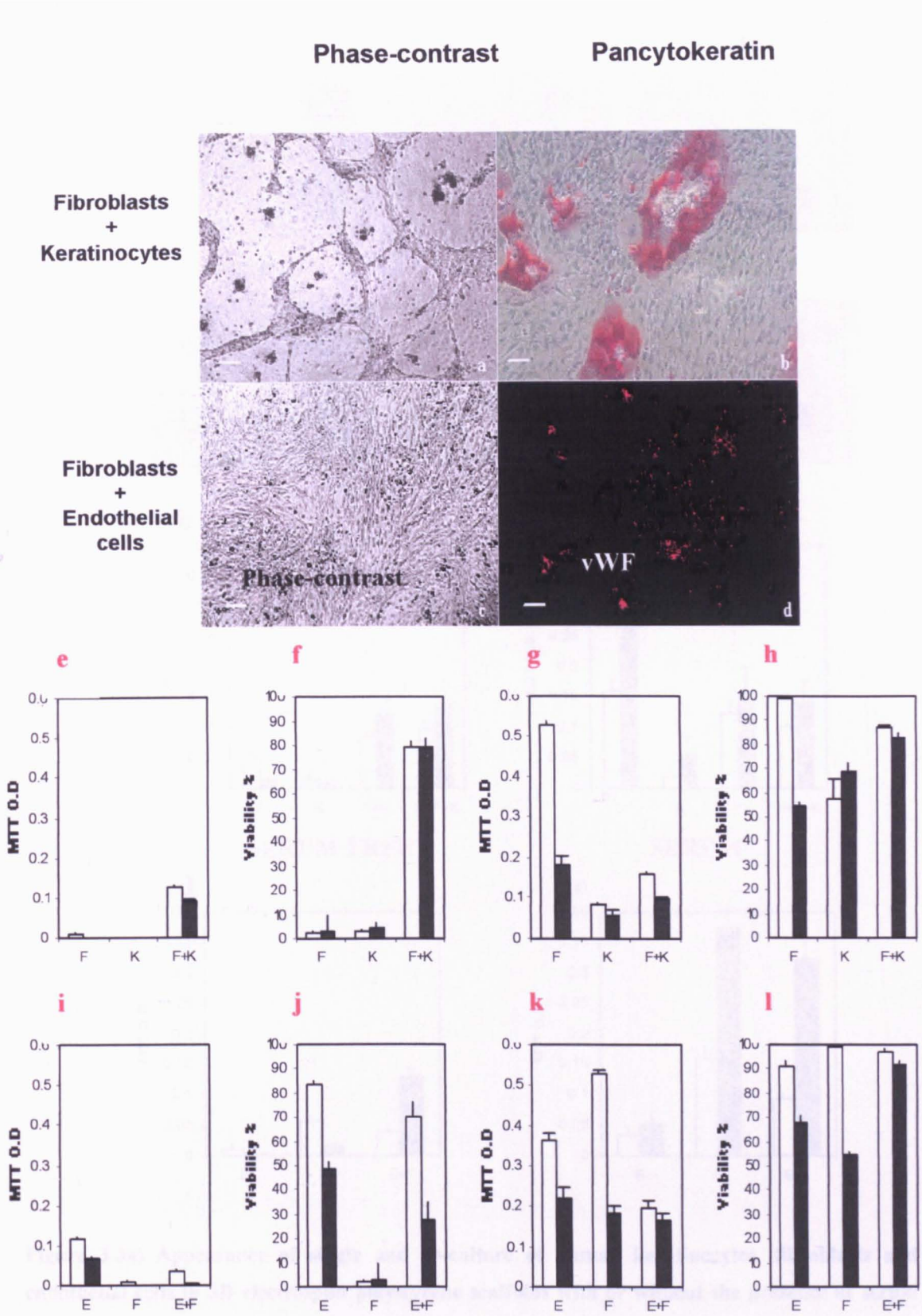

Figure 3.2a) Visual appearance of keratinocytes and fibroblasts in co-culture; b) and after pan-cytokeratin immunostaining to identify keratinocytes. c) Appearance of endothelial cells and fibroblasts in co-culture; d) and following vWF immunostaining for endothelial cells. Total cellular viability of single and co-cultures of human keratinocytes and fibroblasts under serum free conditions e), MTT; f), Hoechst 33342/PI) and serum containing conditions (g), MTT; h), Hoechst 33342/PI). Viabilities of single and co-cultures of human endothelial cells and fibroblasts in serum free conditions (i), MTT; j), Hoechst 33342/PI) and serum containing conditions (k), MTT; l), Hoechst 33342/PI). Time points are: 7 days (□) and 14 days (■) in culture. Results shown are mean ± SD (n=3). Bar = 100μm.

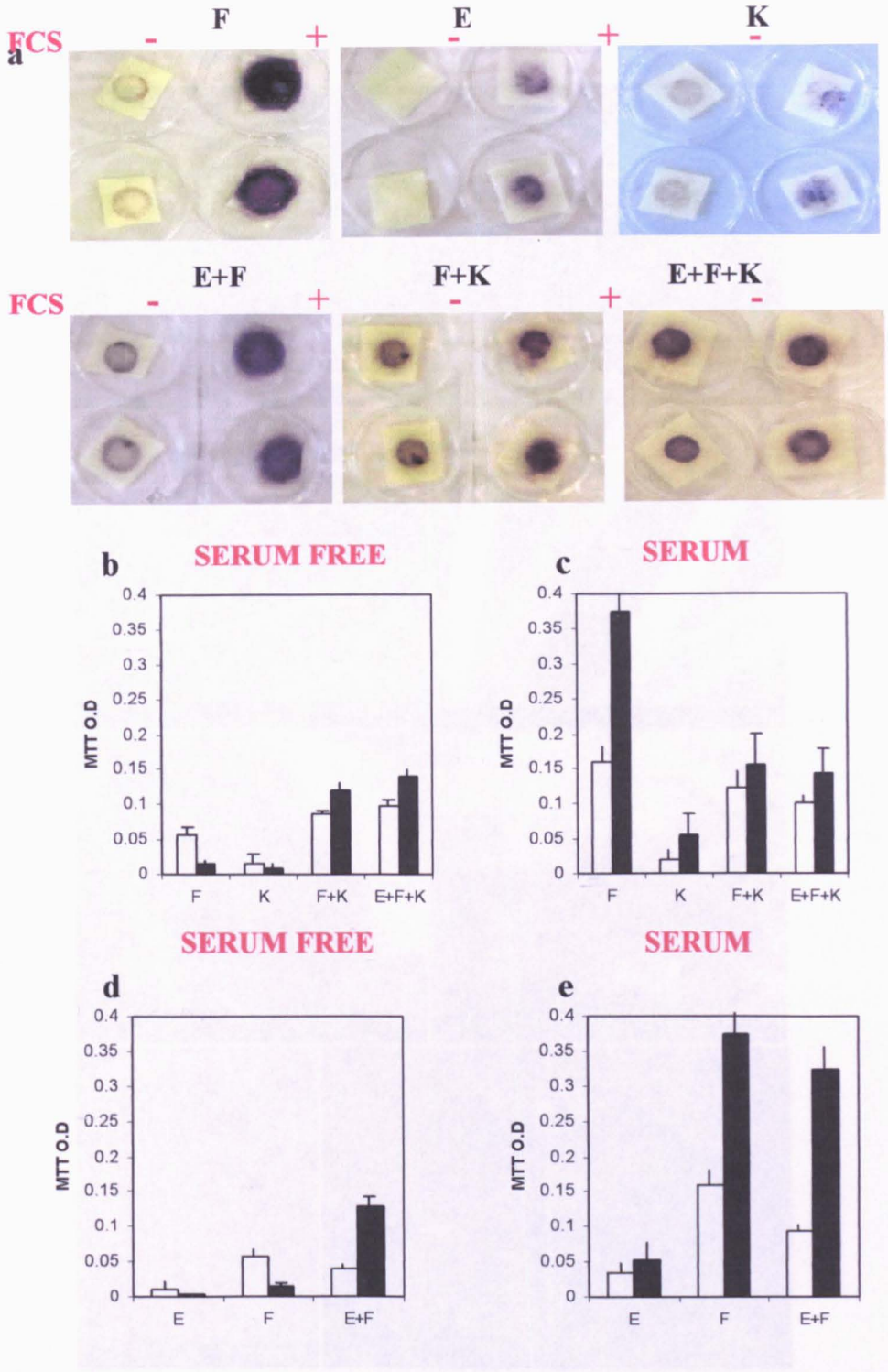

Figure 3.3a) Appearance of single and co-culture of human keratinocytes, fibroblasts and endothelial cells in 3D electrospun polystyrene scaffolds with or without the presence of serum protein after staining with MTT. Viabilities of single and co-cultures of human keratinocytes, endothelial cells and fibroblasts in 3D electrospun polystyrene scaffolds in serum free conditions (b and d) and serum containing conditions (c and e). Time points are: 7 days (□) and 14 days (■) in culture. Results shown are mean ± SD (n=4). E, endothelial cells; F, fibroblasts and K, keratinocytes.

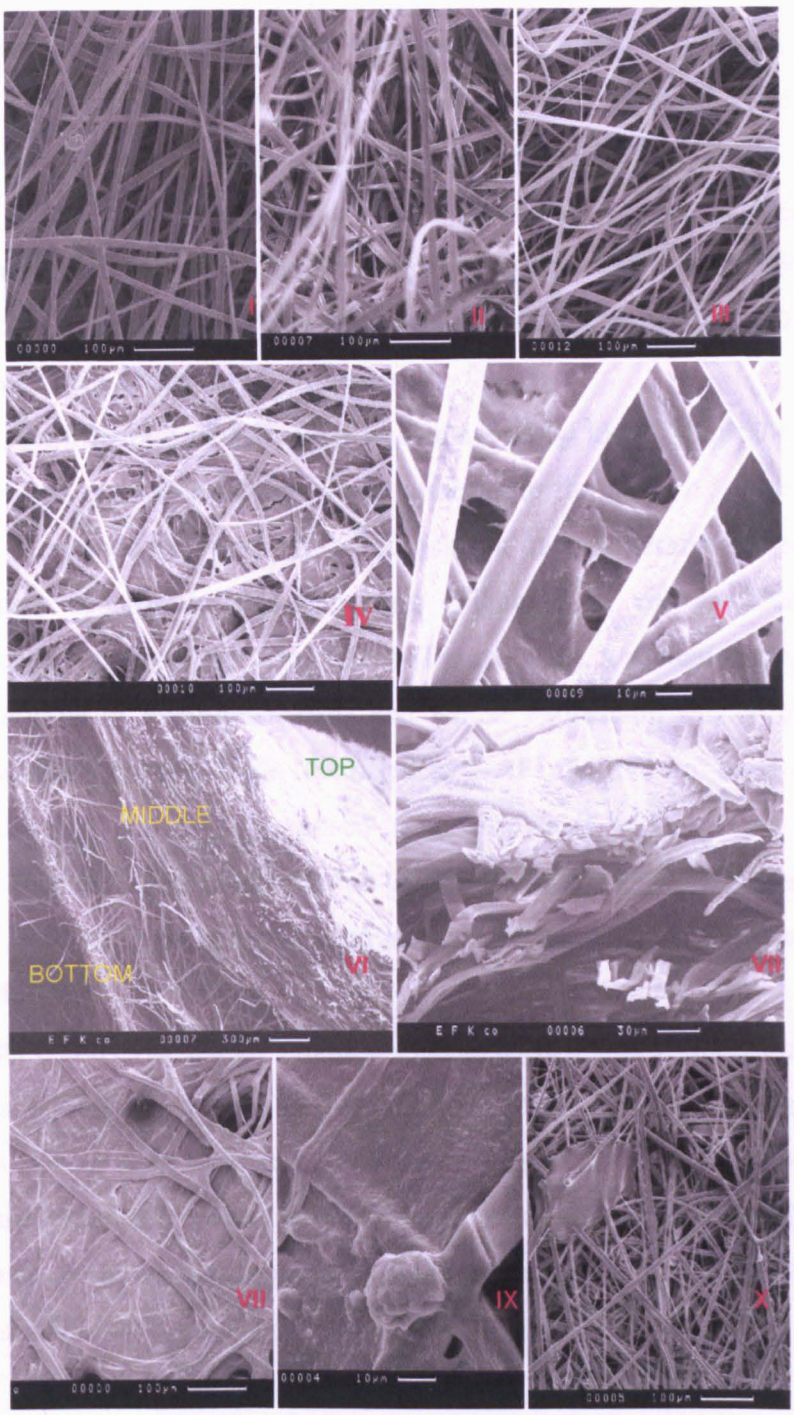

Figure 3.4 SEM micrographs of single and co-culture of human keratinocytes, fibroblasts and endothelial cells in electrospun PS without the presence of serum proteins. (I) electrospun PS, (II) single culture of keratinocytes, (III) single culture of endothelial cells, (IV-V) single culture of fibroblasts, (VI-VII) cross section of scaffolds with three cell types present (VIII-IX). The upper surface of the scaffold with three cell types present. (X) The lower surface of the scaffold with three cell types present.

SEM micrographs of electrospun scaffold (see Figure 3.4I for scaffold alone) showed no cells present when single cultures of keratinocytes (Figure 3.4II) or endothelial cells (Figure 3.4III) were added in serum free conditions. However, a high degree of cell mass was observed when fibroblasts were present (Figure 3.4IV and V). The co-culture of all three cell types together resulted in a high total cell number on the upper surface of the scaffold and through the top third (Figure 3.4VI-IX), with fewer cells observed in the lower two thirds.

Specific identification of cell types was achieved by identifying all the cell nuclei regardless of cell type with DAPI, which attaches to the DNA of the cell and stains the nucleus. Keratinocytes were identified using a pancytokeratin marker which is a protein marker specific to this cell type (Figure 3.5a and b) Identification of endothelial cells was observed using CD31 (Figure 3.5d), a protein that is found in the surface membrane of endothelial cells and whose expression can be used to locate these cells within a culture. Cells identified by DAPI that did not label positively for pancytokeratin or CD31 were supposed to be fibroblasts by deduction. Combination of these markers showed that endothelial cells and fibroblasts were present throughout the scaffold with a higher concentration away from the edges of the scaffold (Figure 3.5 and Table 3.1).

Constructs cultured at the air-medium interface grew more successfully than fully submerged scaffolds and consequently had higher MTT viability (data not shown). As well as this it was seen that and the keratinocytes had migrated to the air liquid interface, mimicking the epidermal positioning of keratinocytes in skin(Figure 3.5e). This contrasts with a less organised distribution of keratinocytes seen in fully submerged scaffolds (Figure 3.5f).

Table 3.1 Summary of immunofluorescence micrograph co-cultures for human keratinocyte, fibroblast and endothelial cells in 3D electrospun polystyrene scaffolds under serum free conditions. -: no cells, -/+: very low cell density, +: low cell density, ++: medium cell density, +++: high cell density.

	Keratinocytes		Endothelial cells		Fibroblasts
	Involucrin	Cytokeratin	vWF	CD31	
Top	+++	+++	-/+	-/+	-/+
Middle	-/+	-/+	+	+	+
Bottom	-	-	-/+	-/+	-/+

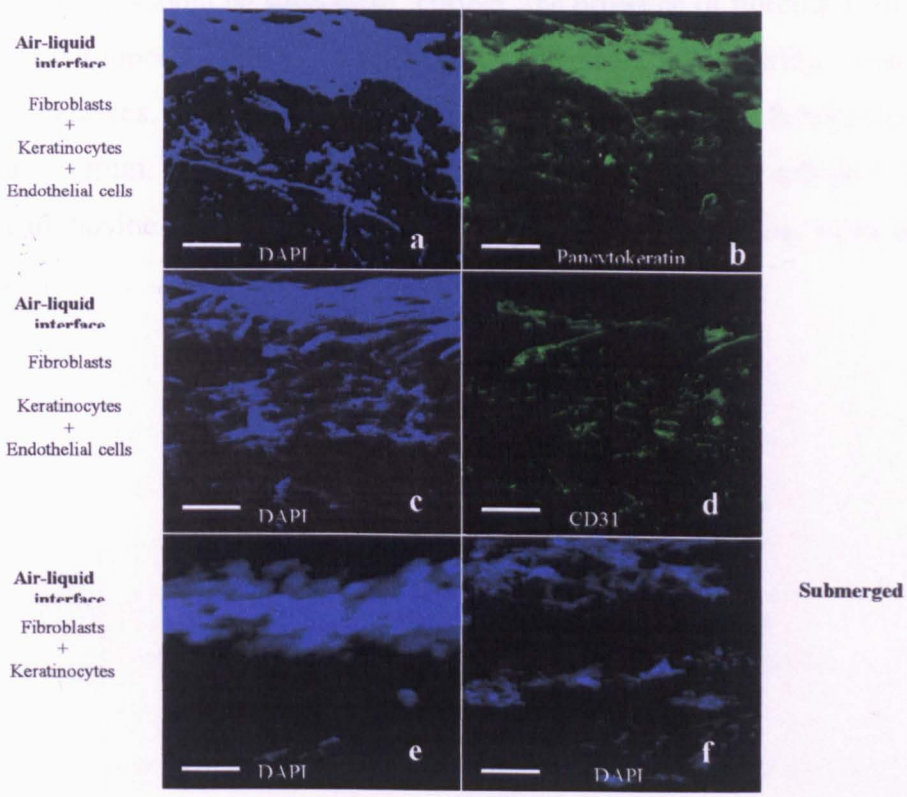

Figure 3.5 Immunofluorescence micrographs of human keratinocytes, fibroblasts and endothelial cells in 3D electrospun polystyrene scaffolds under serum free culture conditions. Three-cell co-cultures were labelled with DAPI (a) and pancytokeratin (b). Three-cell co-cultures labelled with DAPI (c) and CD31 (d). DAPI labelled keratinocyte and fibroblast co-cultures at an air-liquid interface (e) and submerged (f). Scale Bar = 100μm.

3.4 Conclusion – Cell Culture on Polystyrene

In conclusion, it is seen that keratinocytes, endothelial cells and fibroblasts do not proliferate when cultured separately in or on a matrix without the presence of serum. However, when these cells are cultured together within a scaffold they thrive, even under serum free conditions. In the scaffold, keratinocytes formed a continuous 'epidermal' layer at the upper air-facing surface, while fibroblasts and endothelial cells occupied the central and lower regions. Hence, a random co-culture of different cell types introduced into a 3D porous scaffold devoid of molecular cues can self organise. In effect the cells produce their own cues when guided by an air-medium gradient. This suggests that tissue engineering scaffolds do not always have to closely mimic the intended tissue rather act as a guide for the natural proliferation of a co-cultured system. So long as the pores within a scaffold enable relatively unhindered migration of cells it should be successful. Further, the presence of fibroblasts provides an environment supportive for keratinocyte and endothelial cell viability, even under serum-free conditions. Fibroblasts have the ability to secrete growth factors similar to those found in serum, enabling such serum-free co-cultures support cell growth.This elimination of bovine product will be extremely useful in designing materials for clinical use.

3.5 *Biodegradable Fibres*

Following the success with PS a systematic study of biodegradable polymers was initiated, these being Poly (l-lactide) (PLLA) and Poly (d,l – lactide) (PDLA). These polymers were chosen as they were known to be biocompatible and resorbable and had been widely used in bio-medical devices[10,22-25].

Degradation of polylactides occurs through hydrolysis which can lead to acidosis and a decrease in the pH surrounding the material which could result in cell death[11,13]. The small amount of material in electrospun scaffolds, arising from their porous structure, would hopefully mean that any acidosis was not concentrated and easily dispersed.

PDLA (Mw109 $kgmol^{-1}$) was dissolved in DMF at a range of concentrations up to 50wt% at which point the solution was too viscous to be processed. It was found that even at such large concentrations the fibre diameter rarely exceeded 5μm (figure 3.6) as a result of the highly polarisable solvent being used. The scaffolds were easy to handle and were submitted for cell culture. Cells were unable to be seeded due to shrinkage of the material under culture conditions (37°C). This occurs because the glass transition temperature (T_g) of PDLA is ~35°C so the scaffold becomes rubbery at 37°C and shrinks rendering it useless for a tissue scaffold.

In order to overcome the problem of shrinkage crystalline PLLA was used. After many iterations PLLA was spun into fibres of a diameter of roughly 5-15μm with an inter fibre pore size of 30-70μm. PLLA of Mw 152$kgmol^{-1}$ was dissolved in DCM to make a 7.5wt% solution. It was then spun at 20-25kV over 40cm. The long working distance ensured complete fibre dryness and decreased the apparent density of the scaffold due to the gentle deposition of fibres on the reel. Samples of PLLA scaffold were used for cell seeding and early results show even better performance than PS scaffolds.(figure 3.7)

Studies are still ongoing regarding the proliferation of cells in such matrices. Many

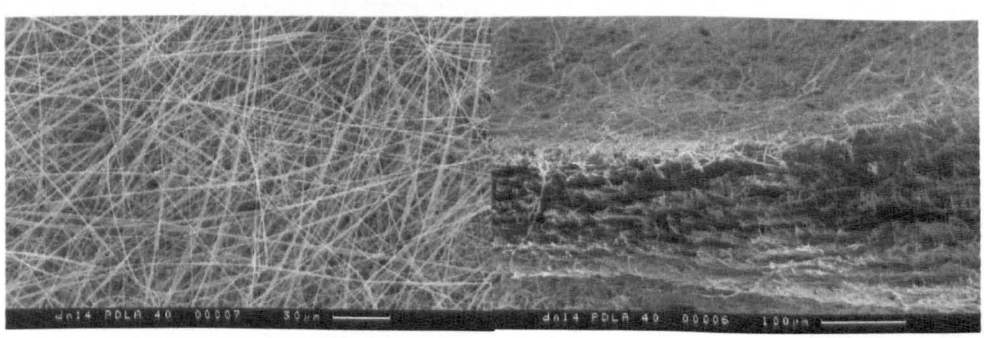

Figure 3.6 SEM micrographs of PDLA spun from 40wt% PDLA in DMF showing both the surface of the scaffold and a cross section. Average fibre diameter is .5um

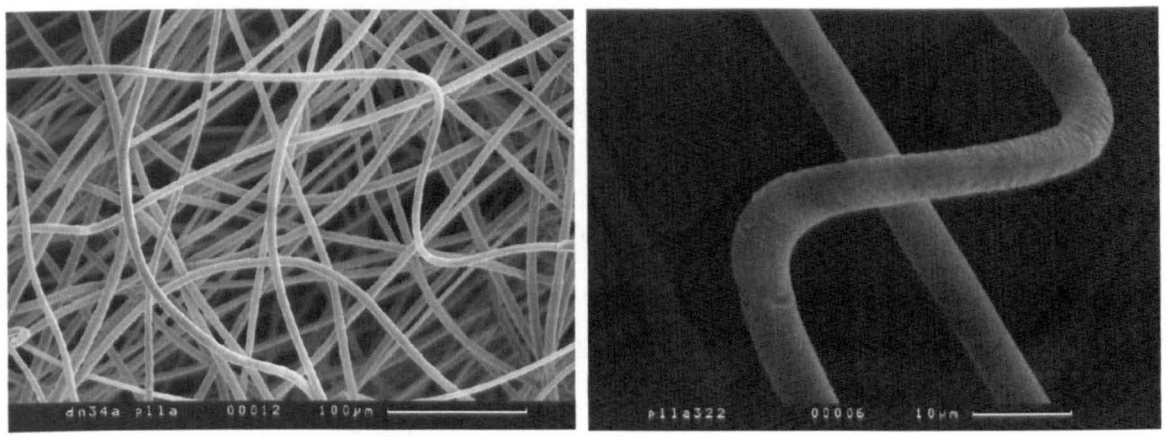

Figure 3.7 PLLA fibres spun from 7.5wt% PLLA in DCM with average fibre diameter of 5µm

seeded PLLA scaffolds have already been implanted in rats and the degradation and immune response is being closely monitored.

Electrospun scaffolds have also been formed from PLLA- PEO diblock copolymers. The PEO content increases the hydrophilicity of the polymer surface which in turn should increase cell adhesion and degradation rates. These studies are still ongoing and beyond the scope of this report. Tailoring the degradation of these scaffolds is the next step which will bring these matrices closer to the clinic. If one can dictate the rate at which these scaffolds degrade and optimise it in the context of the rate of cell proliferation, then the time for complete wound healing can be dramatically reduced.

3.6 Glossary of Terms

MTT- a di*m*ethyl *t*hiazolyl diphenyl *t*etrazolium salt. This is used to quantify the respiratory activity of live cells in cell culture, although it generally kills the cells in the process. metabolite undergoes a colour change which is used to quantify metabolic activity.

Pancytokeratin- antigenic protein marker for tissue of epithelial origin such as keratinocytes

Involucrin- antigenic protein present in keratinocytes of the epidermis which can be immunostained as evidence for the presence of keratinocytes

DAPI- or 4',6-diamidino-2-phenylindole is a fluorescent stain that binds strongly to DNA. It is used extensively in fluorescence microscopy. Since DAPI will pass through an intact cell membrane, it may be used to stain live and fixed cells.

Greens Medium- a modification of DMEM medium, more suitable for the culture of keratinocytes.DMEM (Dulbecco's Modified Eagle Medium) is a standard medium for animal cell culture, which alone is not suitable for kerainocyte culture.

Von Willebrand's Factor (vWF)- is a large multimeric glycoprotein (a macromolecule composed of a protein and a carbohydrate) present in blood plasma and produced constitutively in endothelium by endothelial cells. This can be stained for in immunofluorescent microscopy to indicate the presence of endothelial cells.

Hoechst 33342 and Propidium Iodide – A dual staining technique for the assessment of keratinocyte,fibroblast and endothelial cell viability. Hoechst 33342 stains for all live and dead cells whereas PI stains only for dead cells, so everything that is stained Hoechst 33342 and not PI must be a viable cell.

3.7 References

1. Gawkrodger, D. Dermatology, An Illustrated Colour Text. *Churchill Livingstone*, 27-29 (2002)
2. Rook, A., Burns, T., Breathnach, S., Cox, N. & Griffiths, C. Rook's Textbook of Dermatology. *Blackwell Publishing*, 387-388 (2004).
3. Matthews, J. A., Wnek, G. E., Simpson, D. G. & Bowlin, G. L. Electrospinning of collagen nanofibers. *Biomacromolecules* **3**, 232-238 (2002).
4. Luu, Y. K., Kim, K., Hsiao, B. S., Chu, B. & Hadjiargyrou, M. Development of a nanostructured DNA delivery scaffold via electrospinning of PLGA and PLA-PEG block copolymers. *Journal of Controlled Release* **89**, 341-353 (2003).
5. Sagnella, S. M. et al. Human microvascular endothelial cell growth and migration on biomimetic surfactant polymers. *Biomaterials* **25**, 1249-1259 (2003).
6. Wnek, G. E., Carr, M. E., Simpson, D. G. & Bowlin, G. L. Electrospinning of nanofiber fibrinogen structures. *Nano Letters* **3**, 213-216 (2003).
7. Li, W. J., Laurencin, C. T., Caterson, E. J., Tuan, R. S. & Ko, F. K. Electrospun nanofibrous structure: A novel scaffold for tissue engineering. *Journal of Biomedical Materials Research* **60**, 613-621 (2002).
8. Deitzel, J. M., Kleinmeyer, J., Harris, D. & Tan, N. C. B. The effect of processing variables on the morphology of electrospun nanofibers and textiles. *Polymer* **42**, 261-272 (2001).
9. Zong, X. et al. Electrospun fine-textured scaffolds for heart tissue constructs. *Biomaterials* **26**, 5330-5338 (2005).
10. Yang, F. et al. Fabrication of nano-structured porous PLLA scaffold intended for nerve tissue engineering. *Biomaterials* **25**, 1891-1900 (2004).
11. Boland, E. D., Wnek, G. E., Simpson, D. G., Pawlowski, K. J. & Bowlin, G. L. Tailoring tissue engineering scaffolds using electrostatic processing techniques: A study of poly(glycolic acid) electrospinning. *Journal of Macromolecular Science-Pure and Applied Chemistry* **38**, 1231-1243 (2001).

12. Bacakova, L. et al. Fluorine-ion-implanted polystyrene improves growth and viability of vascular smooth muscle cells in culture. *J.Biomed Mater Res* **49**, 369-379 (2000a).

13. Bacakova, L. et al. Molecular mechanisms of improved adhesion and growth of an endothelial cell line cultured on polystyrene implanted with fluorine ions. *Biomaterials* **21**, 1173-1179 (2000b).

14. Huang, S., Chen, C. S. & Ingber, D. E. Control of cyclin D1, p27(Kip1), and cell cycle progression in human capillary endothelial cells by cell shape and cytoskeletal tension. *Mol Biol Cell* **9**, 3179-3193 (1998).

15. Garcia, A. J., Vega, M. D. & Boettiger, D. Modulation of cell proliferation and differentiation through substrate-dependent changes in fibronectin conformation. *Mol Biol Cell* **10**, 785-798 (1999).

16. Moiseeva, E. P. Adhesion receptors of vascular smooth muscle cells and thein functions. *Cardiovascular Res* **52**, 372-386 (2001).

17. Hynes, R. O. Cell adhesion: old and new questions. *Trends Cell Biol* **9**, M33-M37 (1999).

18. Humphries, J. D. & A.P., M. Molecular basis of ligand recognition by integrin a5ß1. II. Specificity of arg-gly-Asp binding is determined by Trp157 OF THE alpha subunit. *J. Biol Chem* **275**, 20337-20345 (2000).

19. Aplin, A. E. Cell adhesion molecule regulation of nucleocytoplasmic trafficking. *FEBS Lett* **534**, 11-14 (2003).

20. Ingber, D. E., Prusty, D., Sun, Z. & Wang, N. Cell shape, cytoskeletal mechanics, and cell cycle control in angiogenesis. *J.Biomech* **28**, 1471-1484 (1995).

21. Wang, N., Naruse, K., Stamenovic, D. & Ingber, D. E. Mechanical behavior in living cells consistent with the tensegrity model. *Proc Natl Acad Sci USA* **98**, 7765-7770 (2001).

22. Guidoin, M.-F., Guidoin, R., Frayssinet, P., Legrand, A. & How, T. Poly-L-Lactide Surfaces Subjected to Long-Term Cell Cultures. Cell Proliferation and Polymer Degradation. *Artificial Cells, Blood Substitutes, and Biotechnology* **33**, 411-422 (2005).

23. Inai, R., Kotaki, M. & Ramakrishna, S. Structure and properties of electrospun PLLA single nanofibres. *Nanotechnology* **16**, 208-213 (2005).

24. Zu, E.-f., Yang, Q.-f., Ma, A.-j., Shi, K. & Zhu, F. Study on biocompatibility and degradation of poly(L-lactic acid). *Zhongguo Jiaonianji* **14**, 7-10 (2005).

25. Bergsma, J. E., de Bruijn, W. C., Rozema, F. R., Bos, R. R. & Boering, G. Late degradation tissue response to poly(L-lactide) bone plates and screws. *Biomaterials* **16**, 25-31.(1995)

26. Goberdhan, N. J., Dawson, R. A., Freedlander, E. & Mac Neil, S. A calmodulin-like protein as an extracellular mitogen for the keratinocyte. *British Journal of Dermatology* **129**, 678-88 (1993).

27. Ralston, D. R. et al. The requirement for basement membrane antigens in the production of human epidermal/dermal composites in vitro. *British Journal of Dermatology* **140**, 605-615 (1999).

28. Sahota, P. S., Burn J.L, MacNeil, S.J. Development of a human skin model for angiogenesis *J. Wound Care Regen.* **11,** 275-285. (2003)

29. Chakrabarty, K. H, MacNeil, S.J. Development of autologous human dermal-epidermal composites based on sterilized human allodermis for clinical use. *British journal of dermatology* **141**, 811-823(1999)

30. Sun, T., Mai, S.M., Norton, D., Haycock, J.W., Ryan, A.J., MacNeil, S.J. Self-Organization of Skin Cells in Three-Dimensional Electrospun Polystyrene Scaffolds. *Tissue Engineering* **11**, 1023-1033 (2005).

Chapter 4 – Controlled Porosity of PLLA Fibres

4.1 Introduction

When spinning PLLA from DCM and chloroform it was noticed that pores were formed upon the surface of the fibres. Some groups had reported similar surface features on spinning of other polymer systems such as PS from THF[3,4] It was supposed that these features could be a result of condensation or "breath figures" on the surface of the fibre formed during the rapid evaporation of solvent and resultant cooling of the extruded solution.[3-6]

Controlling the formation of these pores was thought to be important for the purposes of tissue engineering as cells often prefer a rough surface upon which they can take hold more easily.[7-11] Also, controlling surface morphology may be another way of controlling degradation rates, as more porous fibres may be prone to faster degradation especially if the core of the fibre is exposed. Sufficiently large pores could allow water to penetrate into the centre of the fibre increasing the rate of hydrolysis.

4.2 Experimental

4.2.1 Spinning Conditions

An environment whereby electrospinning could take place under controlled humidity was created. This consisted of a Pyrex box of dimensions 1000mm x 60mm which adapted so that the needle carrying the solution would be inside the box but all pumping and focussing apparatus outside. The box had a hinged lid to enable easy set up of collecting equipment. The needle could be introduced into the box through a small orifice facing the collector plate. This orifice remained covered with insulating tape during equilibration of the box after which point the needle could be pushed through the tape, and spinning could commence.

The collector used for this experiment was an earthed flat plate covered in aluminium foil, which was placed at a distance of 35cm from the needle for all experiments (this distance was predetermined by spinning the solutions in open air, and was the distance over which dry fibres were collected in all cases). Also inside the box was a temperature/humidity probe (picoRH02, Pico Technology Ltd) which was connected to a laptop. Temperature and humidity readings were taken throughout each experiment.

The solutions to be spun were 6.5, 7.5, and 8.5wt% PLLA in DCM. All three solutions were to be spun inside the box at a minimum of 3 different humidities over a wide range. The three spinning scenarios were a "dry" box (<10% humidity), a "standard" box (20-30% humidity) and a "wet" box (80-100% humidity).

Firstly they were to be spun at low humidity in the "dry" box(figure 4.1). This was achieved by placing flat dishes full of self indicating silica gel into the box and then sealing the box shut with insulating tape. Flat dishes were chosen in order to maximise the amount of silica surface exposed to the atmosphere which enabled a dry environment to be prepared quickly. The box was then left for about 1hr or until the humidity stabilised (checked with picolog program, Pico Technology Ltd). Once the humidity had stabilised spinning could commence.

The next condition under which spinning was to take place was under "medium" or standard humidity. In this instance the box was left open to the atmosphere for about one hour prior to spinning in order for it to equilibrate. Once a steady humidity was recorded the box was once again sealed and spinning could commence.

For spinning at high humidity it was required to make the atmosphere in the box wet without raising the temperature. This was achieved by placing a beaker of hot water inside the box and sealing it. This was then left overnight, by which time the temperature in the box will be the same as room temperature but the atmosphere will be saturated. Electrospinning was then performed into the saturated atmosphere(figure 4.2).

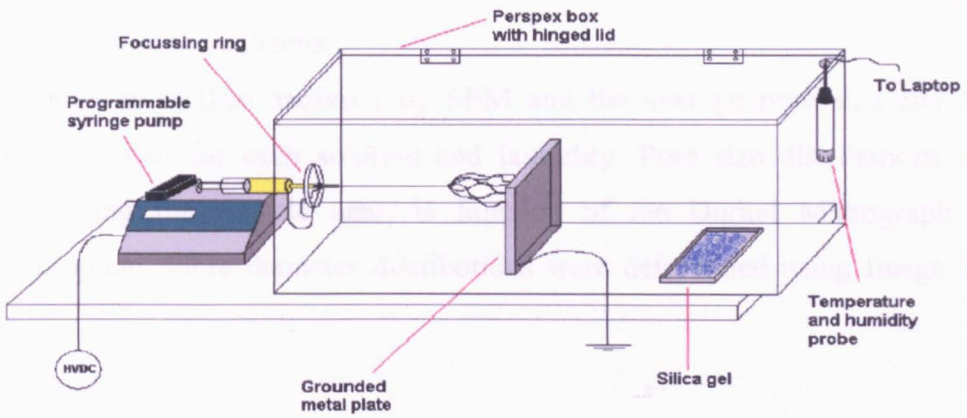

Figure 4.1 Apparatus for electrospinning in a "dry" atmosphere.

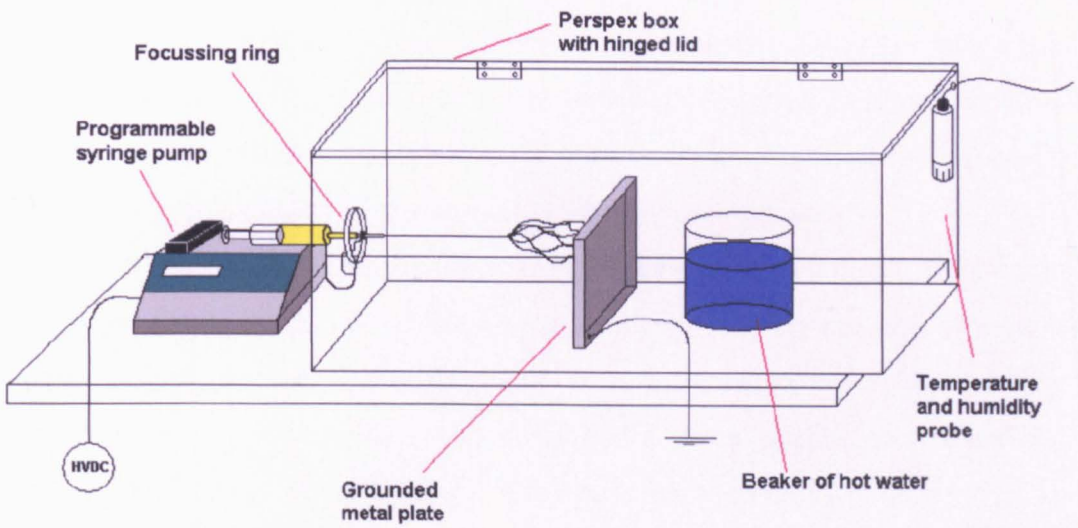

Figure 4.2 Apparatus for electrospinning in a "wet" atmosphere.

Each solution was spun under the same electrospinning conditions at 20kV, 2.2ml/hr and Ga20 needle in order to ensure that the only variable was the humidity. It was noted that the fibre jets were straighter in the box than outside, so a long working distance was required to ensure dryness; this was set at 35cm. This phenomenon was a result of electrostatic insulation from external earth points, which distort the electric field and lead to jet instabilities (i.e. whipping). Reductions in the whipping phenomena means that the fibres get less chance to dry out, and would remain wet upon collection if the working distance was not duly increased. Samples were collected by removing the sealing tape from around the lid and removing the aluminium foil from the collector.

The samples were then analysed by SEM and the average pore size and fibre diameter determined for each solution and humidity. Pore size distributions were determined using the particle analysis function of the Digital Micrograph 365 computer program. Fibre diameter distributions were determined using Image Tool software.

4.3 Fibre Cross-Sections

4.3.1 Resin Mounting

In order to see the depth of pore penetration, a cross section of the fibres needed to be prepared for visualisation with the SEM. The standard procedure for viewing small scale cross sections of materials is to mount the material in either a cold curing resin or a hot mounting compound and then grind the mounting material down to expose the cross section of the embedded substance. Once rough grinding has exposed the area of interest the surface is polished for visualisation under SEM.

Choosing the correct resin for fibres was the first barrier to overcome. Hot mounting is a process whereby the sample is submerged within a thermosetting compound and cured in a mounting press which exerts both heat and high pressure. This mounting method produces hard mounts in a short space of time, however the heating (generally in the order of 120 °C) and considerable pressure applied may be unsuitable for delicate, soft or low melting point specimens. This was certainly the case for PLLA fibres with a melting range of 175-178°C and the delicate nature of the fibres.

The only option for mounting PLLA fibres was therefore a cold mounting resin.[12] A wide range of products are available on the market. Generally faster setting products including acrylic resin types are less favourable, as these tend to develop low hardness and often suffer from 'shrinkage'. Shrinkage is the term given when the resin shrinks away from the sample surface during curing. This is undesirable as the gap which forms harbours contaminants, grit from grinding and polishing stages to cause cross contamination of polishing surfaces. It is difficult to obtain a good polished, scratch free surface when gaps in the mounting material are present.

Epoxy resin types generally have the best characteristics with respect to hardness and shrinkage. However, epoxy resins tend to be slower curing and adequate time should be allowed to ensure that the material is fully cured before proceeding. Epoxies often take a considerable period of time after initial 'setting' to develop full hardness. A drawback of the cold cure resin is that it is not generally possible to make them conductive suitable for SEM examination therefore the mount must be coated in silver conductive paint and gold prior to visualisation which can mask the sample area.

Once the sample is mounted and the resin fully set, it is cut using a circular saw to expose the rough area of interest which is then prepared for SEM with grinding and polishing.

Grinding is performed on rotating wheels of abrasive substrate, lubricated with a constant water supply. Grinding can be achieved in a variety of ways, using a variety of abrasives. Fixed abrasive surfaces were used to grind the resin surface using diamond and cubic boron nitride (CBN) abrasives with abrasive crystals of 10μm diameter. This course grinding process removes much resin material and allows the area of interest to be reached quickly.

Once rough grinding is complete, the defects created by the rough process were smoothed out using silicon carbide (SiC) paper with diamond paste lubricants. SiC paper blunts quickly and therefore should be discarded after a short period of grinding as grinding on a surface that has blunt abrasives causes a great deal of surface damage by smearing, 'burnishing' and local heating. The SiC paper and diamond paste smoothes the surface out to a scale of 1μm defects.

After every grinding stage it is the ground surface was inspected using a light microscope in order to ensure that all damage from the previous stages are removed Care at this stage will greatly reduced the amount of polishing required to achieve a good surface. Polishing of the surface is undertaken with colloidal silica polish with a typical abrasive size is 0.05 micron on a rotating soft cloth. After polishing, the sample was removed and dried using ethanol.

Once dried, the prepared resin was mounted on an SEM stub using a sticky carbon tab, and two of the sides of the resin block not including the polished side are painted

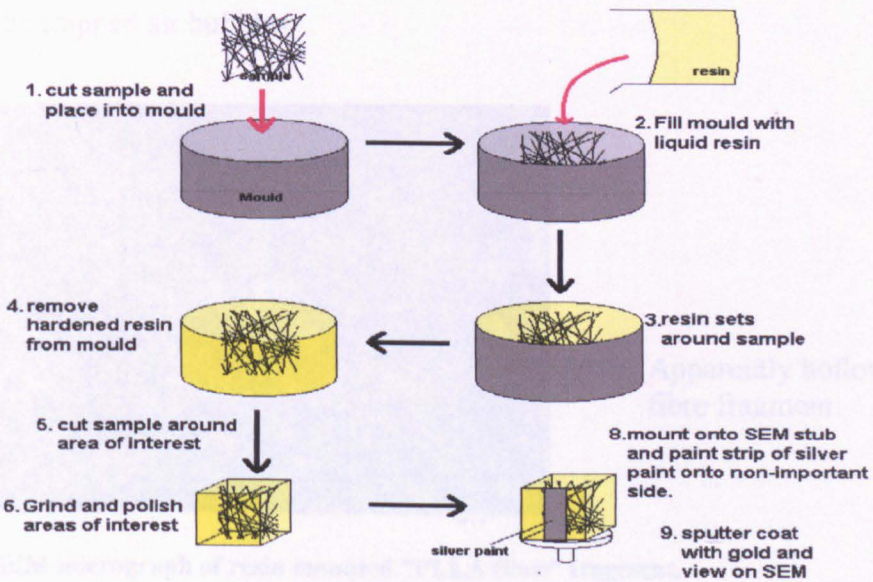

Figure 4.3 Schematic of the resin mounting process.

in silver paint to ensure no charge build up during microscopy. The sample surface was then sputter coated with gold and observed under the scanning electron microscope(Figure 4.3).

4.3.1.1 Resin Mounting Problems

It became apparent rather quickly that resin mounting was not going to yield the cross-sectional images which were required. After much care was taken in preparing a batch of resin mounted samples, the SEM results indicated a number of problems with the technique. The primary concern was that the PLLA samples were actually soluble in the liquid resin, which is indicated by the lack of fibrous material left in the resin and the numerous "fibre" fragments. These fragments were misleading as they suggested that the fibres were indeed profoundly hollow as can be seen in figure 4.3.

A common mistake in microscopy is that you only see what you want to see and artefacts will often be mistaken for products. These fragments were frequent in the resin- but complete fibres were not. Instead of complete fibres, long hollow channels were found with dimension that approximated to those of PLLA fibres (5-15 μm diameter). These hollow channels were also accompanied by holes in the resin surface which were also approximately the diameter of the PLLA fibres (5-15 μm). These holes could be a result of air being trapped in the resin or could be the cross-section of a dissolved fibre (Figure 4.4). Trapped air was always destined to be a problem when setting such a low density material. Fluffy non-woven fabrics trap air between the fibres and as such are excellent thermal insulators. No steps were taken when casting these resin samples to exclude air from the fabric, so many of the visible artefacts could just be trapped air bubbles.

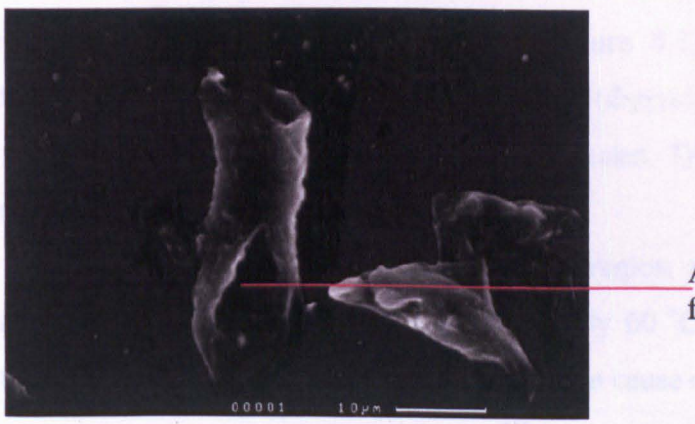

Figure 4.4 SEM micrograph of resin mounted "PLLA fibre" fragment.

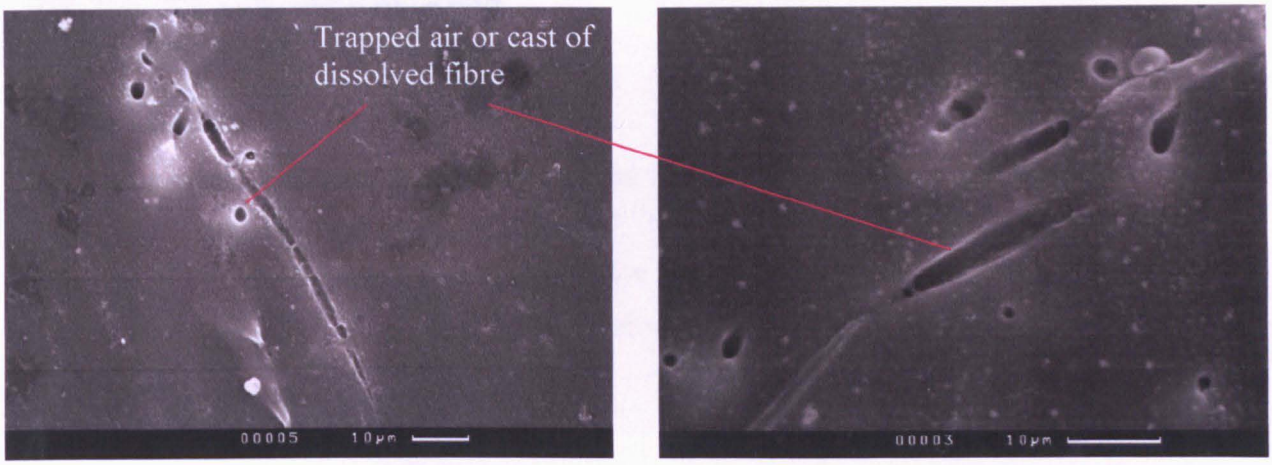

Figure 4.5 SEM micrographs of channels found in epoxy resin. Channels have the same dimensions as electrospun PLLA fibres.

The evidence seemed to suggest that the fibres had indeed been dissolved in the resin as there were no fully formed fibres to be seen. The fragments which were in abundance were therefore not reliable evidence for hollow PLLA fibres. In fact it could not be said for certain that they were even PLLA fragments. We knew that the embedded fibres had pore-rich surfaces from previous "normal" SEM of the fibres but no pores could be seen on these fragment surfaces. This could be due to partial melting of the fibre surface; the fragments not being PLLA; or a lack of contrast on the microscope. Lack of contrast was a serious problem when looking at these resin mounted samples where one is effectively looking for very small blemishes on the surface of the resin. If the embedded sample was more conducting than the resin then the samples would exhibit a great contrast to the insulating resin. The fact that in this case the embedded sample was an insulating polymer meant that the contrast between sample and resin was poor. In turn, this made it extremely difficult to resolve small surface structures of the embedded material (figure 4.5). Solubility experiments showed PLLA to be partially soluble in DEGBA (diglycidyl ether of bisphenol A) which is a major constituent in the epoxy resins used. Dissolution of fibres could therefore have happened prior to the resin hardening.

The melting temperature of PLLA is in the region of 180°C but the curing temperature of the epoxy resin is only approximately 60 °C, so melting of the fibres during the curing process can be ruled out as a possible cause of fibre damage.

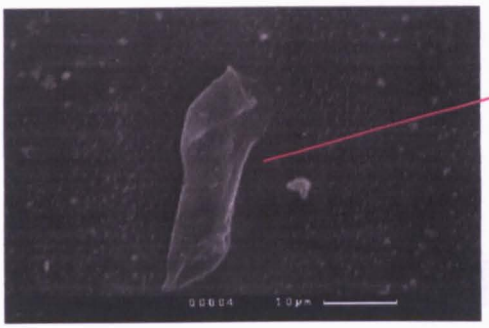

Figure 4.6 SEM micrograph of artefact embedded in resin, highlighting the problems with resolving surface structure of embedded samples

It quickly became apparent that this was not the way to achieve a cross section image of these fibres so a more practical method was sought.

4.3.2 Mount, Freeze and Cut

This method was used as it is quick, simple and brings about the least damage to the fibres. This should ensure that what is seen through the microscope is a fair representation of the sample. The method is very simple as is shown in figure 4.7. A small section of sample is cut and rolled gently into a cylinder. This is then taken and stuck onto a microscope stub with superglue. Once the superglue has set the stub is immersed in liquid nitrogen to make the fibres brittle which takes about twenty seconds. Upon removal from the nitrogen the sample is cut with sharp scissors before being allowed to thaw out. Any delay at this point could lead to "pinching" of the fibre ends. Finally the sample is sputter coated with gold and looked at under the microscope. This must be done quickly to limit the chance of water condensing on the fibre surface. This method was both simple and effective and the resulting cross-section images can be seen in the results section of this chapter.

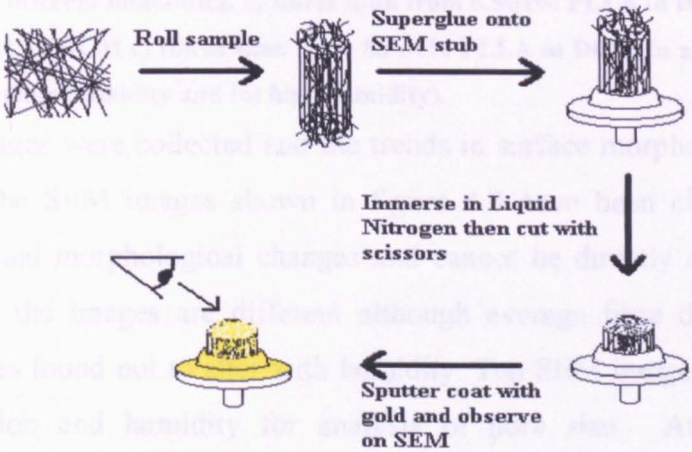

Figure 4.7 Schematic showing how cross section images were prepared for SEM imaging.

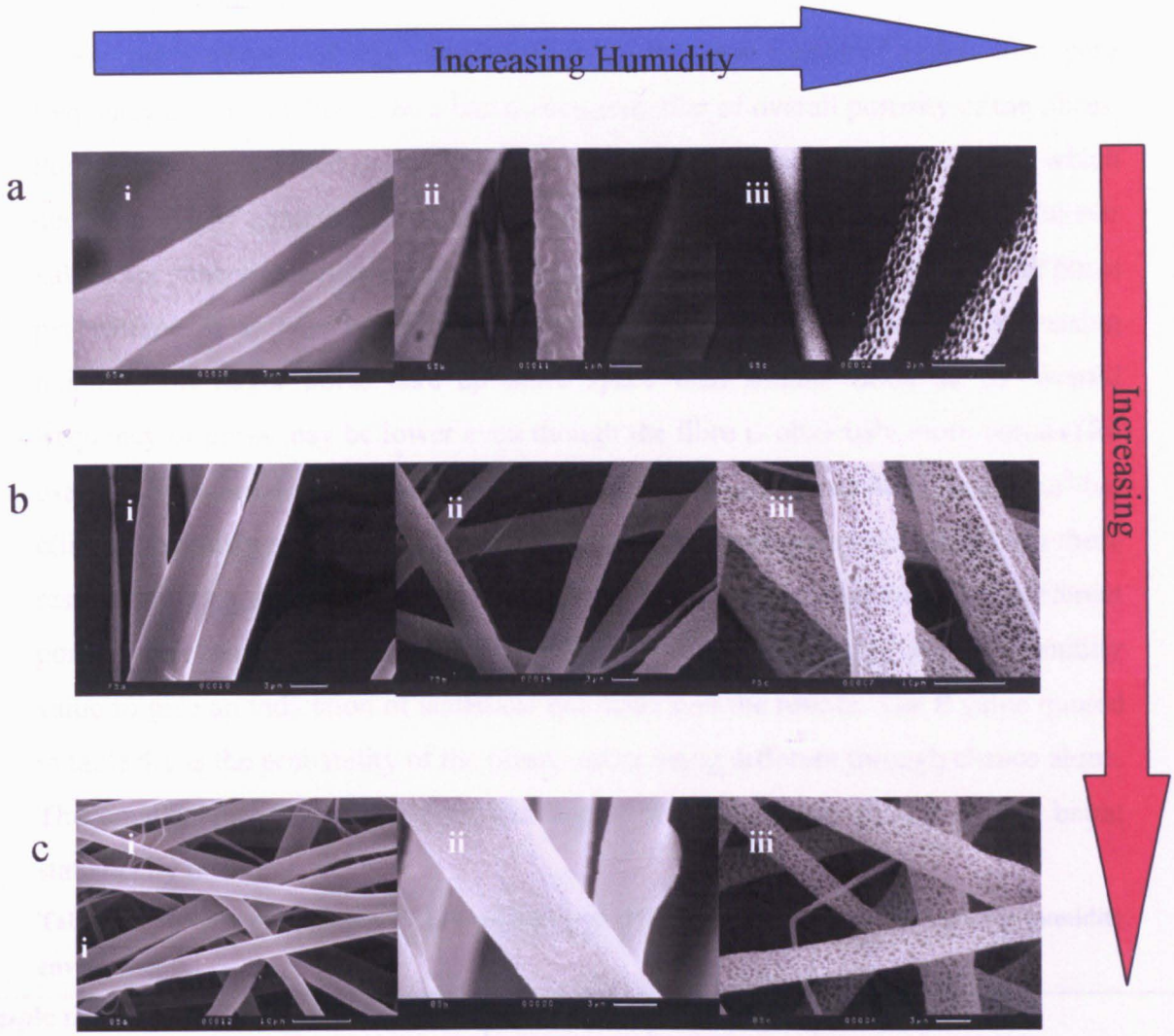

Figure 4.8 SEM micrographs showing evolution of fibre surface morphology for PLLA fibres electrospun under different humidities. a) fibres spun from 6.5wt% PLLA in DCM b) fibres spun from 7.5wt% PLLA in DCM c) fibres spun from 8.5wt% PLLA in DCM(In all cases i) refers to low humidity ii)medium humidity and iii) high humidity).

The SEM images were collected and the trends in surface morphology are shown in figure 4.8. The SEM images shown in figure 4.8 have been chosen merely to highlight the visual morphological changes and cannot be directly compared as the length scales of the images are different although average fibre diameter at each concentration was found not to alter with humidity. Ten SEM images were taken for each concentration and humidity for analysis of pore size. At each spinning concentration, the effect of changing the humidity was the same. In conditions where humidity was low (~ <20%) pore formation was not seen and totally smooth fibres

were produced. Increasing humidity led to an increase in the number of pores on the fibre surface. Pores were non- uniform as opposed to those breath figures seen in static film situations.[2,5,13,14]

For the purposes of this experiment pore size was measured rather than pore frequency as it was taken to be a better representation of overall porosity of the fibres. Pore size was measured using Digital Micrograph particle analysis program, which detects pores by contrast with the fibre surface on SEM micrographs. Pore perimeter values are generated automatically for each image. If pore frequency (number of pores per surface area) was measured one might not see an increase with increasing humidity, as larger pores take up more space than smaller ones, so the overall frequency of pores may be lower even though the fibre is obviously more porous.(for example in figure 4.7 the pore frequencies in c(ii) and c(iii) are both 7 pores/μm^2 but c(iii) is obviously more porous). Average pore perimeters were calculated from these results and also standard deviations to give an indication of the spread of different pore sizes in one sample (table 4.1). Paired t-tests were performed at each humidity value to give an indication of statistical confidence in the results. The P value quoted in table 4.1 is the probability of the mean values being different through chance alone. The smaller the P-value is then the higher the confidence in the results being statistically different.

Table 4.1 Results of spinning PLLA solutions of different concentration in varying humidity environments

Sample description	Mean pore perimeter (μm)	Standard Deviation (μm)	t-test P-value	Comment
6.5wt% normal humidity	0.81	0.95	$3.6x10^{-35}$	Increasing humidity increases mean pore size and distribution. t-test shows the mean perimeters to be statistically different.
6.5wt% high humidity	1.48	1.29		
7.5wt% normal humidity	0.84	1.06	$8.9x10^{-33}$	Pore size increases with humidity. P-value indicates a large degree of confidence in the results.
7.5wt% high humidity	2.59	2.50		
8.5wt% normal humidity	0.37	1.26	$6.4x10^{-28}$	Pore size increases with humidity. Again P-value indicates a statistically significant difference.
8.5wt% high humidity	1.04	2.30		

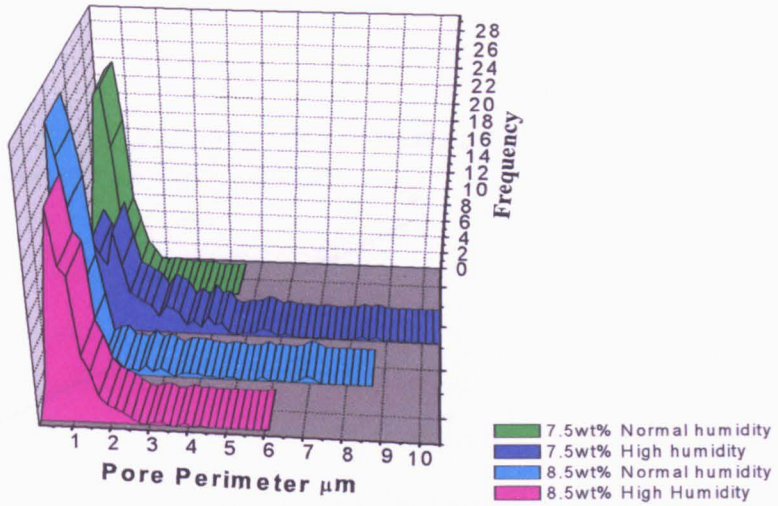

Figure 4.9 Three Dimensional histogram showing relative frequencies of different pore perimeters on fibres spun from different solutions at different humidities.

In an attempt to quantify the effects of humidity on actual pore size, distributions of pore perimeters were measured for each concentration/humidity combination. The results for 7.5wt% and 8.5wt% were plotted as a 3D histogram (figure 4.9). The results from the dry box were not taken into consideration as they always yielded smooth fibres. Also the results from the spinning of 6.5wt% were omitted for clarity As the pores were not symmetrical their area was difficult to calculate using the Digital micrograph program so pore perimeter was used to represent pore size.

Figure 4.9 shows that as humidity increases the pore size distribution shifts to the right regardless of the solution concentration. Some differences could be found between the pore size distributions at different spinning solution concentrations. The fibres spun from 7.5wt% at high humidity (dark blue on figure 4.9) showed the widest range of pore size with the majority having a perimeter of ~2µm, but larger pores also being found with perimeters up to 10µm. It may have been noted that humidity values have not been stated in either figure 4.9 or table 4.1, just the terms "normal" and "high" humidity. This was done for rough comparison purposes only as the actual values for "normal" and "high" were different for the spinning of 6.5wt% to 7.5wt% and so on. In all cases a "dry" humidity corresponded to<10% humidity, a "normal" humidity was 20-30% humidity and a "high" humidity was 80-100% humidity.

The main results to be drawn from this experiment are the effects of humidity on any particular electrospinning solution. Finding a quantitative relationship between humidity, solution concentration and pore size has been left for future work.

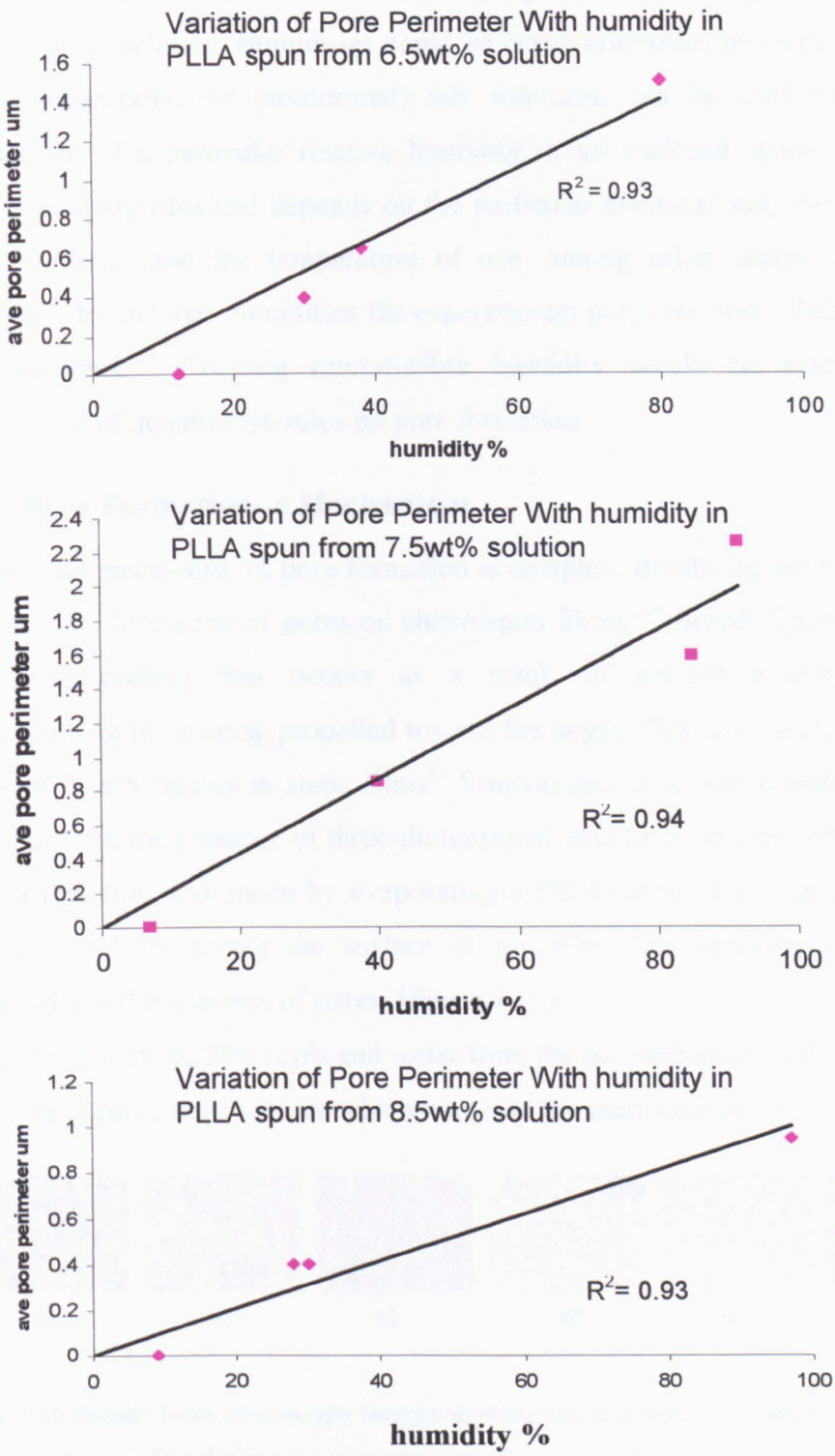

Figure 4.10 Graphs showing the relationship between pore perimeter and relative humidity for 3 different spinning solutions.

Figure 4.10 shows the direct relationships between humidity and pore size with different spinning concentrations. It can be seen clearly here how porosity increases with humidity. The gradients on the graph are just there for a guide but not too much should be read into them as many more experiments at intermediate humidities would

have to be performed to make them statistically relevant although the overall trends are most likely reliable. Humidities could be better controlled by using saturated salt solutions. Saturated (or unsaturated) salt solutions, can be used to generate an environment of a particular relative humidity in an enclosed space. The value of relative humidity obtained depends on the particular chemical salt, the concentration of the solution, and the temperature of use, among other things. Different salt solutions offer tailored humidities for experimental purposes and a definitive list has been published.[15] Creating reproducible humidity would be essential for the development of quantitative rules on pore formation.

4.4.1 Pore Formation- a Mechanism

The exact mechanism of pore formation is complex. Breath figures have been used to explain the formation of pores on electrospun fibers.[3,4] Breath figures form due to evaporative cooling that occurs as a result of solvent evaporating as the electrospinning jet is being propelled toward the target. This is an analogous situation to that of breath figures in static films[13] Srinivasarao et al. use breath figures as an explanation for the presence of three-dimensional structures on a thin PS film. In their work, a thin film was made by evaporating a PS solution in a volatile solvent and passing humid air across the surface of the film. The resulting film contained hexagonally ordered arrays of pores. (figure 4.11)

The surface of the film cools and water from the air condenses on the surface of the film in the form of hard spheres which bore into the malleable polymer surface.

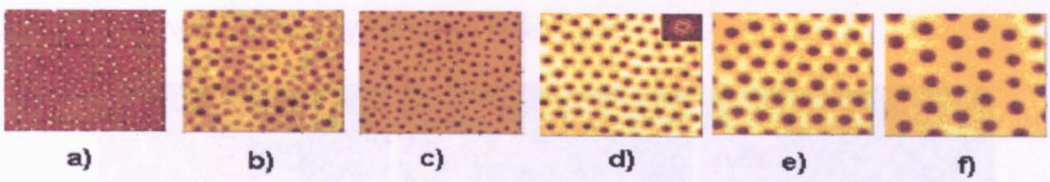

Figure 4.11 Atomic force microscopy images showing the morphology evolution of film surfaces for PS cast from THF solution at a concentration of 4 wt% in different humidity. The humidity is (a) 10%; (b) 15%; (c) 25%; (d) 30%, (e) 50%; (f) 70%, respectively.[13]

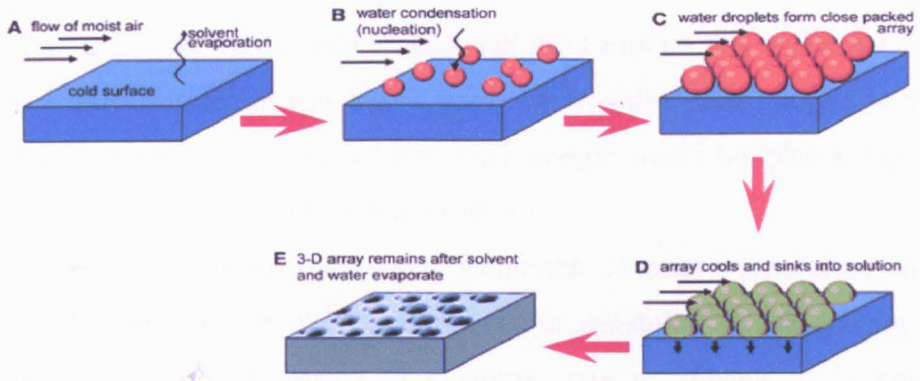

Figure 4.12 Schematic showing the formation of breath figures on a static film.[2]

The pores obtained on the surface of an electrospun fibre are not ordered arrays of uniformly shaped pores but are rather elongated and irregular in shape. The difference in breath figure pores and the pores on an electrospun fibre are most likely due to the motion and elongation of the jet through the moist air, possibly dragging the water droplets along the fibre surface. Also, the fibres carry a charge that may affect the ordering of the pores and their density. Thus, the formation of pores by the electrospinning process is a much more complex process with many variables to be considered.

The formation of pores on the surface of the fibre is not just limited to PLLA in DCM. Casper et al[1] performed a very similar set of experiments on PS spun from THF at approximately the same time as this experiment and found the same relationship between humidity and pore size(figure 4.13).

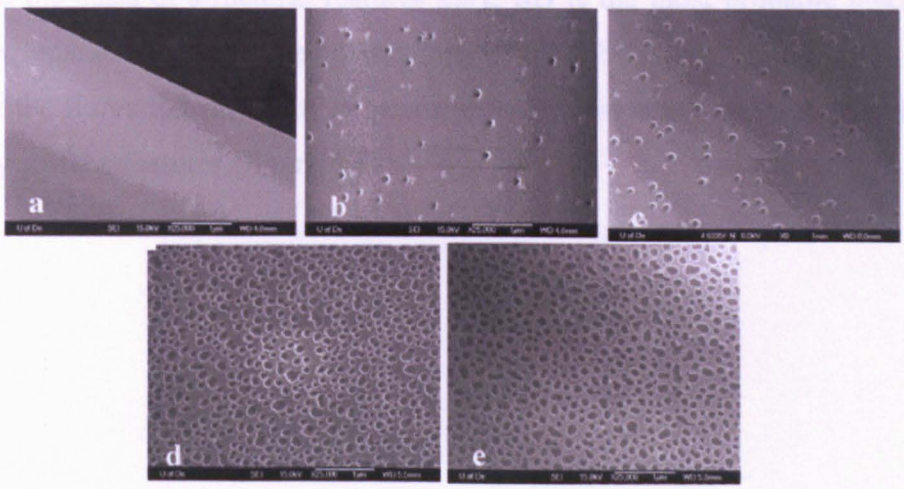

Figure 4.13 SEM micrographs of 190 000 g/mol PS/THF fibres electrospun under varying humidity: (a) <25%, (b) 31-38%, (c) 40-45%, (d) 50-59%, (e) 60-72%[1].

Casper et al[1] also found that pore size was dependent upon the molecular weight, with high molecular weight polymers being less prone to pore formation[4]. They deduced that the concept of breath figures alone would not fully explain this molecular weight dependency. If pore formation was based solely on breath figures, pore size would primarily be a function of humidity and molecular weight would not play a major role in determining the size or shape of porous structures.

Another possible mechanism for pore formation is phase separation as was proposed first by Megelski et al.[3] Thermodynamic instability is the driving force behind phase separation. Decreasing temperature, loss of solvent, or increase in nonsolvent causes a solution to become thermodynamically unstable. During the electrospinning process, all three of these situations are encountered, thus making phase separation a likely contributing mechanism of pore formation. Vapour induced phase separation involves the penetration of a nonsolvent vapour causing phase separation of the polymer solution. In this case water is the nonsolvent, which induces the phase separation of the homogeneous mixture of PS and THF.

Rapid evaporation of the solvent as the jet is being projected from the needle causes lowering of the temperature on the fibre, thus making Thermally Induced Phase Separation (TIPS) a viable explanation for pore formation.[16] During the evaporation of solvent, pore formation begins when the temperature reaches the bimodal temperature and continues to grow until the crystallization temperature of the polymer is reached. Phase separation occurs by the mechanisms of nucleation and growth (NG) and/or spinodal decomposition (SD). Generally, an interconnected pore structure is characteristic of the NG mechanism while closed pores are produced by SD.[5,17] On the basis of structural features only, SD is the most probable mechanism for phase separation in the electrospinning of PS/THF fibres since cross-section images of the fibres indicate that the pores do not interconnect through the fibre and are merely surface features.(figure 4.14)

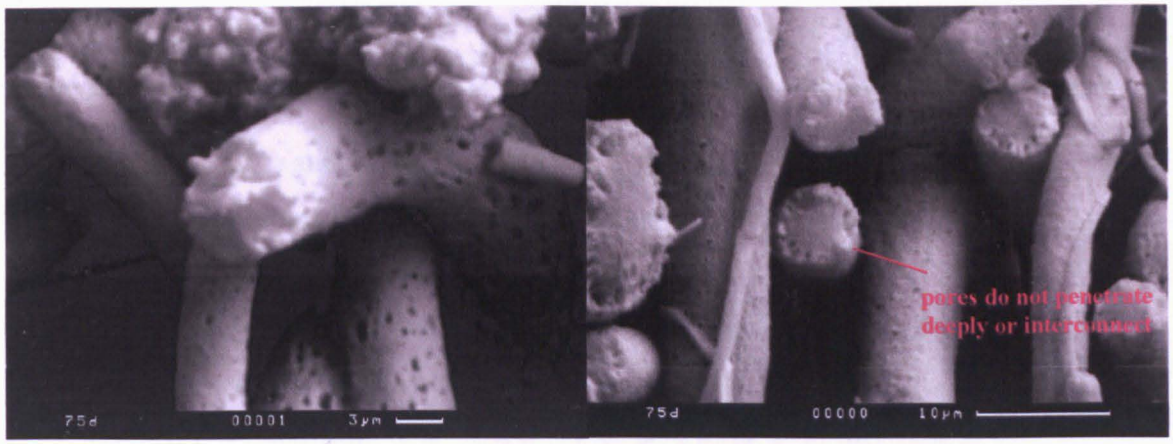

Figure 4.14 Cross section images of PLLA fibres with porous surfaces. It can be seen that the pores do not interconnect and the fibres are solid internally.

The molecular weight effects on pore formation could be due to phase separation or may be just an issue of viscosity, with more viscous jets being less prone to pore formation. What is understood is that neither the phase separation theory nor the formation of breath figures alone fully explains the phenomena of pore formation in electrospun fibres, rather a combination of the two.

4.5 References

1. Casper, C. L., Yamaguchi, N., Kiick, K. L. & Rabolt, J. F. Functionalizing Electrospun Fibers with Biologically Relevant Macromolecules. *Biomacromolecules* **6,** 1998-2007 (2005)
2. Boker, A. et al. Hierarchical nanoparticle assemblies formed by decorating breath figures. *Nature materials* **3,** 302-306.(2004)
3. Megelski, S., Stephens, J. S., Chase, D. B. & Rabolt, J. F. Micro- and nanostructured surface morphology on electrospun polymer fibers. *Macromolecules* **35,** 8456-8466 (2002).
4. Casper, C. L., Stephens, J. S., Tassi, N. G., Chase, D. B. & Rabolt, J. F. Controlling Surface Morphology of Electrospun Polystyrene Fibers: Effect of Humidity and Molecular Weight in the Electrospinning Process. *Macromolecules* **37,** 573-578 (2004).
5. Cui, L., Peng, J., Ding, Y., Li, X. & Han, Y. Ordered porous polymer films via phase separation in humidity environment. *Polymer* **46,** 5334-5340 (2005).
6. Park, M. S. & Kim, J. K. Breath Figure Patterns Prepared by Spin Coating in a Dry Environment. *Langmuir* **20,** 5347-5352 (2004).
7. Boland, T., Dufrene, Y., Barger, B. & Lee, G. Molecular basis of cell adhesion to polymers characterized AFM. *Critical reviews in biomedical engineering* **28,** 195-196.(2000)
8. Khan, S. P., Auner, G. G. & Newaz, G. M. Influence of nanoscale surface roughness on neural cell attachment on silicon. *Nanomedicine* **1,** 125-129 (2005).
9. Min, B.-M., You, Y., Kim, J.-M., Lee, S. J. & Park, W. H. Formation of nanostructured poly(lactic-co-glycolic acid)/chitin matrix and its cellular response to normal human keratinocytes and fibroblasts. *Carbohydrate Polymers* **57,** 285-292 (2004).
10. Phimphivong, S. & Saavedra, S. S. Characterizing cell adhesion to polymers by time-resolved, total internal reflection fluorescence microscopy. *Book of Abstracts, 213th ACS National Meeting, San Francisco, April 13-17,* COLL-303 (1997).

11. Ribeiro, R. et al. Biocomposites: Exploring surface texture for cell adhesion. *Journal of ASTM International* **2**, No pp. given (2005).

12. Oxford, I. *http: www.ebsd.com/sampleprep3.htm* (2004).

13. Srinivasarao, M. Three-Dimensionally Ordered Array of Air Bubbles in a Polymer Film. *Science* **292**, 79 (2001).

14. Srinivasarao, M., Collings, D., Philips, A. & Patel, S. Three-dimensionally ordered array of air bubbles in a polymer film. *Science* **292**, 79-83(2001)

15. Greenspan, L. 'Humidity fixed points of binary saturated aqueous solutions. *J. of Research, National Bureau of Standards* **81A**, 89-96 (1977).

16. Ryan A, J. Wilkinson, A. N. Polymer processing and structure development. Kluwer Academic Publishers (1998).

17. Bognitzki, M. et al. Preparation of fibers with nanoscaled morphologies: Electrospinning of polymer blends. *Polymer Engineering and Science* **41**, 982-989 (2001).

Chapter 5 - Drug Delivery from PLLA Fibres

5.1 Introduction

PLLA has been widely used in drug delivery applications due to its high biocompatibility and its propensity to degrade in aqueous conditions,[1-5] Drug delivery from electrospun fibres has also been studied quite extensively, for a wide range of polymer/drug systems [6-16]and the relationship between fibre diameter and rate of delivery has been widely reported. The relationship between fibre porosity and drug delivery however, has not yet been studied. Being able to control the surface morphology of electrospun fibres opens up the possibility of "fine tuning" the release of drugs from electrospun fibres.

The polymer/drug system chosen was PLLA/tetracycline. PLLA was chosen as it has been extensively studied in previous work and the porosity control was predictable (see chapter 4). Tetracycline was chosen in order that the results could be compared to those of *L. Wang* who studied the release of tetracycline from collagen fibres.[16] Also tetracycline is a common broad spectrum antibiotic which has been intensively studied so there was much information available on its release from different systems.[8,17-23]

The term broad-spectrum antibiotic refers to an antibiotic with activity against a wide range of disease-causing bacteria.[24] This is in contrast to a narrow-spectrum antibiotic which is effective against only specific families of bacteria. Tetracyclines are oral antibiotics often used to treat skin diseases such as acne and perioral dermatitis.[25] Release from electrospun fibres may enable the development of new generation micro-capsules with tailored release properties, which could replace old generation pills and capsules which have more crude "all at once" release profiles. There is also the potential to use electrospun products as "smart" wound dressings which can release antibiotics directly to the point of infection.[6,26-28]

5.2 *Experimental*

5.2.1 *Calibration of UV Spectrometer*

Fine ground Tetracycline Hydrochloride powder was obtained from Sigma-Aldrich. The powder was dissolved in distilled water to a concentration of 0.20mg/mL and a UV/Vis (Ultraviolet/Visible) spectrum was taken on a Cary 50 UV/Vis spectrophotometer. From this spectrum the wavelength of maximum absorbtion for the antibiotic was determined. This was noted to be at 355.5nm.

A calibration curve for Tetracycline in water was then constructed by making up a range of solutions of increasing concentration. Very accurate solutions of tetracycline in distilled water with the concentrations 0.025, 0.05, 0.075 and 0.15 mg/ml were made up in volumetric flasks and the absorbance of each at 355.5nm was measured. When concentration was plotted against Absorbance, a straight line was obtained from which the extinction coefficient could be calculated this being the gradient of the graph (using Beer-Lambert law[29])(figure 5.1). This calibration allows tetracycline release to be quantified. Tetracycline release will be monitored by the UV/Vis spectrometer, whereby the absorbance levels at 355.5nm of a sample solution will be monitored over time and converted to concentrations of antibiotic released into solution using the extinction coefficient.

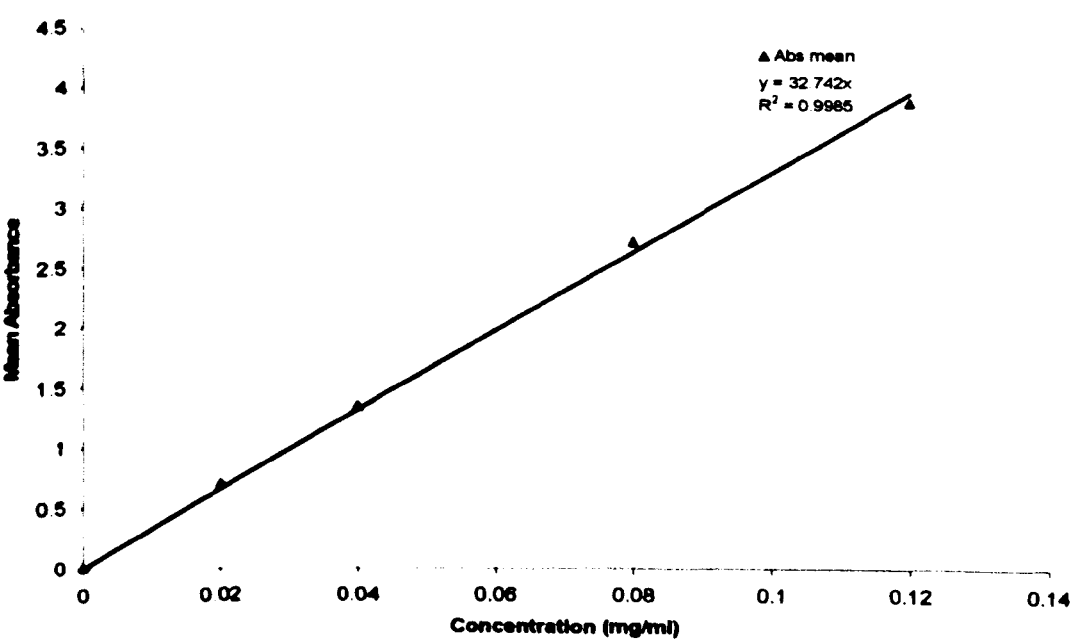

Figure 5.1 Calibration Curve for Tetracycline Hydrochloride in Water at 355.5nm.

5.2.2 *Electrospinning*

The electrospinning solutions were prepared as suspensions of tetracycline in a 7.5wt% solution of PLLA in dry DCM as tetracycline is insoluble in organic solvents. In order to increase the encapsulation of the tetracycline in the fibres the powder was further ground with a pestle and mortar to give extremely fine particles (<1μm measured by light microscopy).The ratio of PLLA to tetracycline was 10:1 (wt:wt). The solutions were stirred extensively and then placed in a sonic bath for 10 minutes to ensure an even distribution of the drug in solution. The time between sonication and spinning was kept to a minimum in order to reduce the amount of settling of the suspension.

The solution was drawn up into a 2ml disposable syringe which was then fitted with a Ga20 blunt-ended dispensing needle. The electrospinning rig was the one used for the controlled porosity experiment (chapter 4)(figure 5.2). The solution was pumped at 2.2ml/hr, over a distance of 35cm, toward a flat metal plate collector covered with aluminium foil, with a voltage of 20kV. 2 ml of solution was spun for each humidity used. Three different humidities were used (15%, 34% and 90%) in order to produce smooth, slightly porous and very porous fibres. Samples were removed from the collector after spinning.

Each sample was scraped off the aluminium foil and weighed and then cut into 2.8mg pieces, placed in sealed bags and refrigerated.

On removing samples from the fridge care was taken to let them warm to room temperature before opening the bags in order to reduce condensation on the fibres.

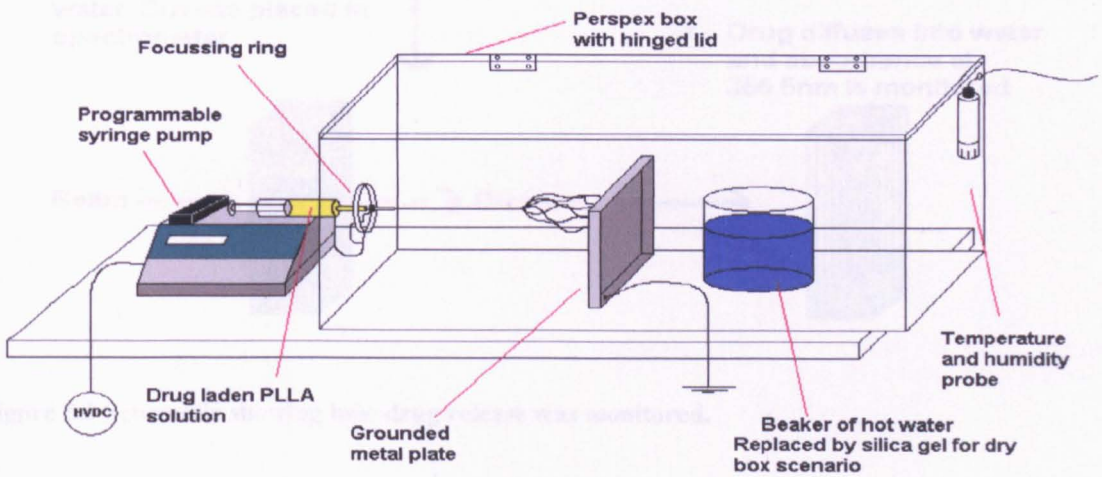

Figure 5.2 Electrospinning apparatus for incorporation of tetracycline into fibres with a controlled surface morphology.

5.2.3 Drug release studies

A cuvette was firstly filled with distilled water and placed in a UV/Vis spectrophotometer and held at 37°C for 10 minutes. After 10 minutes a fixed-wavelength scan was run on the water at 355.5nm. This was taken as the blank and the machine was zeroed accordingly.

One of the previously cut pieces of electrospun product was taken with tweezers and carefully placed on the surface of the water in the cuvette and a lid placed on the cuvette. The lid was designed such that it would push the sample under the water and fully submerge it. Care was taken not to allow fibres to stray in front of the beam as this would cause erroneous results. Once the sample was fully submerged the sampling began. Sampling involved a scan (at 355.5nm) of the solution being taken every minute for 30 minutes, and every 30 minutes thereafter for a period of 24hrs. Throughout this period the temperature was held at 37°C (figure 5.3).

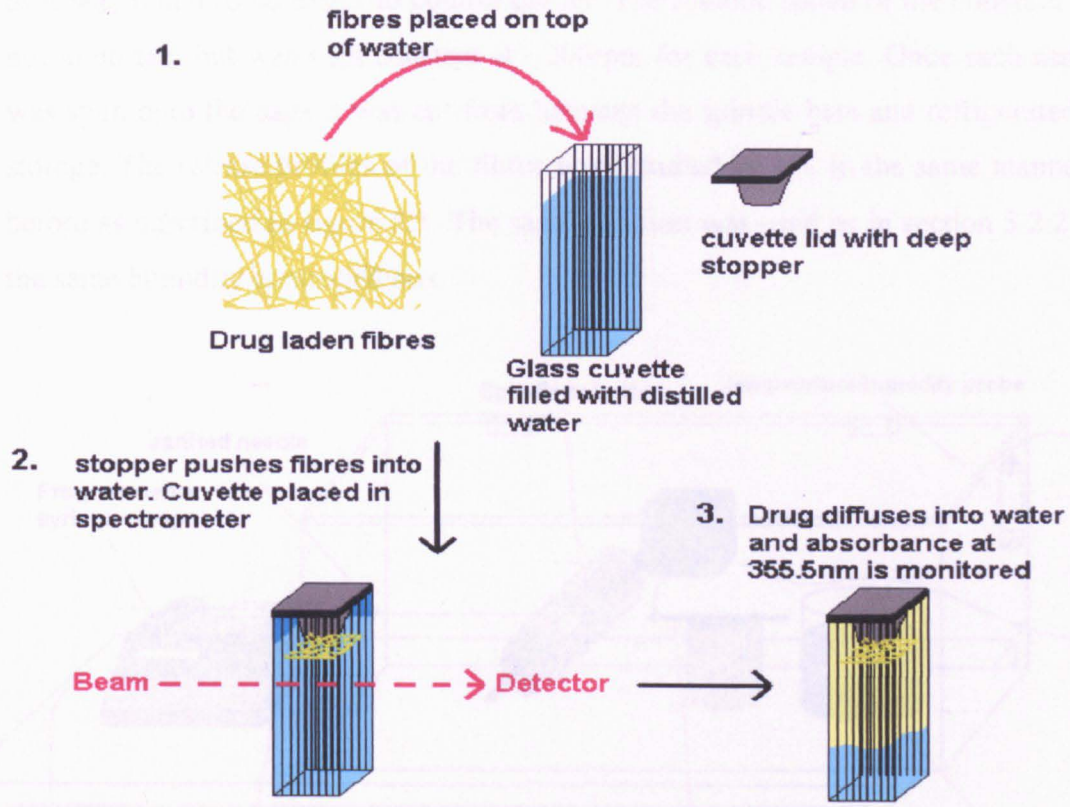

Figure 5.3 Schematic showing how drug release was monitored.

5.2.4 *Electrospinning of Evenly Distributed Drug-Laden Fibres*

A limitation of collecting fibres on a flat plate meant aggregation of drug on the foil side of the fibre mat, giving rise to a concentration gradient of drug throughout the mat. This concentration gradient probably arose as a result of condensation on the surface of the metal collector tetracycline is very soluble in water so his condensation would draw out the drug from the fibres making drug release studies very difficult to control and reproduce.

Ensuring even distribution of drug throughout the sample required the collection of fibres on an open cage structure. The apparatus used was the same as that used in chapter 5 for the alignment of fibres with a reverse polarity needle-to-needle setup. This apparatus was then placed inside the humidity controlled box (figure 5.4).

Alignment of the fibres was not essential but reverse polarity spinning was still used with the collector being charged to 20kV and the delivery needle being earthed, as it was found to be easier to control the jet. The rotation speed of the collector was not important but was kept constant at ~200rpm for each sample. Once each sample was spun onto the cage it was cut from between the spindle bars and refrigerated for storage. The release profiles of the fibres were studied by UV in the same manner as before as described in figure 5.3. The same solution was used as in section 5.2.2 and the same humidity controlled box.

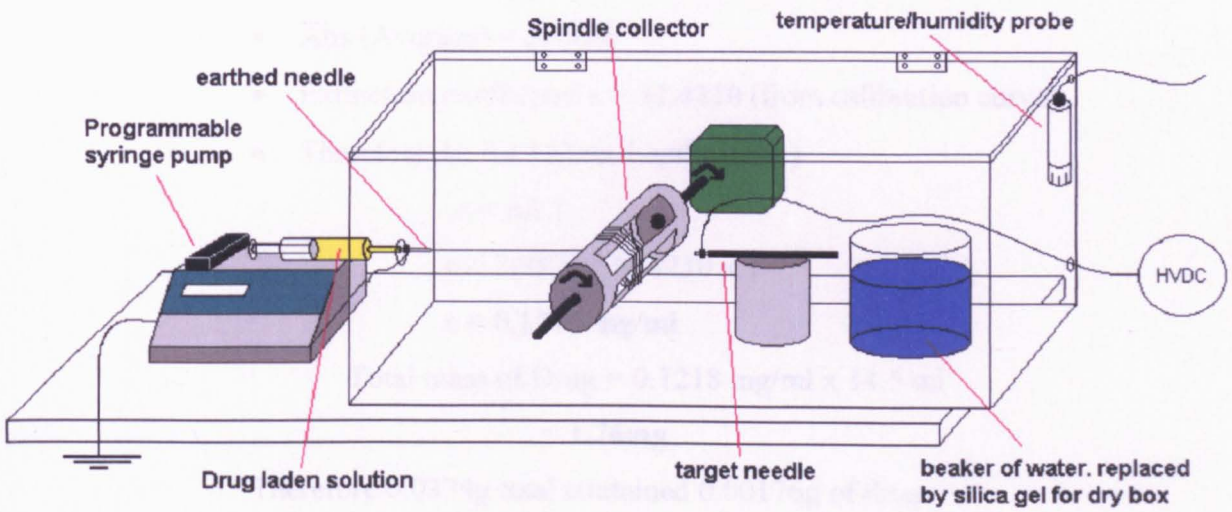

Figure 5.4 Apparatus for ensuring even distribution of drug throughout electrospun fibre.

5.2.5 Encapsulation

The degree of encapsulation was calculated for each sample. Encapsulation refers to the percentage of drug that ended up in the final electrospun mat from the amount that was put into the spinning solution. It is a method of showing the efficacy of a drug loading technique. In order to work this out a known amount (~0.05g) of product was taken and dissolved in DCM in a separating funnel. This has the effect of dissolving all the fibres and releasing the encapsulated drug into the DCM as a suspension. Distilled water was then added to the solution into which the highly hydrophilic drug would separate. The aqueous layer was then separated from the organic and the organic layer washed through three times to remove all of the drug. All the aqueous washings were collected together and weighed to get a total volume of water.

A small sample of this water was then put in a cuvette and an absorbance reading taken on the UV/Vis Spectrometer at 355.5nm. This was compared to the calibration curve to give a concentration of drug in the washings. From this, the total mass of drug in the fibre sample could be determined.

Sample Calculation:-

- Mass of Fibres Dissolved in DCM = **37.4mg**
- Mass of Washings = 14.5g ≡ **14.5ml**
- Abs (Average) = **3.9876**
- Extinction coefficient ε = **32.4210** (from calibration curve)
- Therefore A= ε c l (Beer Lambert law)

$$c = A/\varepsilon l$$

$$c = 3.9876 / 32.4210 \times 1$$

$$\mathbf{c = 0.1218\ mg/ml}$$

Total mass of Drug = 0.1218 mg/ml x 14.5 ml

= **1.76mg**

Therefore 0.0374g total contained 0.00176g of drug

i.e PLLA : TC = 0.03564 : 0.00176

Ratio pre-spinning = 10 : 1 or **0.03564 : 0.003564**

Degree of encapsulation = 0.00176 / 0.003564 x 100

= **49. 4%**

The significance of this result is that it shows how inefficient the drug loading of tetracycline into PLLA fibres is using this method. Tetracycline is highly soluble in water but insoluble in all PLLA electrospinning solvents (DCM, chloroform, THF). The result of this is that tetracycline must be loaded into PLLA fibres from a suspension of the drug in PLLA/DCM solution. A known amount of drug is suspended in the viscous spinning solution which is stirred and sonicated to evenly distribute the drug particles. This solution is then transferred to a spinning syringe and then spun. The calculation for the degree of encapsulation shows just how much drug is lost in the transferral process probably as a result of the suspension settling out. Knowing the degree of encapsulation is essential to calculate the amount of drug present in a sample.

5.3 Results and Discussion

5.3.1 Fibre Morphologies

To test the hypothesis that controlling the pore size on the fibres could control the rate of drug release from the fibres, with more porous PLLA fibres allowing faster release of tetracycline into aqueous medium, a series of experiments were conducted. Fibres were spun at four different humidities, these being 7%, 40%, 84% and 90% relative humidity. The average pore perimeters of the fibres are shown in figure 5.5 and SEM micrographs of the drug laden fibres in Figure 5.6.

As can be seen from figures 5.5 and 5.6 the fibres become more porous as humidity increases. What can also be seen is the difference between these fibres and those spun without tetracycline in chapter 4. Whereas the fibres spun from 7.5wt% PLLA/DCM in chapter 4 were all roughly the same diameter there is a far wider distribution of diameters in the samples here. Also the fibres spun with tetracycline are less uniform and have many additional large surface features.

The variations in diameter are most probably a result of the drug being ionic. As discussed in chapter 1.6.8, the addition of ionic salts leads to a decrease in the diameter of the fibre. One assumes that the addition of tetracycline hydrochloride will affect the spinning, and sections of the electrospinning jet with a higher concentration of drug will be thinner.

As for the additional large surface features it is believed that these are crystals of tetracycline which have not been completely encapsulated by the fibre. The non-uniform nature of the fibre surface also suggests large drug particles encapsulated under the fibre surface, whereby the fibre isn't quite large enough to accommodate the particle(figure 5.7).

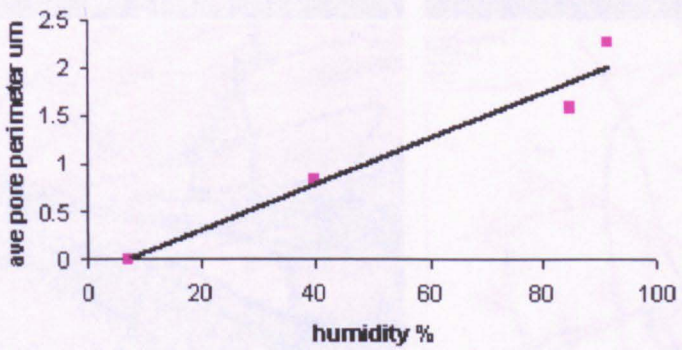

Figure 5.5 Graph showing variation of pore perimeter with humidity in tetracycline- laden PLLA fibres spun from 7.5wt% solution of PLLA in DCM. PLLA:Tetracycline = 10:1.

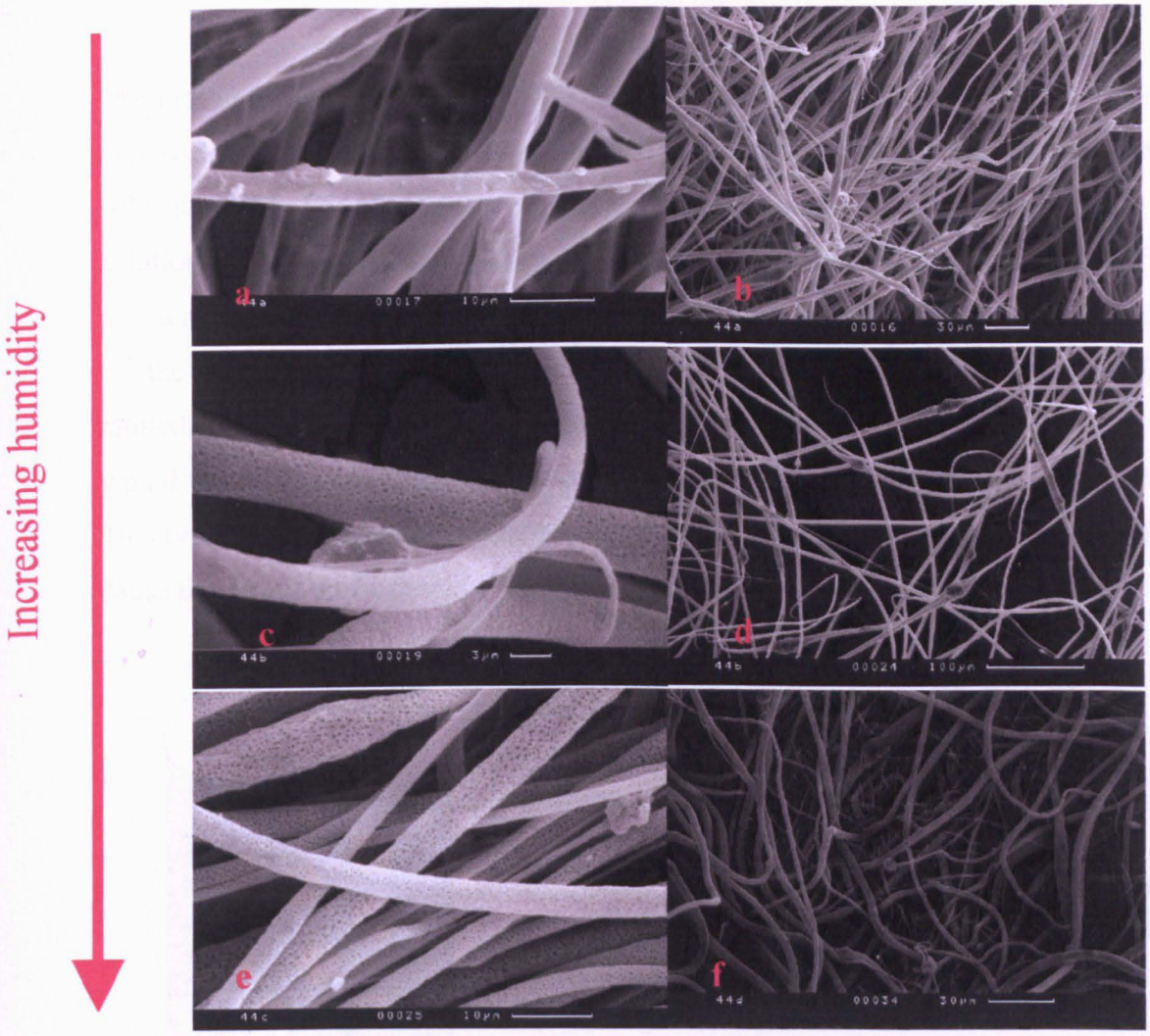

Figure 5.6 SEM micrographs of tetracycline-laden PLLA fibres : (a) and (b) spun at 7% relative humidity (R.H), (c) and (d) spun at 40% humidity, (e) and (f) spun at 84% humidity.

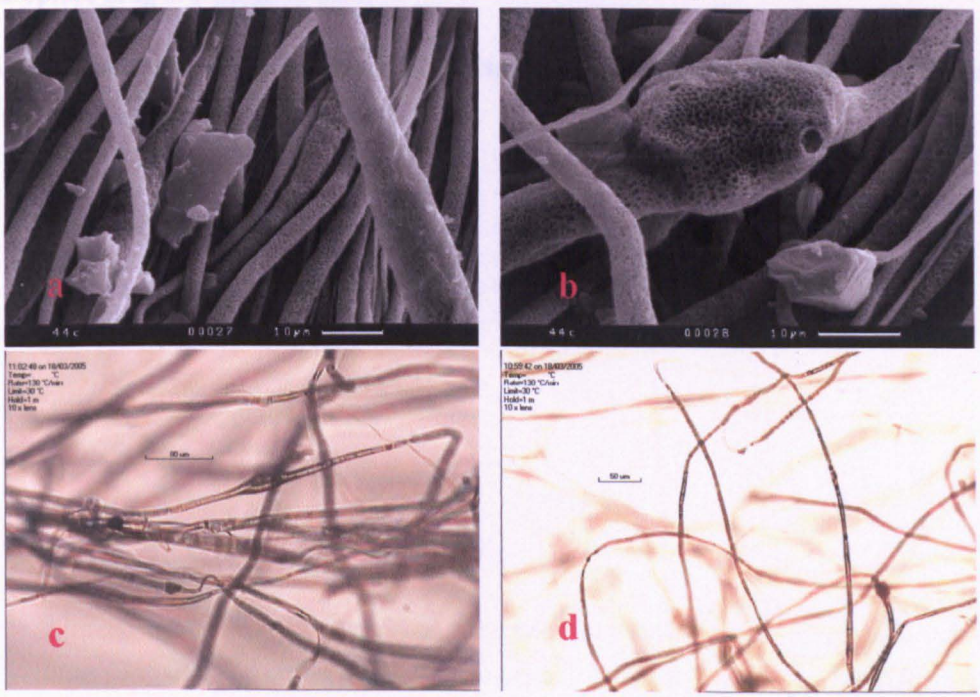

Figure 5.7 a) SEM micrograph showing surface crystals of tetracycline on PLLA fibres b) SEM micrograph of drug-laden PLLA fibre showing encapsulated tetracycline stretching the walls of the fibre and below that a surface crystal of tetracycline c) and d)Light microscope images showing tetracycline encapsulated in PLLA.

The reason for the formation of these surface crystals and large encapsulated particles comes down to the insolubility of tetracycline hydrochloride in the electrospinning solvent DCM. For this reason the drug will always form a suspension with the solution and not actually dissolve. This is the reason why the drug was ground in a pestle and mortar prior to being added to the solution. It was inevitable then that some of the ground particles would be too large to become encapsulated. With a monodisperse particle diameter of less than or equal to that of the fibre diameter one would expect the drug-laden fibre to have a "string of pearls" structure (figure 5.8). This type of encapsulation can be seen in figure 5.7 but it is the larger particles which cause the deviation from this.

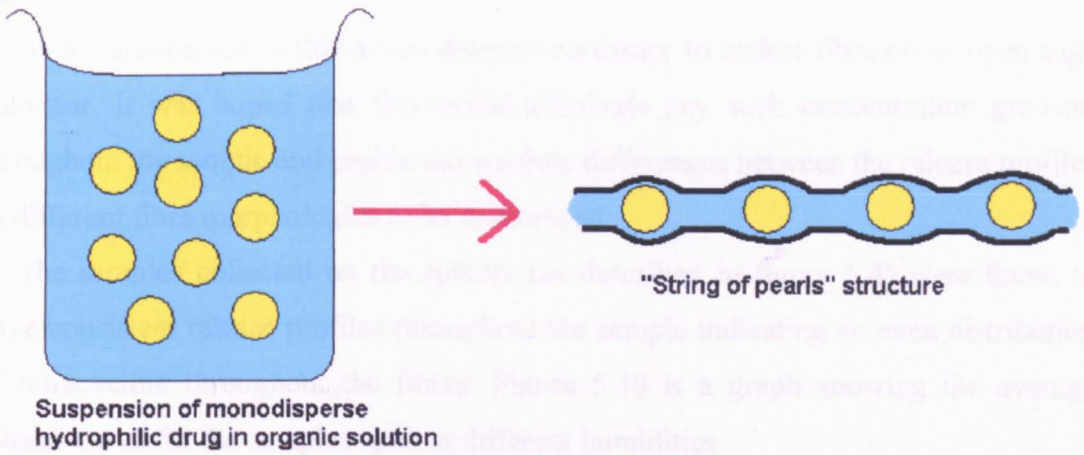

Figure 5.8 Schematic showing formation of a "string of pearls" structure when electrospinning a solution of monodisperse insoluble particles.

5.3.2 Drug Release

The first samples to be monitored for drug release were those collected on a flat plate collector (figure 5.2). The shortcomings of this method quickly became apparent when it was found that results were non-reproducible. The release profiles all had the same general shape but were inconsistent in the amount of tetracycline being released. On closer inspection it was found that fibres which were closest to the metal collecting surface released far more tetracycline than those collected later. This confirmed what was mentioned in 5.2.4, that the tetracycline was probably drawn toward the collector surface as a result of condensation upon that surface. Figure 5.9 shows two release curves for the same fibre mat with sample a) being taken from closer to the metal surface(i.e earliest collected fibres) and b) from fibres which were deposited later.

As a consequence of this it was deemed necessary to collect fibre on an open cage collector. It was hoped that this would eliminate any such concentration gradient throughout the sample and enable more subtle differences between the release profiles of different fibre morphologies to be determined.

The samples collected on the spindle (as described in figure 5.4) were found to have consistent release profiles throughout the sample indicating an even distribution of tetracycline throughout the fibres. Figure 5.10 is a graph showing the average release curve for the samples spun at different humidities.

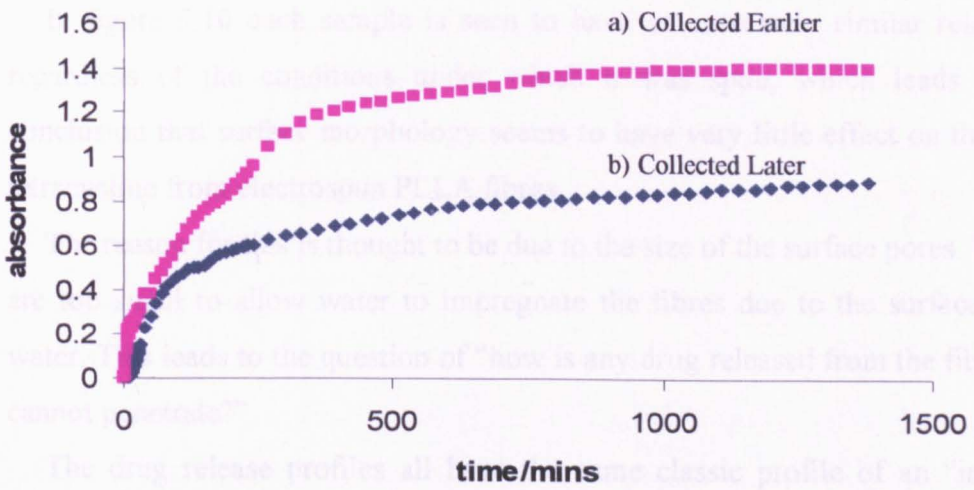

Figure 5.9 Release curves from two sections of the same electrospun sample. The earlier collected fibres a) closest to the metal surface release more drug than those collected further from the metal surface b). Absorbance is related to drug concentration by extinction coefficient ε=32.42 and the equation c=A/ εl.

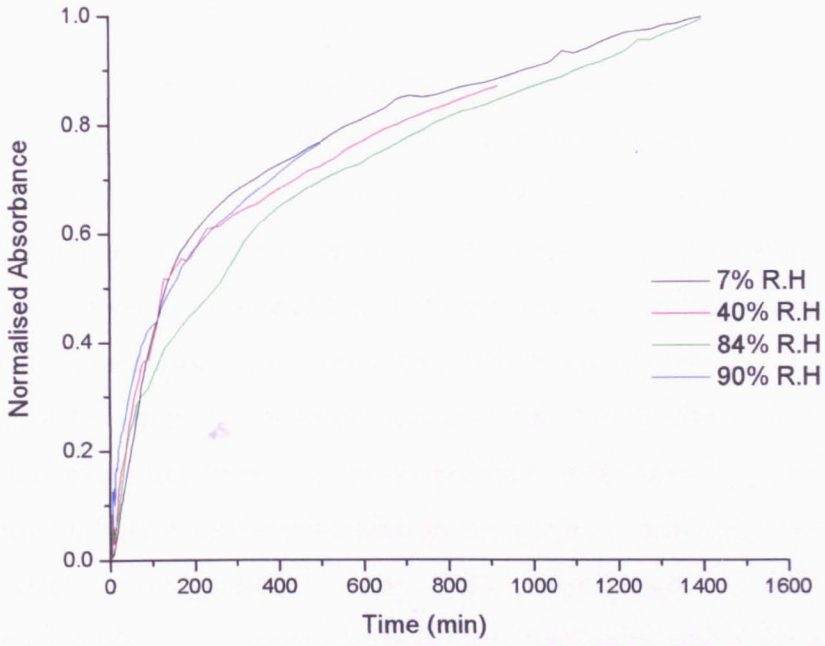

Figure 5.10 Graph showing the average release curves of tetracycline from PLLA fibres spun at different humidities.

Even though the problem of concentration gradients throughout individual samples had been overcome, the total encapsulation in different samples was still slightly different so in order to compare the release curves for fibres spun at different humidities the absorbance values were firstly normalised.

In figure 5.10 each sample is seen to have an extremely similar release profile regardless of the conditions under which it was spun, which leads one to the conclusion that surface morphology seems to have very little effect on the release of tetracycline from electrospun PLLA fibres.

The reason for this is thought to be due to the size of the surface pores. These pores are too small to allow water to impregnate the fibres due to the surface tension of water. This leads to the question of "how is any drug released from the fibres if water cannot penetrate?"

The drug release profiles all have the same classic profile of an "initial burst" followed by a "sustained release". This "initial burst" comes about though the release of drugs either on the fibre surface, half penetrating the fibre surface or very close to the fibre surface but still within the fibre. All three of these situations lead to rapid

dissociation of the drug from the fibre and are a result of incomplete encapsulation. The average encapsulation for these drug/fibre combinations worked out at ~50%.

The "sustained release" comes from the degradation of the PLLA fibres in the water which eventually releases the tetracycline from deep within the fibre. PLLA fibres can take over 2-3 months to degrade[1,2] and expose their core to surrounding aqueous medium. The effects of surface morphology on the degradation of PLLA fibres have not yet been studied and there may well be a relationship between the two over longer time periods. This could lead to finer control over the "sustained release" of encapsulated drugs but certainly not over the "initial burst". A better method of control however, may be to change the polymer rather than its morphology. Release from within a fibre could be controlled by using more easily degraded polymers such as poly(lactide-co-glycolide)[30,31], or block co-polymers of PLLA with poly-ethyleneoxide (PEO), examples of which have been made within the research group.[32] The hydrophilic nature of PEO increases the rate of degradation within the block copolymer and would increase the rate of release of encapsulated drugs.

In order to control the "initial burst" the fibres could firstly be washed in a non-solvent for both the fibre and drug in order to remove any loose drug crystals on the fibre surface. This alone would not be sufficient in stopping the "initial burst". In order to achieve this one would have to increase drug encapsulation either by decreasing particle size or increasing fibre diameter. Average drug encapsulation for this system was only ~50% so half of the drug did not find it's way into the fibres and was either lost in transferral of solution or was too large to become incorporated. Light microscopy showed the tetracycline particles to have an average diameter of <1μm which is small enough to comfortably fit inside most PLLA fibres. However, aggregation of particles in the suspension gives rise to particles which are much larger than the average fibre diameter.

Work done on tetracycline release from cellulose fibres shows how changing the fibre diameter has a drastic effect on the release profile (figure 5.11)[16], whereby a larger diameter fibre shows a much more sustained release than a thinner one of the same polymer. Encapsulation data was not supplied but it can be assumed that the thicker fibres had incorporated more tetracycline than the thinner ones.

This increased encapsulation has the effect of decreasing the initial burst as there is less free drug on the surface of the fibre of protruding from the walls of the fibres.

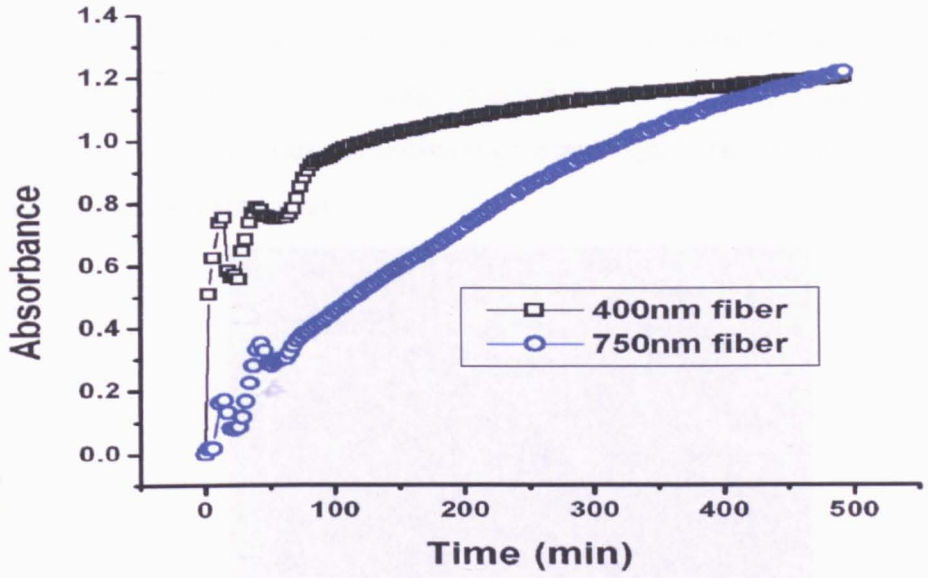

Figure 5.11 Release profiles of tetracycline from electrospun fibres of cellulose. The black curve corresponds to the release from fibres with an average diameter of 400nm, the blue curve from fibres with an average diameter of 750nm.[16]

The limitations of such drug suspension systems are brought about by the different solubilities of the drug and carrier. An improvement to the system could be brought about by either using a polymer which was soluble in water, or a drug which was soluble in the spinning solvent. A situation whereby a drug/polymer solution rather than a suspension was produced would ensure complete encapsulation of the drug inside the fibres and would probably yield more consistent fibre morphologies as opposed to the inconsistent ones seen in figures 5.6 and 5.7. The question would arise as to how the drug would be distributed within the fibre if it were totally miscible with the polymer solution; would it, for example be more prevalent in the outer surface or the core of the fibre, or equally abundant in both? We have an indication of how a soluble drug may be distributed from pictures of rhodamine-laden fibres spun for use in chapter 6.5 for differentiation of cells from fibres using fluorescent microscopy. Rhodamine is a fluorescent dye which is soluble in DCM and when introduced to a spinning solution of PLLA in DCM mixes evenly throughout the solution. Spinning of the solution yields rhodamine-stained fibres which glow red under UV excitation. Images taken with a confocal microscope of unaligned rhodamine-stained PLLA fibres are shown in figure 5.12 (rhodamine has been assigned a yellow colour using

the imaging software). These images show a seemingly even distribution of rhodamine dye throughout the PLLA fibres with no discrete "pockets" of rhodamine dye. This suggests that a drug/carrier system whereby both constituents were dissolved in the same solution, rather than a suspension of drug in carrier, would yield evenly laden fibres. It does not however give any insight of how such a system would release its encapsulated load.

Figure 5.12 Rhodamine-laden PLLA fibres(spun from 7.5wt% PLLA in DCM with 0.5wt% rhodamine) showing even distribution of dye throughout the fibres. It is expected that a drug which was soluble in the spinning solvent would be distributed as evenly as the rhodamine is in this system.

5.4 References

1. Zu, E.-f., Yang, Q.-f., Ma, A.-j., Shi, K. & Zhu, F. Study on biocompatibility and degradation of poly(L-lactic acid). *Zhongguo Jiaonianji* **14**, 7-10 (2005).
2. Guidoin, M.-F., Guidoin, R., Frayssinet, P., Legrand, A. & How, T. Poly-L-Lactide Surfaces Subjected to Long-Term Cell Cultures. Cell Proliferation and Polymer Degradation. *Artificial Cells, Blood Substitutes, and Biotechnology* **33**, 411-422 (2005).
3. Cam, D., Hyon, S. H. & Ikada, Y. Degradation of high molecular weight poly(L-lactide) in alkaline medium. *Biomaterials FIELD Publication Date:1995* **16**, 833-43. FIELD Reference Number: FIELD Journal Code:8100316 FIELD Call Number:.
4. von Recum, H. A., Cleek, R. L., Eskin, S. G. & Mikos, A. G. Degradation of polydispersed poly(L-lactic acid) to modulate lactic acid release. *Biomaterials FIELD Publication Date:1995* **16**, 441-7. FIELD Reference Number: FIELD Journal Code:8100316 FIELD Call Number:.
5. Bergsma, J. E., de Bruijn, W. C., Rozema, F. R., Bos, R. R. & Boering, G. Late degradation tissue response to poly(L-lactide) bone plates and screws. *Biomaterials FIELD Publication Date:1995* **16**, 25-31. FIELD Reference Number: FIELD Journal Code:8100316 FIELD Call Number:.
6. Casper, C. L., Yamaguchi, N., Kiick, K. L. & Rabolt, J. F. Functionalizing Electrospun Fibers with Biologically Relevant Macromolecules. *Biomacromolecules*, ACS ASAP.
7. Hansen, L. M., Kataphinan, W., Reneker, D. H. & Smith, D. J. Production of superabsorbent electrospun nanofibers. *Abstracts of Papers, 227th ACS National Meeting, Anaheim, CA, United States, March 28-April 1, 2004*, PMSE-303 (2004).
8. Kenawy, E. R. et al. Release of tetracycline hydrochloride from electrospun poly(ethylene-co-vinylacetate), poly(lactic acid), and a blend. *Journal of Controlled Release* **81**, 57-64 (2002).
9. Sanders, E. H., Kloefkorn, R., Bowlin, G. L., Simpson, D. G. & Wnek, G. E. Two-Phase Electrospinning from a Single Electrified Jet: Microencapsulation of Aqueous Reservoirs in Poly(ethylene-co-vinyl acetate) Fibers. *Macromolecules* **36**, 3803-3805 (2003).

10. Tan, S. T., Wendorff, J. H., Pietzonka, C., Jia, Z. H. & Wang, G. Q. Biocompatible and biodegradable polymer nanofibers displaying superparamagnetic properties. *ChemPhysChem* **6**, 1461-1465 (2005).

11. Bhide, M. Controlled release of nitric oxide from electrospun nanofiber transdermal matrices. *Abstracts, 35th Great Lakes Regional Meeting of the American Chemical Society, Chicago, IL, United States, May 31-June 2*, 251 (2003).

12. Chew, S. Y., Wen, J., Yim, E. K. F. & Leong, K. W. Sustained Release of Proteins from Electrospun Biodegradable Fibers. *Biomacromolecules* **6**, 2017-2024 (2005).

13. Gibson, P. W., Schreuder-Gibson, H. L. & Rivin, D. Electrospun fiber mats: Transport properties. *Aiche Journal* **45**, 190-195 (1999).

14. Jiang, H., Fang, D., Hsiao, B., Chu, B. & Chen, W. Preparation and characterization of ibuprofen-loaded poly(lactide-co-glycolide)/poly(ethylene glycol)-g-chitosan electrospun membranes. *Journal of Biomaterials Science, Polymer Edition* **15**, 279-296 (2004).

15. Kenawy, E. R. et al. Release of tetracycline hydrochloride from electrospun polymers. *Abstracts of Papers of the American Chemical Society* **223**, 95-POLY (2002).

16. Wang, L. Electrospinning Cellulose derivative fibres. *Presentation to NCD Group, Sheffield* (2004).

17. Bajpai, A. K., Bajpai, J. & Shukla, S. Release dynamics of tetracycline from a loaded semi-interpenetrating polymeric material of polyvinyl alcohol and poly(acrylamide-co-styrene). *Journal of Materials Science: Materials in Medicine* **14**, 347-357 (2003).

18. Markman, C., Fracalanzza, S. E. L., Novaes, A. B., Jr. & Novaes, A. B. Slow release of tetracycline hydrochloride from a cellulose membrane used in guided tissue regeneration. *Journal of Periodontology* **66**, 978-83 (1995).

19. Park, Y. J. et al. Enhanced guided bone regeneration by controlled tetracycline release from poly(L-lactide) barrier membranes. *Journal of biomedical materials research FIELD Publication Date:2000* **51**, 391-7. FIELD Reference Number: FIELD Journal Code:0112726 FIELD Call Number:.

20. Petratos Peter, B., Chen, J., Felsen, D. & Poppas Dix, P. Local pharmaceutical release from a new hydrogel implant. *Journal of surgical research FIELD*

Publication Date:2002 **103**, 55-60. FIELD Reference Number: FIELD Journal Code:0376340 FIELD Call Number:.

21. Pevzner, V., Ruderman, M. & Avramoff, A. in *Brit. UK Pat. Appl.* 45 pp. ((Dexcel Ltd, Israel). Gb, 2005).
22. Schwach-Abdellaoui, K., Monti, A., Barr, J., Heller, J. & Gurny, R. Optimization of a novel bioerodible device based on auto-catalyzed poly(ortho esters) for controlled delivery of tetracycline to periodontal pocket. *Biomaterials FIELD Publication Date:2001* **22**, 1659-66. FIELD Reference Number: FIELD Journal Code:8100316 FIELD Call Number:.
23. Song, Z., Zhou, D., Yin, G. & Zheng, C. In vitro release of tetracycline hydrochloride from a-TCP cement. *Shengwu Yixue Gongchengxue Zazhi* **20**, 586-589 (2003).
24. Wikipedia. *http://en.wikipedia.org/wiki/Broad-spectrum_antibiotic* (2005).
25. Dermatology, N. *http://dermnetnz.org/treatments/tetracycline.html* (2003).
26. Huang, L., Nagapudi, K., Apkarian, R. P. & Chaikof, E. L. Engineered collagen-PEO nanofibers and fabrics. *Journal of Biomaterials Science-Polymer Edition* **12**, 979-993 (2001).
27. Huang, L., Apkarian, R. P. & Chaikof, E. L. High-resolution analysis of engineered type I collagen nanofibers by electron microscopy. *Scanning* **23**, 372-375 (2001).
28. Kenawy, E. R. et al. Electrospinning of poly(ethylene-co-vinyl alcohol) fibers. *Biomaterials* **24**, 907-913 (2003).
29. Atkins, P. W. The Elements of Physical Chemistry. *Oxford University Press*, 414 (1996).
30. Chen, X., Ooi, C. P., Lye, W. S. & Lim, T. H. Sustained release of ganciclovir from poly(lactide-co-glycolide) microspheres. *Journal of Microencapsulation* **22**, 621-631 (2005).
31. Win, K. Y. & Feng, S.-S. In vitro and in vivo studies on vitamin E TPGS-emulsified poly(,-lactic-co-glycolic acid) nanoparticles for paclitaxel formulation. *Biomaterials* **27**, 2285-2291 (2006).
32. Mai, S. M. A., A. ; Norton, D ; Ryan, A J. Synthesis and Charaterisation of Block Co-polymers of Poly-ethyleneoxide and PLLA with Different Architechtures. *Unpublished work* (2006).

6.1 Current Technology

Electrospinning is used widely to obtain non-woven materials which have a wide range of applications (see chapter 1). Fibre size can be changed, beaded fibres can be made and porosity of the fibres increased; but the end product is still a non-woven which inherently limits its application.

To broaden the possible application of electrospinning a tighter control over the morphology of bulk electrospun materials is needed. If aligned fibres can be produced for example, then a whole new set of possibilities open up for electrospun products.

Much work has been carried out to achieve this aim. The simplest method involves collecting electrospun fibres onto a rapidly rotating earthed drum or spindle[1-4]. Increasing speed of rotation gives the fibres a degree of orientation in the direction of rotation to the point at which the drum is spinning faster than the fibres are being deposited and orientation then decreases. However, orientation is never that extensive with this method due to the random fibre deposition resulting from fibre whipping. Often all semblance of alignment is lost over longer spinning times and eventually non-wovens are collected.

Using a sharpened disc collector alters the electric field so that fibres collect in parallel along the edge of the disc[5,6]. This method gives highly aligned fibres but with the major drawback of the collection being over a small area (the disc edge)(figure6.1)

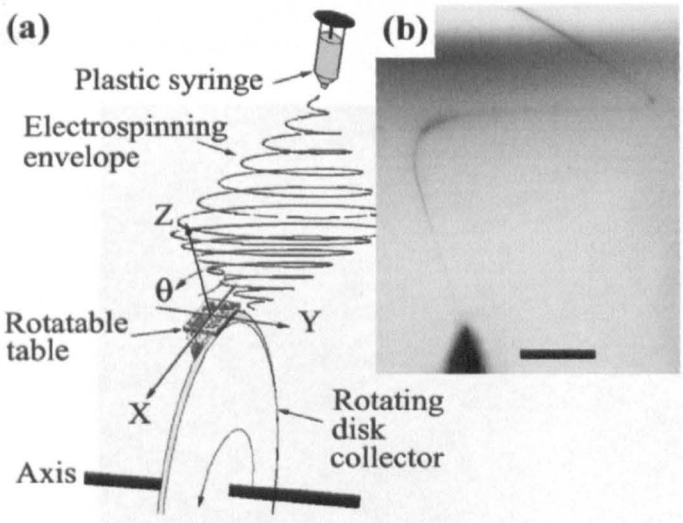

Figure 6.1 Diagram showing a) a schematic of electrospinning onto a gounded disc edge and the associated focussing of the jet and b) fast shutter speed image of fibre focussed onto disc edge.[5]

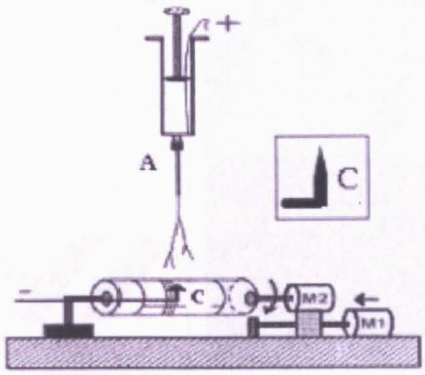

Figure 6.2 Experimental set-up for polyester drum electrospinning. Pin C is earthed. The polyester drum can move from side to side as well as rotating. Polymer solution A must be close to drum (2-8cm) for alignment.[7]

Another collection device involves collection upon a polyester drum. The earthed target for the charged fibres is a pin mounted within the drum(figure 6.2). Before reaching the pin the fibres are collected upon the rotating polyester drum. By moving the pin from side to side and altering the rotation speed of the drum, aligned fibres can be obtained. For this method to work well, short path lengths are needed and low voltages in order to minimise jet whipping[1,7].

Another method involves spinning of fibres onto a specially constructed wire drum (figure 6.3)[8]. Rather than a solid surface for the fibres to collect on, the drum is made of many parallel copper wires separated by a distance of 0.5cm. Upon rotation of this drum(up to 10r.p.m) collected fibres are oriented perpendicular to the copper wires. The effect of increasing speed has not yet been studied but higher speeds should yield more alignment.

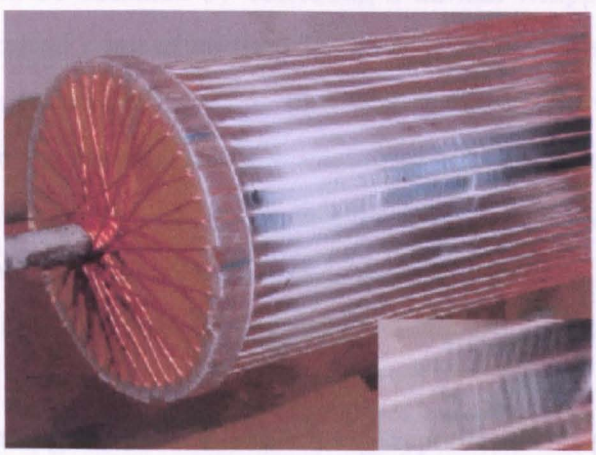

Figure 6.3 electrospun nylon fibres are collected on the wire drum. The magnified image shows stratified layering associated with alignment.[8]

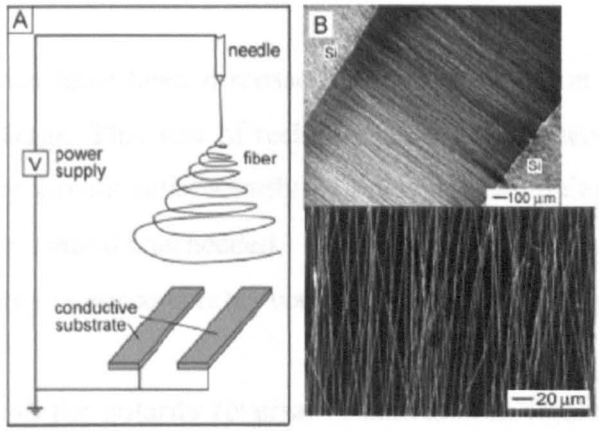

Figure 6.4 Method of alignment of nanofibres using a two-strip conductive collector[2].A) shows the basic set-up, B) is a light microscope image showing large scale alignment and C)SEM micrograph of aligned Poly(2-vinylpyridine).[2]

A drawback of this method is the small amount of aligned material which can be used. Alignment only occurs between the copper wires, over a span of only 0.5cm. The surface of the wires still yields a non-woven material.

A recent novel approach involves collection of fibres on a grounded electrode consisting of two conductive silicon strips separated by a gap[2]. Fibres are attracted to the grounded target and are suspended over the gap in an aligned fashion (figure 6.4). Improvements on this method involved filling the void gap with an insulating material and changing the silicon strips for gold.

This is again not a practical solution to the alignment problem as it only gives aligned fibres over a small area.

6.2 *Needle to Needle Spinning*

Aligned fibres can be obtained by collecting a normal whipping jet on a rapidly rotating spindle or cylinder but often the alignment is poor and isn't maintained over long spinning times (over 1 minute)[1,3]. This is a result of the wildly whipping jet landing randomly on the spindle. Initially alignment will be inferred by the direction of rotation but over time it will be lost, as further random deposition takes place. The nature of the whipping jet in electrospinning is both attractive, in terms of making useful non-wovens; and destructive, in terms of making alignment difficult.

In order to collect aligned fibres the following hypothesis was put forward

"Eliminate jet whipping and collect a straight jets and aligned fibres will result"

Focussing methods have been discussed in the introduction and usually involve rings of stepped voltage. This sort of technology seemed unnecessarily complex for our needs and rarely gave a satisfactorily straight, non-whipping jet. It was decided that a new focussing method was needed.

The innovative step in our apparatus was to reverse the polarity of the rig and use a point charge target.

The Theory behind the polarity reversal is indicated in figure 6.5. By replacing a large area target with a charged needle creates a more focussed electric field in which jet instabilities will be minimised.

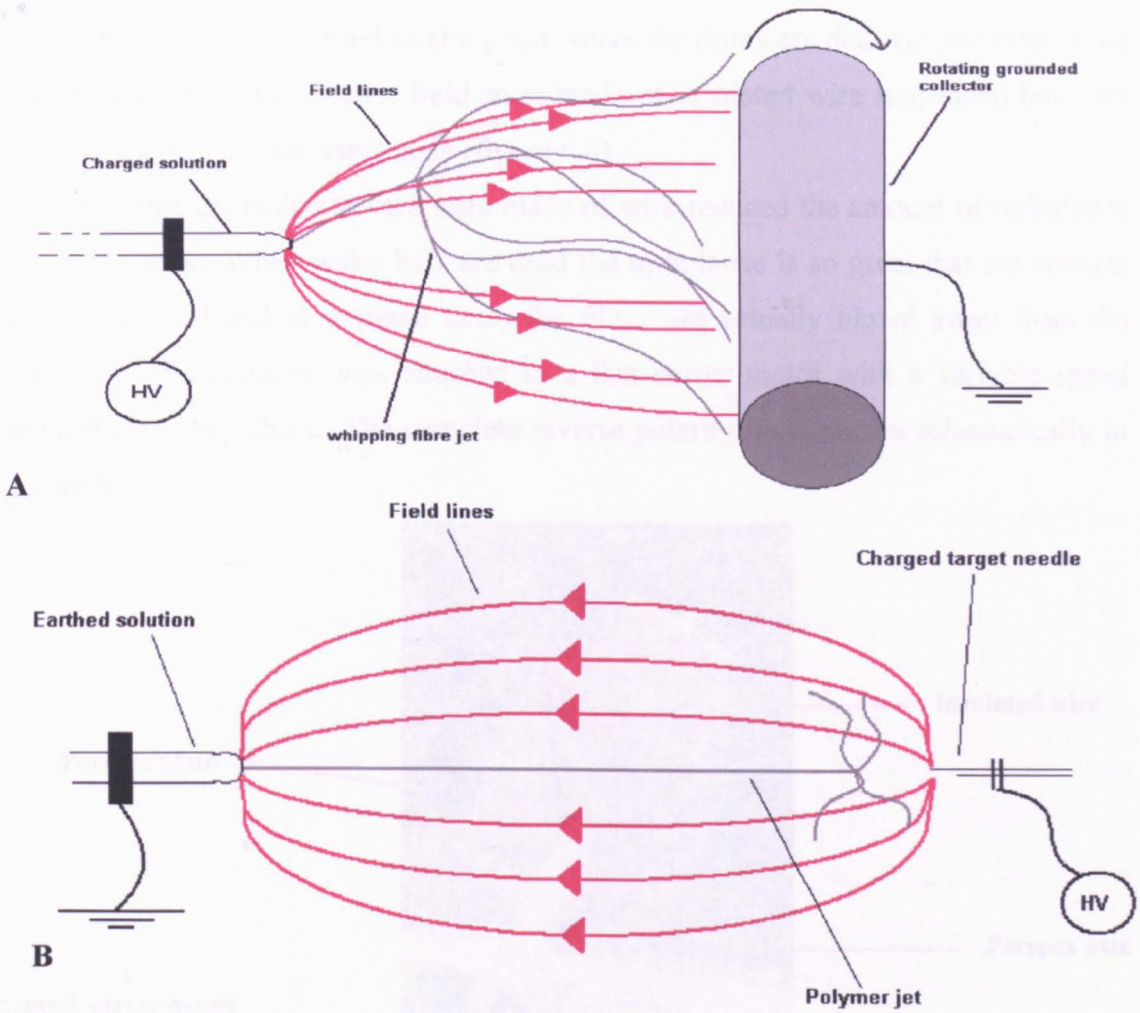

Figure 6.5 A)Schematic of "normal" electrospinning showing electic field lines and the whipping jet. No matter how fast the rotation, orientation will eventually be lost due to random deposition.B) Focussed field lines give a focussed jet the point charge being highly attractive.

In situation A, the jet will always whip as the electric field is less focussed. Also, because the target is at earth potential any object in the vicinity with that potential will be attractive to the jet and distort the field. This distortion leads to instabilities and whipping. All other alignment methods involve collecting on an earthed collector[1,5,7-14], so this instability will always be a limiting factor.

Situation B removes these instabilities by changing the polarity of the system around. This method only works with a needle point charge to really focus the field. Using a more diffuse charged target such as a metal plate or drum does not yield any fibres at all.

In order to collect aligned fibres the collector must be placed in the straight part of the jet between the two needles at a point where the fibres are dry. The collector must not interfere with the electric field so is made of insulated wire suspended between Perspex plates with a Perspex axle (figure 6.6).

The fact that the collector bars were made of wire reduced the amount of turbulence during rotation. When wider bars are used the turbulence is so great that the straight jet is disturbed and in extreme cases the fibres are actually blown away from the collector. The collector was attached to a fast stirrer motor with a variable speed control via a drill chuck. The complete reverse polarity rig is shown schematically in figure 6.7.

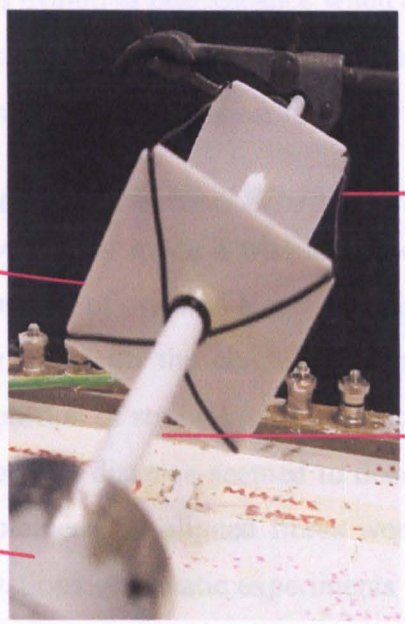

Figure 6.6 The insulated collector.

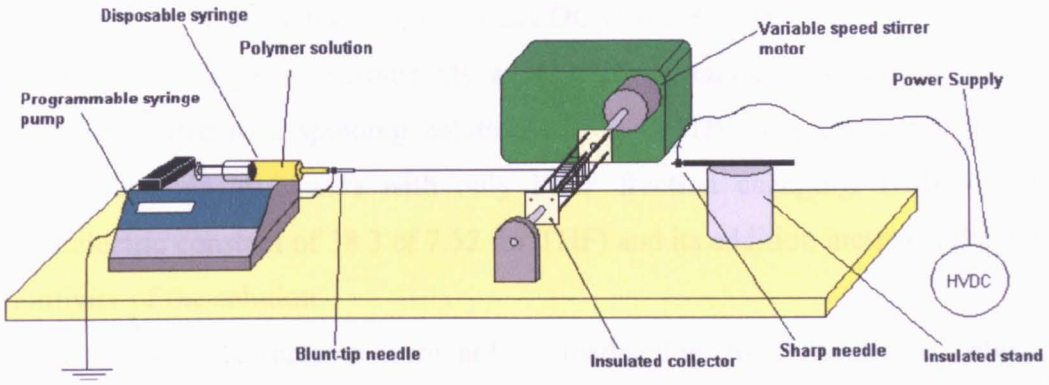

Figure 6.7 A schematic of the reverse polarity rig. The distances from needle to needle and needle to collector are all easily changed.

6.3 *Experimental*

A wide range of solutions of polystyrene (PS) and Poly(l-lactic acid) (PLLA), were made up and spun using this apparatus. Much iteration was required in order to optimise the spinning conditions; notably the needle to needle distance and the position of the collector. Another variable was the speed of rotation of the collection spindle. A summary of the early experiments is given in result table 6.1.

Once aligned fibres of PS and PLLA were obtained, high Mw ($8.5x10^5$g mol^{-1} to $1.2x10^6$ g mol^{-1}) triblock copolymers (AP, courtesy of Andy Pryke) were also spun on the apparatus. These polymers exhibited pearlescance when cast in films as a result of microphase separation, The purpose of electrospinning these polymers was to try to induce such microphase separation under the shear forces of electrospinning.

6.3.1 *Systematic Studies of Oriented Fibre Spinning*

The earlier experiments were very much a trial and error process with the main objective of proving the hypothesis of oriented electrospinning. The next stage was to take a more systematic approach with the conditions chosen. We saw that when concentration increased, the portion of straight jet seemed to increase too. Also when more polar solvents were used this distance seemed to decrease to point where very little straight jet could be obtained and aligned fibres were difficult to achieve. In order to quantify these observations systematic experiments were undertaken whereby the portion of straight jet (l_{whip})was measured along a concentration gradient and a solvent permittivity gradient.

The effect on l_{whip} of changing concentration was observed for two different polymer/solvent systems, these being PLLA/DCM and PS/THF.

In order to change the permittivity an increasing amount of Dimethylformamide (DMF) was added to a spinning solution of PS in THF. The concentration of the solution was held at 25wt% with only DMF fraction changing. DMF is highly polar(dielectric constant of 38.3 cf 7.52 for THF) and its addition increases the overall permittivity of the solution.

Permittivity measurements were not made due to difficulty in obtaining values with the apparatus available, so the results will only show a quantitative relationship between DMF volume fraction and l_{whip} in the case of the PS/THF:DMF system rather than between permittivity and l_{whip}. For the purposes of this experiment it is assumed that increasing DMF volume fraction does increase permittivity and that this relationship is additive[15-17].

6.4 Results and Discussion

6.4.1 Easily Aligned Polymers

The polymers discussed in this section were easily aligned. At each concentration a number of needle to needle and needle to collector distances were tested (table 6.1)

Results table 6.1 Showing a selection of results from spinning of PS, PLLA and AP.

Polymer/Mw/ Solvent	Needle to needle distance/ cm	Needle to collector distance/ cm	Concentration/ wt%	Fibres y/n	Alignment y/n
PLLA/152 $kgmol^{-1}$ /DCM	55	50	6.5	n	n
			7	y	n but better
	45	40	7.5	y	y but only sustained over 2 minutes spinning
			8	y	y but only sustained over 2 minutes spinning
			8.5	y	y sustained over 5 minutes spinning
			9	y	y sustained over 10 minutes spinning
			10	y	y sustained over 10 minutes spinning
			11	n unprocessable	n
PS/ 200 $kgmol^{-1}$/THF	35	28	22.5	y	n
			25	y	n
			27.5	y	y sustained over 5 minutes
			30	y	y sustained over 15 minutes
			35	y	y sustained over 15 minutes
AP 850K/CH_3Cl (M_w 850 $kgmol^{-1}$)	17	10	18-20	y	y sustained over 20 minutes
AP 1200K/CH_3Cl (M_w 1200 $kgmol^{-1}$)	15	8	15-20	y	y sustained over 20 minutes

Polystyrene

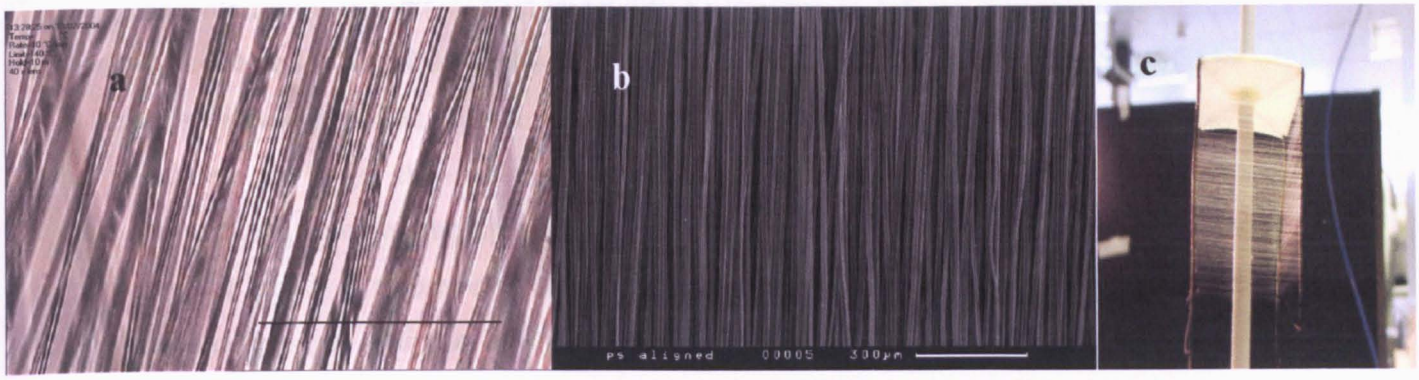

Figure 6.8 a) Light microscope image PS fibres spun from 27.5wt% PS in THF (scale bar is 500µm) b) SEM micrograph showing perfect alignment of PS fibres spun from 35wt% PD inTHF over 15 minutes c)PS fibres seen on the spindle collector.

Poly(l-lactic acid)

Figure 6.9 Light microscope images of PLLA fibres showing increasing alignment with increasing concentration a)10x image of fibres spun from 7.5wt% PLLA in DCM b) 20x image of fibres spun from 8.5wt% PLLA in DCM c) 20x image of fibres spun from 10wt% PLLA in DCM.

AP-850K and AP-1200K

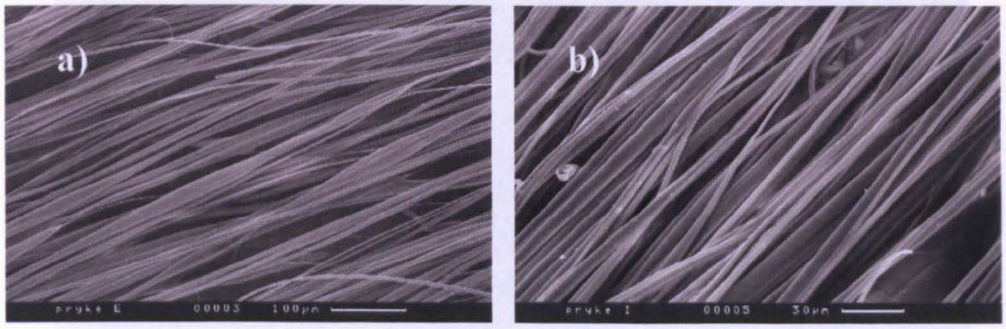

Figure 6.10 SEM micrographs of a)AP-850K fibres spun from 18wt% solution of AP-850K in CH_3Cl b)AP-1200K fibres from 16wt% AP-1200K in CH_3Cl.

For all four polymers, alignment increases with increasing concentration. As concentration was increased jet instabilities were minimised and a perfect straight jet was collected. The collector was positioned in such a place as to collect the straight jet before it was repelled by the target needle. It should be noted that the collection distances are larger than for conventional spinning in order to collect dry fibres. In conventional spinning the fibre drying process is greatly increased during whipping as the path length is effectively much longer. By eliminating the whipping motion the fibres take longer to dry so in compensation the path length must be increased.

The portion of straight jet increases with increasing concentration. This is denoted l_{whip} and is the length of straight jet before repulsive back-whipping ensues. l_{dry} is the critical distance over which a straight, non-whipping jet must fly to dry out completely. l_{dry} is inversely proportional to the concentration.

So, for aligned dry fibres $l_{whip} > l_{dry}$, it is also imperative when $l_{whip} > l_{dry}$ that the collector is placed in a position which is less than l_{whip} and more than l_{dry}. By placing it too close to the source needle wet fibres will be obtained.(figure 6.11)

Collection of wet fibres yields very few aligned fibres which is probably a major factor in our inability to align more dilute solutions.

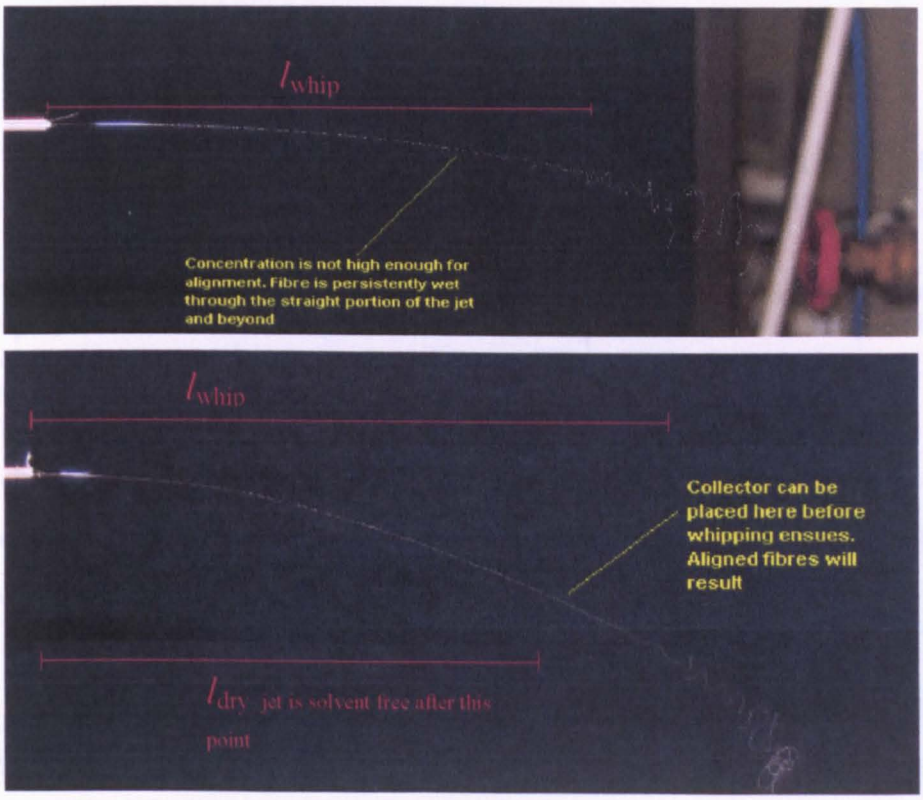

Figure 6.11 Diagram explaining the terms l_{whip} and l_{dry}.

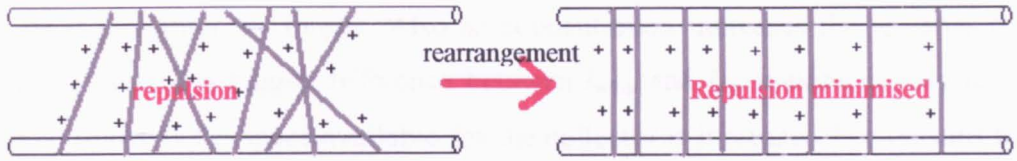

Figure 6.12 The insulating bars of the collector mean that fibres cannot discharge. Fibres which overlap or are not aligned repel each other and can rearrange with the help of the torsional force of the spinning collector. Wet fibres stick to the bars and do not rearrange.

With such solutions the fibres remain "tacky" upon reaching the collector. If these fibres are not laid down perfectly perpendicular to the spindle bars they stick in that position and are unable to reposition themselves. Repositioning of dry fibres occurs under the torsional force imparted by the spindle bars and also by repulsion from adjacent fibres. This repulsion only arises when an insulated collector is used. As an insulated collector is unable to discharge, each fibre retains its charge and repels adjacent fibres, further increasing alignment (figure 6.12). This repulsion is analogous to the alignment method used by Li et al[2] illustrated in figure 6.4 .

6.4.2 Results of Systematic Studies

6.4.2.1 Effect of concentration

The polymer/solvent systems under investigation here were PLLA in DCM and PS in THF. The experiments were repeated twice. The results are shown in figure 6.13.

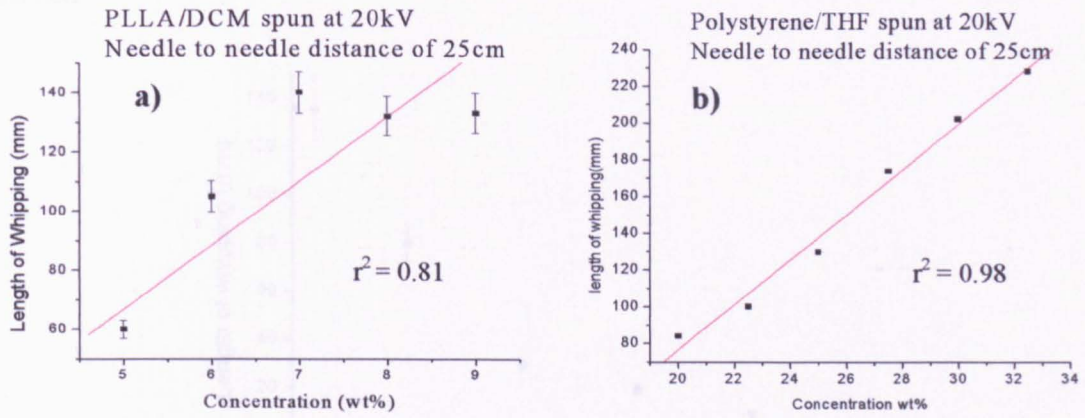

Figure 6.13 a) Graph showing relationship between l_{whip} and concentration of PLLA in DCM. Line is one of best fit calculated by Origin. b) Graph showing relationship between l_{whip} and concentration of PS in THF.

It can be seen that as concentration increases l_{whip} increases too. This means that the jet is straighter for longer. Also as concentration increases the jet dries quicker meaning there is a bigger difference between l_{whip} and l_{dry} making it easy to collect aligned fibres as the space available for the collector is increased.The reasons for this relationship are not fully understood. Why should a more concentrated solution yield a more stable jet?

Concentrated solutions certainly yield thicker fibres (chapter 1.6.2) so the extra momentum associated with thicker jets could make them more resilient to instabilities. Vigorous whipping would be more difficult to achieve with a thicker, heavier jet. To fully understand this phenomenon, this study would need to be subject to some mathematical modelling.

6.4.2.2 Effect of solvent permittivity

The distance l_{whip} was plotted against volume fraction of DMF in the PS in THF/DMF system. Concentration of PS is 25wt%.

It is seen clearly that when the % of DMF in the spinning solution is increased the length of whipping decreases. Since no permittivity readings were taken successfully it is not known whether or not this is a linear relationship or otherwise. This data may only be used as an experimental indication of this phenomenon.

It appears that jets of more polar solutions are less easily controlled even with the well defined electric field of the reverse polarity rig. As l_{whip} decreases, so does the difference between l_{whip} and l_{dry} so the chance of collecting dry, aligned fibres is lessened.

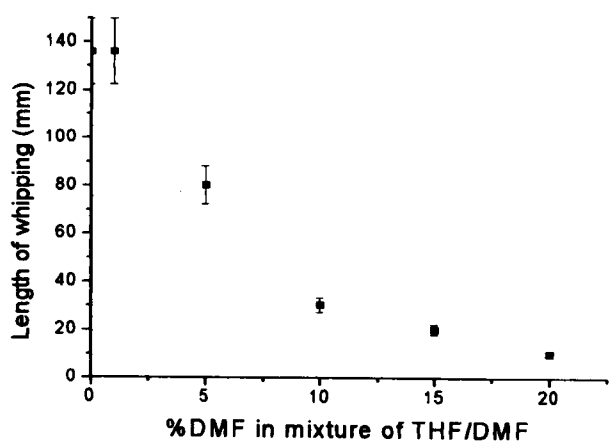

Figure 6.14 Plot of l_{whip} vs %DMF for a jet of 25wt% PS in a mixed solvent of THF and DMF.

The reasons for this relationship between l_{whip} and permittivity as yet unknown however a major problem with spinning from highly polar solvents is excessive "back-whipping". It follows then that adding polar solvent to a solvent mixture increases the likelihood of "back-whipping" instabilities. This phenomena is explained in section 2.4.4.

The findings of the systematic experiments are summarised in figure 6.15.

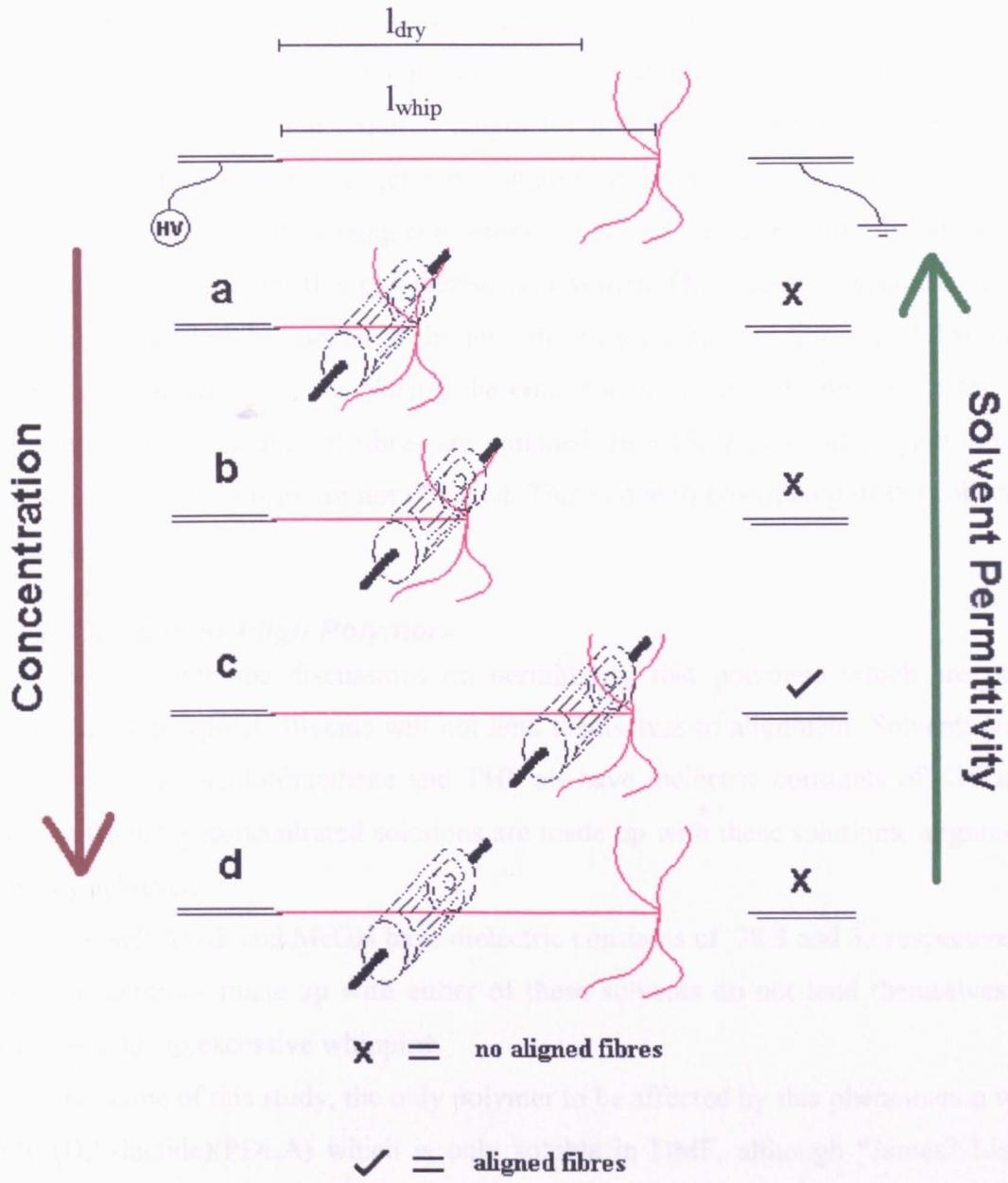

Figure 6.15 Schematic to show relationship between the length of the straight portion of jet (l_{whip}) and changing concentration/permittivity. situations a-d) show different positions for the collector, with a tick or a cross indicating whether or not aligned fibres are obtained. l_{dry} for this polymer/solvent system is shown at the top of the diagram.

From figure 6.15 it can be seen that as concentration increases l_{whip} increases, and as permittivity increases l_{whip} decreases. In figure 6.15a we have a situation of either low concentration or high solution permittivity. The straight portion of the jet is short, in fact far shorter than the required length for drying (l_{dry}). When the collector is placed in the straight portion of jet wet, non-aligned fibres will result. In figure 6.15b l_{whip} has increased with increasing concentration (or decreasing permittivity), however it is still less than l_{dry} for this polymer/solvent system. Once again, placement of the collector in the straight portion of the jet will not yield aligned fibres. In 6.15c l_{whip} becomes longer than l_{dry}. By placing the collector in the straight portion of the jet between l_{dry} and l_{whip} aligned fibres are obtained. In 6.15d l_{whip} is once again longer than l_{dry} but aligned fibres are not obtained. This is due to positioning of the collector before l_{dry}.

6.4.3 Difficult to Align Polymers

It follows from the discussions on permittivity that polymers which are only soluble in highly polar solvents will not lend themselves to alignment. Solvents such as Chloroform, Dichloromethane and THF all have dielectric constants of <10 and when sufficiently concentrated solutions are made up with these solutions, alignment is easily achieved.

Conversely DMF and MeOH have dielectric constants of 38.3 and 33 respectively. Polymer solutions made up with either of these solvents do not lend themselves to alignment due to excessive whipping.

In the scope of this study, the only polymer to be affected by this phenomenon was Poly (D,L-lactide)(PDLA) which is only soluble in DMF, although "James" Linge Wang from the NCD group studied the electrospinning of polymers which were soluble only in MeOH. He reported difficulty in aligning fibres of these polymers.

PDLA was spun from a range a concentrations but a situation whereby l_{whip} was longer than l_{dry} was never reached. For this reason the collector could only be placed in the rapidly whipping region of the jet as in conventional electrospinning(figure 6.16).

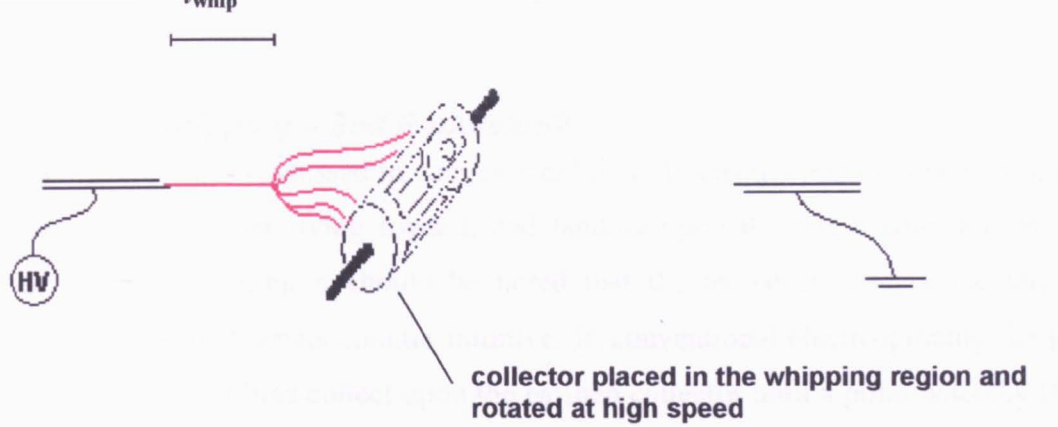

Figure 6.16 Schematic showing collection of fibres spun from highly polar solvents.

Since only a whipping jet could be collected the only alignment achieved was one enforced by rapid (>400r.p.m) rotation of the collector as in the work done by Chew et al[4], Li et al[1], and that reported by Huang in his review paper[3]. The fact that the collector was a spindle probably helped to align the polymer more than a solid drum would have.

Increasing rotation speed has the effect of increasing alignment when collecting a whipping jet but only up to a point. Once the collector rotates faster than the fibres are being deposited the fibres are prone to breakage and alignment is lost. This trend is illustrated in figure 6.17

The broken fibres can be seen clearly in 6.17c. There is an underlying orientation in the fibre mat with snapped fibres in their "relaxed" state lying throughout the material.

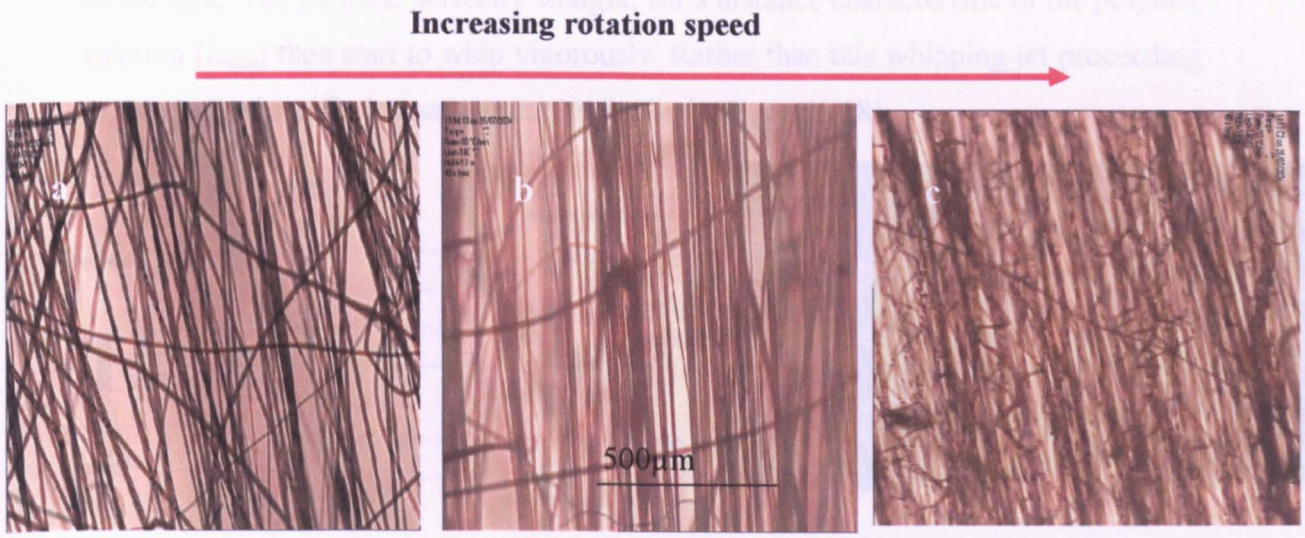

Figure 6.17 PDLA fibres spun from a solution of 40wt% PDLA in DMF. a)rotation speed 200 r.p.m b) 550 r.p.m c) 650 r.p.m.

6.4.4 Back Whipping – Self Repulsion?

When whipping is discussed in conventional polarity electrospinning one imagines a rapidly oscillating jet flying toward, and landing upon the target collector. With reverse polarity spinning it should be noted that the jet never reaches the target needle, which at first seems counter intuitive. In conventional electrospinning the jet travels towards and fibres collect upon the earthed collector until a point whereby the collector becomes insulated by the deposited polymer. When this happens the jet diverts to the next most attractive (i.e nearest) earth source, be that the bench top, a belt buckle or any part of one's anatomy. The jet travels down the potential gradient towards earth and lands upon an earthed conductor in its path as there are no more attractive places (electrostatically speaking) for it to do so. With this conventional spinning method the jet will nearly always whip extensively as the electric field isn't particularly well defined due to the many other earth points in the vicinity. The field lines are non-uniform and as a result the jet is destabilised and whips.

By swapping the charges and spinning point to point, these instabilities are almost completely lost. The target for the charged solution is no longer one of many earths in the room but a discrete concentrated point. As was shown in figure 6.5 the field lines will be focussed on the target needle and the jet will be funnelled toward the target. Originally it was expected that fibre would land upon the tip of the charged target needle in a fashion analogous to conventional electrospinning. This was found not to be the case. The jet flies, perfectly straight, for a distance characteristic of the polymer solution (l_{whip}) then start to whip vigorously. Rather than this whipping jet proceeding to the charged needle it was seemingly repelled. (Figure 6.18)

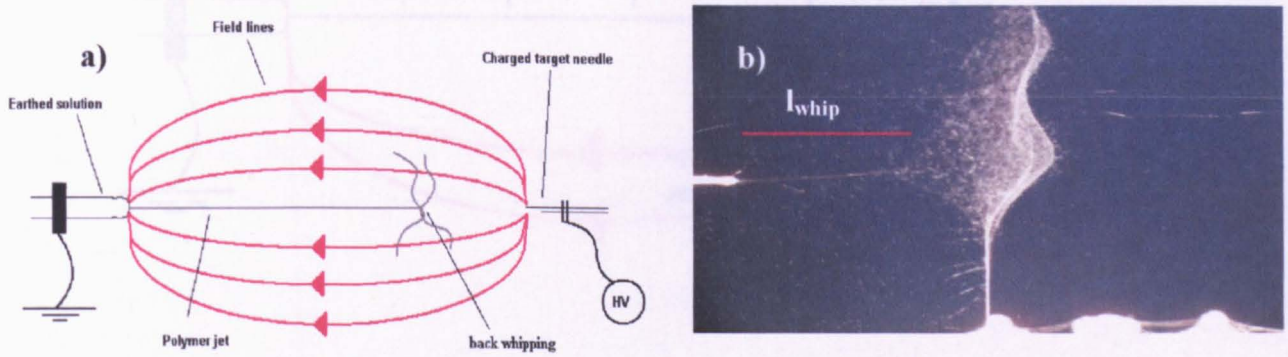

Figure 6.18 a)Schematic of a "back whipping" jet b) photograph of an extreme back whipping scenario using 40wt% PDLA in DMF- notice the short straight jet distance (l_{whip}).

The reasons for back-whipping are not well understood. It is proposed that once the jet is initiated it follows the potential gradient toward the charged collector. Over its flight the jet becomes more and more charged as it comes closer to the target needle (a very high point charge). In fact, the jet is effectively being charged from zero potential (earth) up to that of the target needle. It is proposed that once the jet reaches a potential of a similar magnitude to that of the target voltage it is actually repelled from what attracted it in the first place (figure 6.19). The jet is thus destabilised and whips. It then proceeds to collect on the nearest earth point. In effect, at the point where back whipping occurs, the attraction for earth outweighs the attraction of the target needle.

As discussed in 2.4.2.2 and 2.4.3 whipping happens as shorter path length for more polar solvents. Polar solvents take on induced charge more readily than less polar ones therefore are more quickly repelled by the target needle and attracted to earth.

With less polar solvents such as THF and DCM the "back-whipping" phenomenon doesn't affect the ability to collect aligned fibre as it happens sufficiently close to the target needle to allow a collector to be placed beyond l_{dry}. It is however a major problem when using more polar and less volatile solvents such as DMF as discussed in 2.4.3.

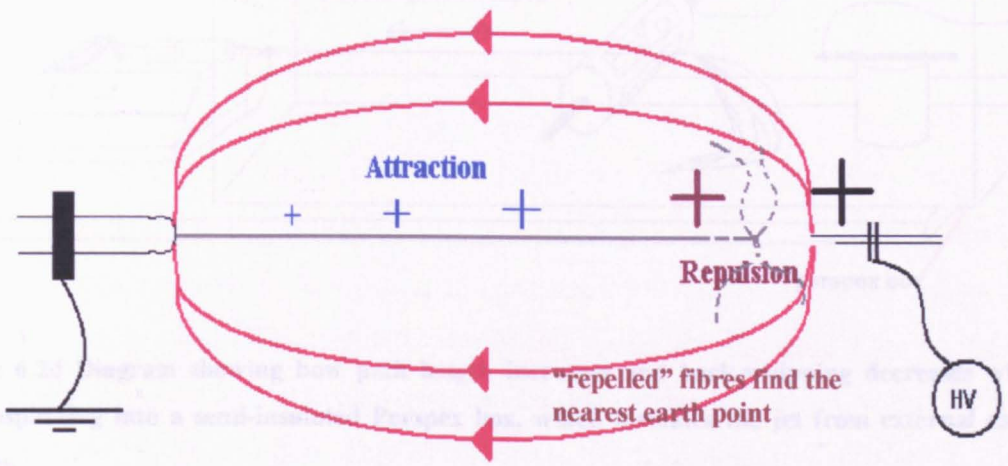

Figure 6.19 Repulsion from the target needle occurs when the jet reaches a similar potential to that of the initiating voltage. The repelled fibres collect on the nearest earth surface.

Evidence for this comes when needle-to-needle reverse polarity spinning is performed in a semi-insulated box. In this experiment the electrospinning rig was mounted inside a Perspex box (the same one used in chapter 4 for controlling humidity). This Perspex box insulates the jet from external earth sources. When spinning in the box l_{whip} increases (up to a three fold increase with DMF as a solvent). The jet is attracted to the needle for longer as it has no earth points to compete with. In some cases the jet actually reaches the target needle. This indicates that the most important factor in back-whipping is not in fact the "self-repulsion" but rather the "preferred attraction" to earth, although the effect is governed by a combination of the two(figure 6.20).

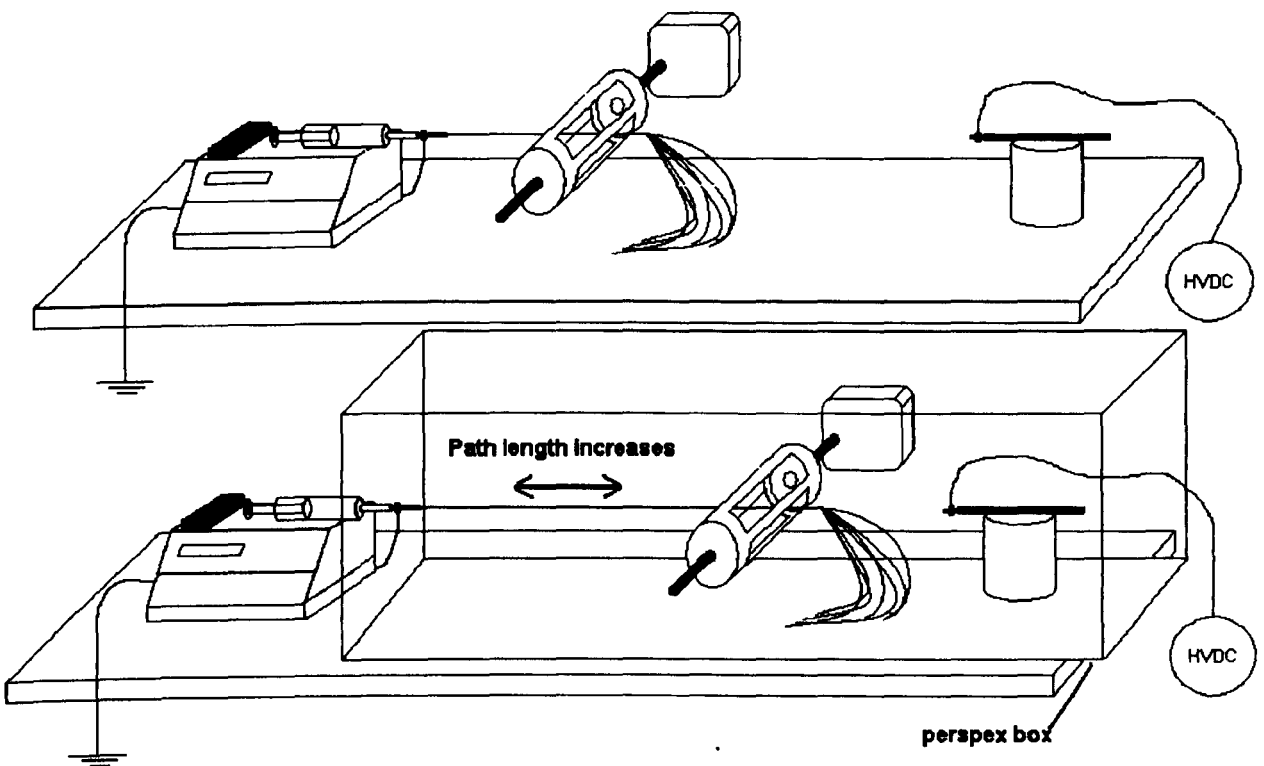

Figure 6.20 Diagram showing how path length increases and back-whipping decreases when electrospinning into a semi-insulated Perspex box, which insulates the jet from external earth sources.

6.5 Cell Growth on Aligned and Separated Fibres

Recent studies involved the seeding of skin cells (fibroblasts) on aligned parallel fibres[18]. The methods discussed in this chapter have been used to produce aligned fibres of PS and PLLA. Fibres are collected on an open spindle and the longer they are allowed to collect for then the closer the aligned fibres become. By collecting for different lengths of time the separation between adjacent fibres can be controlled. The reason for performing this experiment is to ascertain the length scale over which cells can span a fibre gap. This knowledge will provide a valuable insight into the mechanism of cell migration and proliferation within fibrous scaffolds.

Fibres are removed from between the bars of the spindle collector and mounted straight onto a special bioreactor microscope slide, which consists of a silicon rubber well glued to a standard glass slide (made by Sun Tao). The silicon rubber is covered in quick setting glue and the fibres stuck to the silicon (figure 6.21). The silicon is used to raise the fibres above the glass surface, ensuring all cell proliferation happens on the fibres and not the glass.

Once the fibres are glued down, fibroblasts are seeded upon them and allowed to proliferate. Staining is performed on the cells once again and the cells visualised under a fluorescent microscope. To aid visualisation of the cells upon the fibres a fluorescent dye was introduced into the fibres. This was achieved by adding 0.5wt% rhodamine dye was to the spinning solution. Adding the dye at this stage of the electrospinning procedure ensures even distribution of the dye throughout the fibres once spun. By staining the cells with a blue dye (DAPI), they could be easily distinguished from the red fibres.

Figure 6.22 shows how cells can span between adjacent fibres. On each slide is a wide range of gap sizes between adjacent fibres. Using fluorescence microscopy the maximum gap over which cells can span can be determined. It was found that all cells could successfully span a gap of up to 100μm within two weeks of incubation. Over distances greater than 200μm no cells would span, and between 100 and 200μm approximately 50% of the cultured cells would bridge the gap.

As well as studying the bridging behaviour of fibroblasts their response to different fibre diameters was measured. Varying the concentration of PLLA solutions enabled fibres of 1-10μm to be spun, with PS solutions yielding fibres with a diameter range of 10-30μm. Thicker fibre diameters were achieved by finding adjacent fibres which

had stuck together. The behaviour of cells on thin to thick fibres was monitored through cell staining and fluorescent microscopy. It was found that there is a minimum fibre diameter of 10μm required to promote cell attachment and migration along the fibre Currently a paper is in progress reporting the spanning of cells between a systematic range of gap sizes and fibre diameters.

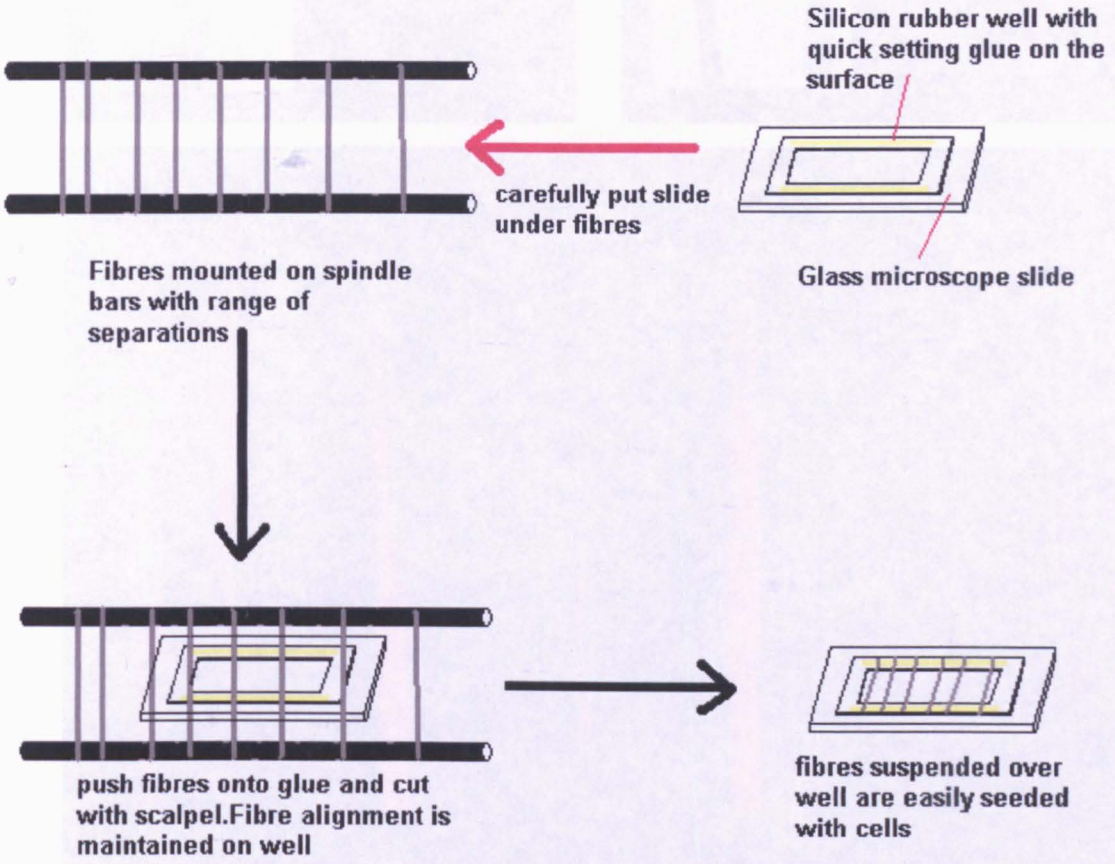

Figure 6.21 Schematic showing preparation of aligned fibres for cell seeding.

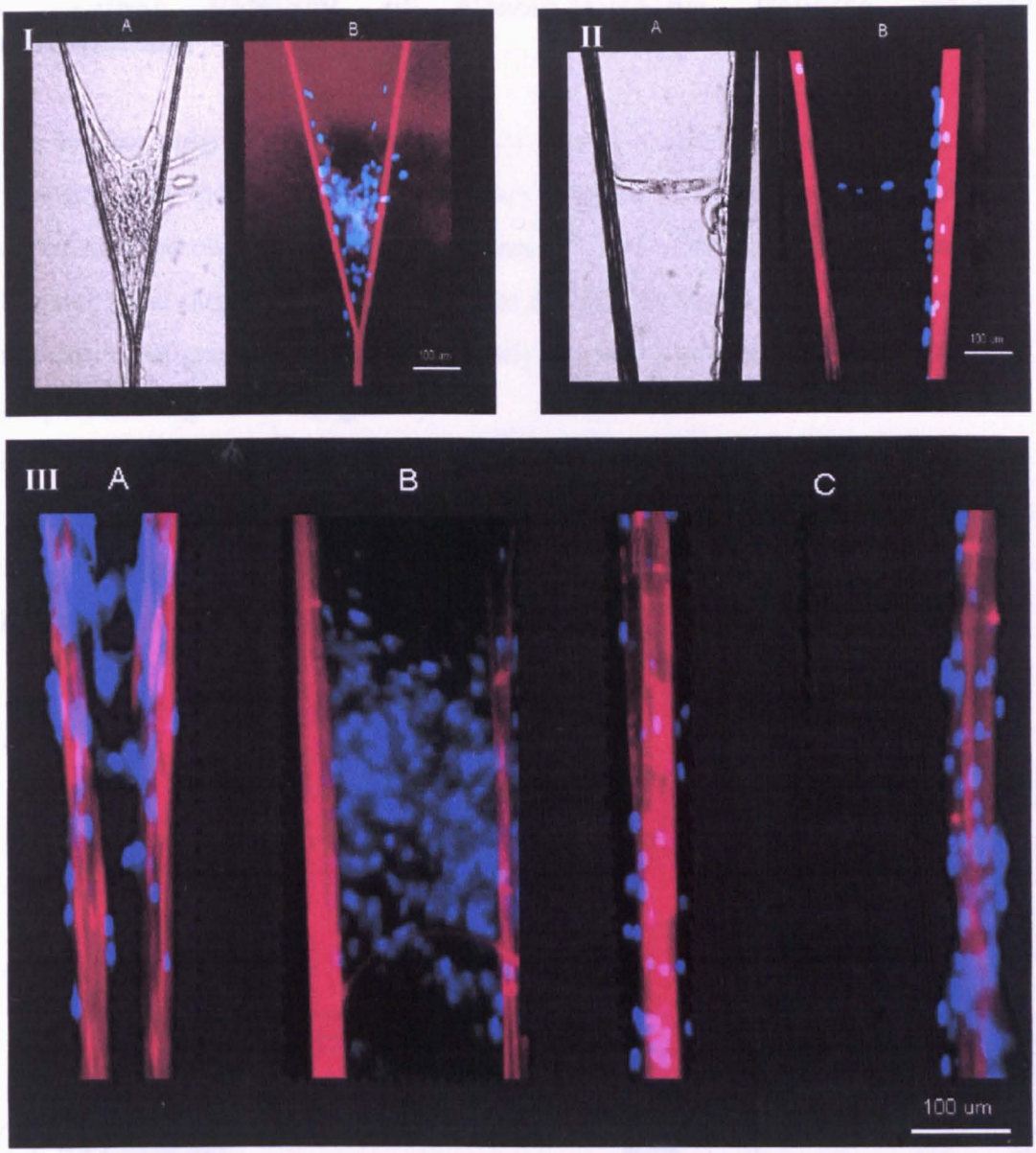

Figure 6.22 (I) Phase contrast normal light (A) and fluorescent (B) micrographs of normal human dermal fibroblasts cultured on a V-shape void in the 3D cell culture system for 2 weeks. Cells can span the smaller gaps but stop spanning when the gap is too large (II) Phase contrast normal light (A) and fluorescent (B) micrographs of normal human dermal fibroblasts cultured on open pore structure in 3D cell culture system for 2 weeks. (III) Fluorescent micrographs of normal human dermal fibroblasts cultured on aligned fibres with increasing gaps between them in the 3D cell culture system for 2 weeks. Fibroblast nuclei were stained with DAPI as blue and the fibres were labelled as red. Scale bars are 100μm.

6.6 Further Potential of Needle-to-Needle Reverse Polarity Electrospinning

The reverse polarity rig will enable easy fabrication of composite materials and also relieve some potential mass production problems. Different polymer solutions could be mounted on the same pump, or many syringes of the same material, and fired at the same point target Without the need for external focussing devices such as rings, composites of aligned fibres would be easily produced as would large quantities of single polymer aligned fibre(fig 6.23).

Early tests show that this rig works very well indeed and up to six jets have been fired at one time and aligned fibres collected. So far this has only been done with jets of the same polymer but will work just as well with different solutions as long as they maintain straight jets over long enough path lengths.

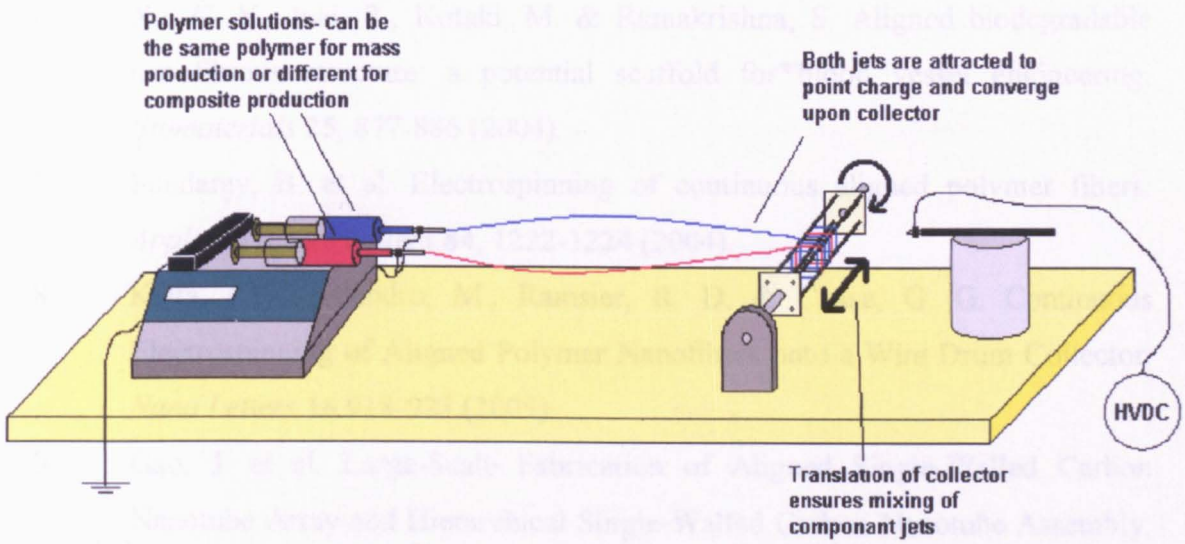

Figure 6.23 Mass production of aligned fibres/ making composites should be straight forward on the reverse polarity rig.

6.7 References

1. Li, D. & Xia, Y. Electrospinning of nanofibers: Reinventing the wheel? *Advanced Materials (Weinheim, Germany)* **16**, 1151-1170 (2004).
2. Li, D., Wang, Y. & Xia, Y. Electrospinning nanofibers as uniaxially aligned arrays and layer-by-layer stacked films. *Advanced Materials (Weinheim, Germany)* **16**, 361-366 (2004).
3. Huang, Z.-M., Zhang, Y. Z., Kotaki, M. & Ramakrishna, S. A review on polymer nanofibers by electrospinning and their applications in nanocomposites. *Composites Science and Technology* **63**, 2223-2253 (2003).
4. Chew, S. Y., Wen, J., Yim, E. K. F. & Leong, K. W. Sustained Release of Proteins from Electrospun Biodegradable Fibers. *Biomacromolecules* **6**, 2017-2024 (2005).
5. Theron, A., Zussman, E. & Yarin, A. L. Electrostatic field-assisted alignment of electrospun nanofibres. *Nanotechnology* **12**, 384-390 (2001).
6. Xu, C. Y., Inai, R., Kotaki, M. & Ramakrishna, S. Aligned biodegradable nanofibrous structure: a potential scaffold for blood vessel engineering. *Biomaterials* **25**, 877-886 (2004).
7. Sundaray, B. et al. Electrospinning of continuous aligned polymer fibers. *Applied Physics Letters* **84**, 1222-1224 (2004).
8. Katta, P., Alessandro, M., Ramsier, R. D. & Chase, G. G. Continuous Electrospinning of Aligned Polymer Nanofibers onto a Wire Drum Collector. *Nano Letters* **16** 918-923 (2005)
9. Gao, J. et al. Large-Scale Fabrication of Aligned Single-Walled Carbon Nanotube Array and Hierarchical Single-Walled Carbon Nanotube Assembly. *Journal of the American Chemical Society* **126**, 16698-16699 (2004).
10. Kahol, P. K. & Pinto, N. J. Electron paramagnetic resonance investigations of electrospun polyaniline fibers. *Solid State Communications* **124**, 195-197 (2002).
11. Kessick, R., Fenn, J. & Tepper, G. The use of AC potentials in electrospraying and electrospinning processes. *Polymer* **45**, 2981-2984 (2004).

12. Teo, W. E., Kotaki, M., Mo, X. M. & Ramakrishna, S. Porous tubular structures with controlled fibre orientation using a modified electrospinning method. *Nanotechnology* **16**, 918-924 (2005).

13. Yang, F., Murugan, R., Wang, S. & Ramakrishna, S. Electrospinning of nano/micro scale poly(L-lactic acid) aligned fibers and their potential in neural tissue engineering. *Biomaterials* **26**, 2603-2610 (2005).

14. Zussman, E., Theron, A. & Yarin, A. L. Formation of nanofiber crossbars in electrospinning. *Applied Physics Letters* **82**, 973-975 (2003).

15. Turky, G. M. A. Dielectric studies of dilute solutions of binary mixtures of N,N-dimethylformamide and 1-hexanol in the non-polar solvent mesitylene. *Physics and Chemistry of Liquids* **34**, 15-24 (1997).

16. Valisko, M., Boda, D., Liszi, J. & Szalai, I. Relative permittivity of dipolar liquids and their mixtures. Comparison of theory and experiment. *Physical Chemistry Chemical Physics* **3**, 2995-3000 (2001).

17. Theron, S. A., Zussman, E. & Yarin, A. L. Experimental investigation of the governing parameters in the electrospinning of polymer solutions. *Polymer* **45**, 2017-2030 (2004).

18. Sun, T. et al. Tissue Engineering: Nano, Micro or Macro-fibres? *Submitted for assessment* (2005).

Chapter 7 – Summary and Future Work

7.1 Summary

A range of electrospinning machines were built in order to produce electrospun fibres for specific purposes. For non-woven electrospun fabrics the SESM MkIII was favoured as it enabled collection of thick samples. The major application of these samples was in tissue engineering. Using the SESM MkIII it was possible to produce PS fibres with a suitable geometry for the proliferation of skin cells throughout the scaffold. By creating a scaffold of a suitably porous nature and seeding it with a mixture of skin cell types (fibroblasts, keratinocytes and endothelial cells), it was discovered that these cells would not only proliferate in the absence of bovine calf serum, but also self-organise when in contact with an air-water interface. Effectively this enables the production of a synthetic dermis without the need for complex proteins to act as molecular cues, these cues being produced by the cells and aided by the scaffold geometry. The lack of need for serum also lessens safety worries associated with using bovine products. It was found that the SESM MkIII was also suitable for producing tissue engineering scaffolds of biodegradable polymers (Poly-(l- lactide) (PLLA) and poly- (D,L- lactide) (PDLA)) with suitable modifications to the electrospinning solutions and electrospinning parameters. The biocompatibility of such biodegradeable scaffolds has yet to be elucidated.

Control over the surface morphology of electrospun fibres has been achieved using a modified version of the SESM MkIII whereby the apparatus is encased within a perspex box. The humidity of the atmosphere within this box is easily manipulated and has a direct bearing on the porosity of the fibre surface of polymers spun within the box. In this study more humid atmospheres have been found to give rise to more porous fibres of PLLA. It has been proposed that the mechanism of such a phenomenon is a combination of condensation effects and phase separation. It was hoped that by increasing the surface porosity of electrospun PLLA that the rate of release of a drug encapsulated within the fibre could be increased. A method was designed by which the antibiotic Tetracycline could be encapsulated within fibres of PLLA with different surface porosities. Unfortunately it was found that surface porosity has very little bearing on the rate of drug release from the fibres.

A completely novel electrospinning technique has been invented which enables the production of aligned electrospun fibres. Commonly the technique of electrospinning yield only non-woven materials as result of jet whipping during spinning. By reversing the polarity of the conventional electrospinning apparatus and targeting the jet at a needle point rather than a diffuse collector, jet-whipping is minimised. Collection of a straight jet upon a spindle yields aligned fibres. Conditions for the successful collection of aligned fibres have been observed and relationships between solution properties and propensity for fibre alignment have been determined. Aligned fibres of PLLA, Polystyrene (PS) and a high molecular weight block copolymer have all been produced. It has been found that aligned fibres are difficult to obtain when the electrospinning solution has a large dielectric constant (ε), although the threshold value for ε whereby alignment can no longer be achieved has not been determined.

Skin cells (fibroblasts) have been cultured successfully on the surface of aligned PLLA and PS fibres and have been seen to migrate along fibres over 10μm in diameter. Fibroblasts have also been seen to span the gaps between aligned fibres up to a maximum distance of 200μm. This information is important as it gives insight into the mechanism of cell proliferation within 3-D scaffolds. By knowing the distances over which cells can span and the fibre diameters upon which cells can proliferate a scaffold can be designed in which cells will thrive.

7.2 Future Work

Electrospinning will always be closely related to tissue engineering. Work still needs to be done on the proliferation of skin cells within biodegradable scaffolds such as those made from PLLA and modified versions of PLLA with controllable rates of degradation. At the time of writing in-vitro studies of PLLA scaffolds are being performed whereby the scaffolds will be extracted from the hosts after different periods of time, and the degradation of the scaffolds determined. These experiments are important in order to determine whether or not any serous inflammatory responses are caused or whether any modifications to the polymer's degradability are needed.

So far the only cells to have been seeded on these electrospun fibres have been skin cells. These scaffolds could also be used to culture other cell types. The aligned fibres in particular are an attractive tissue engineering substrate for cell types which require

some sort of guidance. Cells such as tenocytes (which form tendons) and neurones (which form nerves) cold both benefit from the guidance effect of an aligned fibre scaffold.

The future of electrospinning is limited only to the imagination of the polymer scientist. Most polymers can be electrospun into a range of fibre diameters or topographies depending upon the required purpose. Co- spinning of different polymers on the modified SESM MkIII apparatus or the modified alignment apparatus offers an attractive route to making smart materials, coupling the properties of each polymer spun. Polymers have been synthesised which swell and contract in solution when the pH of that solution is altered. Electrospinning of such polymers would increase the surface area of the material and as such increases the rate of diffusion and swelling. Work has already begun on the spinning of such polymers but none has been done on the co-spinning of such polymers with other materials.[1] An example would be to co-spin such a polymer with an elastin (an elastic polymer) which would work as an antagonistic force to the swelling of the pH responsive polymer. Swelling of the pH responsive fibres would occur under acid or base conditions (depending upon the polymer used). Once the pH is changed in order to stop the swelling, the co-spun material could "snap back" to its original dimensions as the elastin relaxes. Spinning such composites as bundles of aligned fibres would give the swelling and contraction some direction and power.

Scale-up of the electrospinning process is a major consideration for the future. Whilst methods of scale-up for conventional electrospinning have been devised (see section 1.2), no techniques for increasing rates of production of aligned fibres have been found. Whilst some methods have been suggested in section 6.6 none of these have been taken beyond the early trail stage.

7.3 References

1. Topham, P. D. Study of pH Responsive Polymer Systems for use in Molecular Machines. *PhD Thesis* (2006).

7.4 Publications

1 Sun T., Norton D., McKean R., Haycock J., Ryan A.J., MacNeil S.. Self-organization of skin cells in three-dimensional electrospun polystyrene scaffolds. *Tissue Engineering* **11**, 1023-1033 (2005).

2. Sun, T., Norton, D., Haycock, J. W., Ryan, A. J. & MacNeil, S. Development of a Closed Bioreactor System for Culture of Tissue-Engineered Skin at an Air-Liquid Interface. *Tissue Engineering* **11**, 1824-1831 (2006).

3. Sun T., Norton D., McKean R., Haycock J., Ryan A.J., MacNeil S.. Tissue Engineering: Nano, Micro or Macro-fibres? *Submitted for assessment* (2005).

4. Sun T, Norton D., McKean R , Haycock J, Ryan AJ, MacNeil S. Fibroblasts walk the plank- do tissue engineered scaffolds need to incorporate macro, micro and nano features? *Submitted for assessment* (2006).